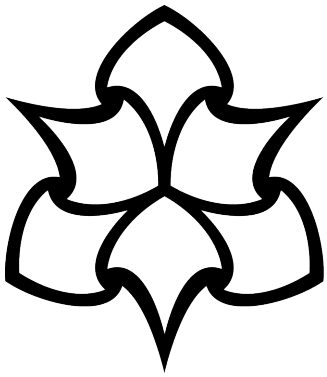

Novel, rapid and sensitive detection of isomeric fluorinated New Psychoactive Substance(s) and their principal metabolites using analytical techniques

A thesis submitted in fulfilment of the requirements of the Manchester Metropolitan University for the degree of Master by Research.

A. Hayatbakhsh
Department of Chemistry
Manchester Metropolitan University 2018

A thesis submitted in fulfilment for the degree of Master by Research at Manchester Metropolitan University. I declare that none of the work detailed herein has been submitted for any other award at Manchester Metropolitan University or any other Institution. I declare that, except where specifically indicated, all the work presented in this report is my own and I am the sole author of all parts. I understand that any evidence of plagiarism and/or the use of unacknowledged third part data will be dealt with as a very serious matter.

Armita Hayatbakhsh 13154590

Supervisors: Dr. Oliver B. Sutcliffe and Dr. Ryan Mewis

Sign:  Date: 08/08/18

Word count: 16567

Abstract:

In the last few years, there has been a remarkable increase in the prevalence and use of New Psychoactive Substances (NPS) within the global recreational drugs market. The biological activity of NPS, formally known as “legal highs”, exhibit similarities to illicit drugs of abuse. Different regioisomers, such as those of fluorocathinone, can have different toxicological and biological effects. As such, it is vital to distinguish between their isomers. Therefore, a simple, accessible and selective analytical method is promptly required to differentiate positional isomeric *N*-substituted fluorocathinones.

In this project, a combination of GC–MS, LC-MS, IR, presumptive testing and thin layer chromatography have been employed for full chemical characterization of the regioisomers of cathinone derivatives. GC-MS and LC-MS are essential for the screening of compounds in illicit drug products. The LC-MS spectrum presents information about the molecular weight, and the GC-MS spectrum gives structural information about the molecule. *N*-alkylated *ortho*-, *meta*- and *para*-fluoro*eth*cathinones were unequivocally separated by GC-MS, using product ion spectrometry of the hydrogen fluoride loss ions.

These compounds were also characterized and identified using full analysis of ^{1}H and $^{13}C\{^{1}H\}$, $^{19}F\{^{1}H\}$, ^{1}H-^{1}H COSY, HMQC and HMBC using high-field nuclear magnetic resonance (NMR) spectroscopy.

Isomeric fluorinated *N*-ethylcathinone (FEC) is structurally similar to fluoromethcathinone (FMC) isomers, with only the methyl group at the end of the side chain substituted for an ethyl group. Therefore, *J*-resolved and HETCOR spectroscopy were employed to resolve the positional regioisomers using low-field bench top NMR (1.4 T). In reality, however, due to similarities in their structures, this was difficult to achieve. It was possible to separate the FEC and FMC isomers within their own class but not an individual FEC/FMC regioisomer from a FEC/FMC mixture.

Acknowledgements:

I would like to express my sincere appreciation and gratitude to the people who supported and helped me throughout this research project.

Firstly, I would like to thank my supervisors, Dr Ryan Mewis and Dr. Oliver B. Sutcliffe, for providing me the opportunity to join their remarkable team and fulfill this project. Also, I am grateful for their continuous support and guidance and great knowledge throughout this research and writing of the thesis.

I would also like to thank my fellow lab-mate Matthew Hulme for his constant help throughout this project.

Finally, I am greatly thankful to my family and friends, for their support and encouragement, I am truly grateful for their constant support financially and spiritually.

Table of Contents

List of Figures

List of tables

Overview of the Synthesis Routes

Abbreviations:

^{13}C NMR	13-Carbon NMR
^{19}F NMR	19-Fluorine NMR
^{1}H NMR	Proton NMR
4-MMC	Mephedrone
ATR–	Attenuated Total Reflectance-Fourier Transform Infrared
FTIR	Spectroscopy
Br_2	Bromine
CNS	Central Nervous System
COSY	Homonuclear correlation spectroscopy
D_2O	Deuterated water
DCM	Dichloromethane
DEPT	Distortionless Enhancement by Polarization Transfer
DMSO	Dimethyl sulfoxide
EMCDDA	The European Monitoring Centre for Drugs and Drug Addiction
FEC	Fluoroethcathinone
FEC.HCl	Fluoroethcathinone Hydrochloride
FMC	Fluoromethcathinone
GC-MS	Gas Chromatography-Mass Spectroscopy
HBr	Hydrobromic Acid
HETCOR	Heteronuclear-Correlation
HMBC	Heteronuclear Multiple Bond Coherence
HMQC	Heteronuclear Multiple Quantum Coherence

HPLC	High Performance-Liquid Chromatography
HRMS	High-Resolution Mass Spectrometry
Hz	Hertz
IR	Infrared Spectroscopy
J_{CF}	Carbon-Fluorine *J*-couplings
J_{CH}	Carbon-Hydrogen *J*-couplings
J_{HF}	Hydrogen-Fluorine *J*-couplings
J_{HH}	Hydrogen-Hydrogen *J*-couplings
J-RES	*J*-resolved Spectroscopy
LC-MS	Liquid Chromatography–Mass Spectrometry
MDA	3,4-Methylenedioxyamphetamine
MDMA	3,4-methylenedioxy-*N*-methylamphetamine
mg	Milligram
$MgSO_4$	Magnesium Sulfate
mL	Millilitre
mL min^{-1}	Millilitre per minute
MSD	Mass spectrometric detector
NHEt	Dimethylamine
NMR	Nuclear Magnetic Resonance
NPSs	New Psychoactive Substances
ppm	Parts Per Million
PS	Psychoactive Substance
R_f	Retention factor
RSD	Relative Standard Deviation

TFA	Trifluoroacetic Acid
TLC	Thin Layer Chromatography
TSP	Trimethylsilylpropanoic acid
UNODC	United Nations Office on Drugs and Crime
UV	Ultraviolet
δ	Delta (ppm)

Chapter 1 Introduction

1.1 New psychoactive substances (NPSs)

Definition of NPS: New psychoactive substances are the recreational drugs that are intended to mimic the desired effects of other illegal substances such as cannabis, amphetamine, cocaine, heroin and MDMA (3,4-methylenedioxy-*N*-methylamphetamine), commonly known as "Ecstasy".[1] These drugs are broadly sold as "legal highs", but all psychoactive substances are now controlled under the Misuse of Drugs Act 1971 or the Psychoactive Substances Act 2016 (PS Act).[2] They are controlled as Class B drugs in the United Kingdom under the Misuse of Drugs Act 1971 since April 2010.[3] Figure 1-1 illustrates the increase in the number of NPSs reported between 2009 -2014.

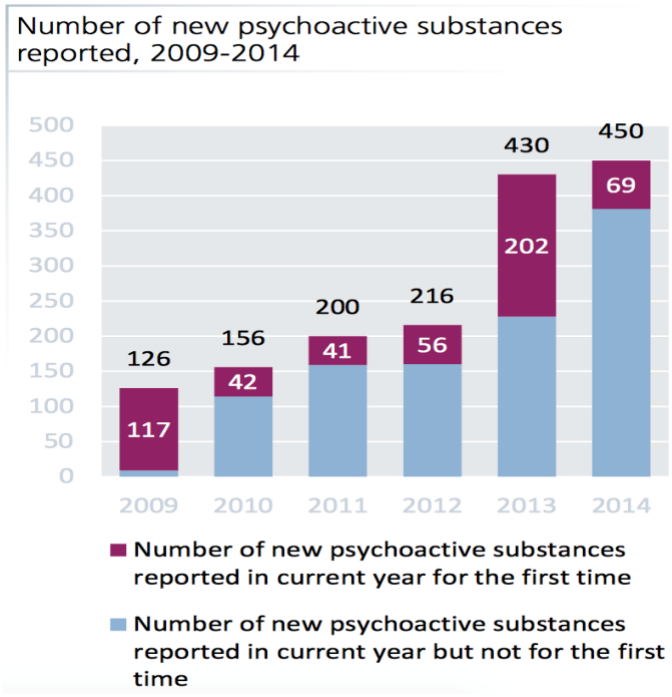

Figure 1-1. Number of New Psychoactive Substances reported between 2009 -2014.[4]

A drug's harmful effects must be recognized before it can be controlled under the Misuse of Drugs Act 1971; however, this demands major intensive resources and could be time consuming. Furthermore NPSs have been appearing at an extraordinary rate.[5] Therefore, to control and illegalize the selling, making, and possession of NPSs, the government introduced the legislation of the Psychoactive Substances (PS) Act 2016, which was originated on 26 May 2016.[5] However, these drugs are chemically altered to avoid international legislations and, therefore, this causes major problems for the police force, in that if a sample is found, the police will be unsure as to whether to charge the person with the Misuse of Drug Act or the PS Act.[6]

Furthermore, in the past decade, there has been a rapid increase in recreational intoxication substances including synthetic cathinones, hence, these drugs have become popular drugs of abuse, mainly due to ease of purchase and low cost in comparison to their subsequent illicit drugs of abuse. These substances are easily sold as powders or even tablets in pet shops, on the dark web and by high street suppliers, as 'plant food' and 'bath salt' as well as 'research chemicals'. These products are specifically labelled as not suitable for human consumption.[7] In particular 4-methylmethcathinone (4-MMC, mephedrone) (**1**) and 3,4-methylenedioxypyrovalerone (MDPV) (**2**) are the most regularly sold illicit substances within Europe, North America and Oceania.[8]

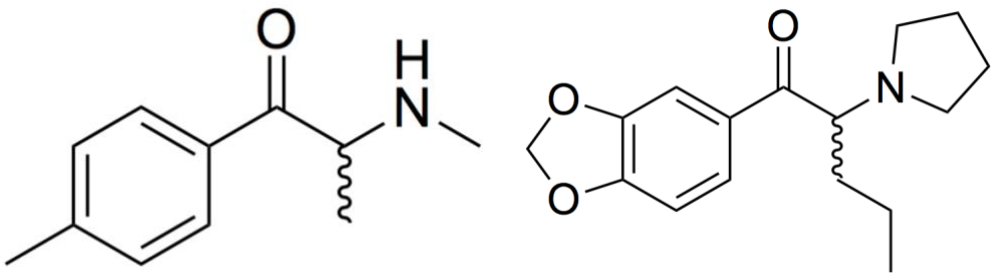

1 **2**

Figure 1-2. (**1**) Mephedrone; (**2**) 3,4-methylenedioxypyrovalerone

Consequently, the United Nations Office on Drugs and Crime (UNODC) reported more than 600 substances by the end of 2015, which has doubled since 2013. From 2005 to 2011, 150 NPSs were recorded by The European Monitoring Centre for Drugs and Drug Addiction (EMCDDA); 34 of these registered drugs were synthetic cathinones, which increased to 50 new synthetic cathinones by 2013.[9] The synthetic cathinone trade is significantly growing with the emerging synthetic cathinones in comparison to the synthetic cannabinoids and other psychoactive substances. Although, synthetic cathinones are fast growing in the illegal drug market, very limited information is known about the chemical characteristics and side effects associated with these drugs. Fig. 1-3 shows the global emergence of NPSs up to December 2015.

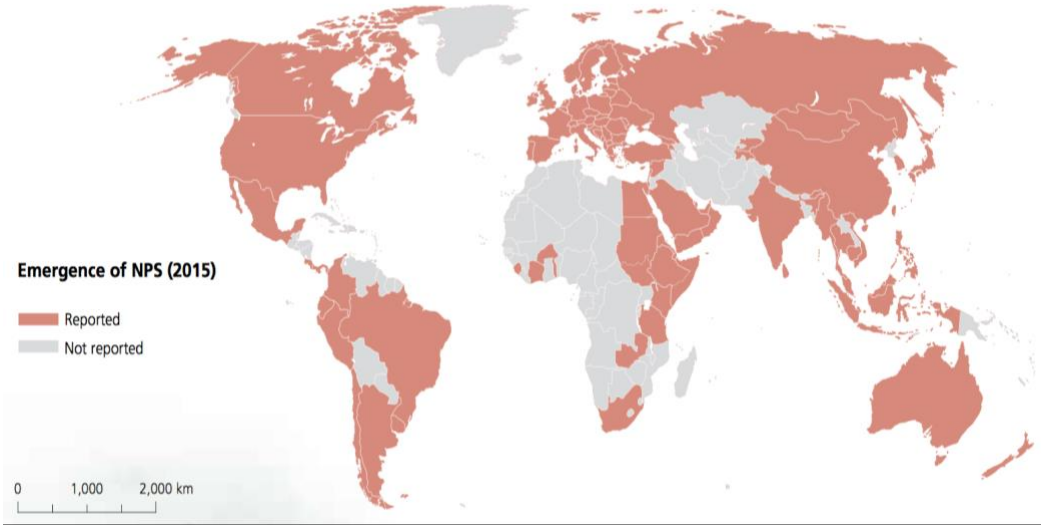

Figure 1-3. Global emergence of New Psychoactive Substances (NPSs) up to December 2015.[10]

The biological activity of NPS exhibit similarities to illicit drugs of abuse and have the potential to cause serious risk to public health and safety and can even be fatal. The NPSs are classified into the following sub-categories: synthetic cannabinoids, synthetic (meth)cathinones, ketamine, phenethylamines, piperazines and plant-based.[9] Different regioisomers of these drugs can have different toxicological and biological effects; as a consequence, it is vital to distinguish between their isomers. Therefore, a simple, accessible and selective detector with affinity for NPS is promptly required to develop proficiency within the forensic science sector. Consequently, decreased international trading (of NPS) may result, possibly leading to a safer and securer society.

1.2 Synthetic Cathinone

Cathinone is a naturally occurring phenylalkylamine derived from Khat leaves, which is a plant or tree that grows in East Africa and the Arabian Cape mainly Somalia and Ethiopia. Historically people chewed Khat leaves for their overjoyed and stimulating properties; this tradition is still predominant in countries such as Somalia, Yemen, Kenya, and Ethiopia.[11] The plant leaves are called different names in these regions for instance, Arabian Tea, Abyssinian Tea, Chat Tree, Cafta or even Khat.[11]

Figure 1-4. Khat leaves. [12]

The properties of Khat leaves (Fig. 1-4) are due to its ingredients comprising of phenylalkylamine alkaloids that contain L-ephedrine (**3**), cathinone (2-amino-1-phenylpropan-1-one, α-aminopro-piophenone) (**4**) and cathine [norpseudoephedrine, (1S, 2S)-2-amino-1-phenylpropan-1-ol, (+)-nor-Ψ-ephedrine] (**5**).[11] In the 1930s, researchers found that the psychoactive properties of Khat initially was mostly due to norpseudoephedrine, although in 1975, cathinone was isolated from Khat leaves and was studied for its

psychoactive components. It was found that although cathinone exists as a chiral molecule, only the S-(-) enantiomer is detected in Khat leaves and its racemic mixture was produced after 1982. Moreover, only fresh leaves have been used for chewing because the cathinone in the leaves have a short lifetime and decompose quickly. On the other hand, unlike synthetic cathinones, Khat chewing allegedly results in mild psychological addiction and mild withdrawal symptoms. [13]

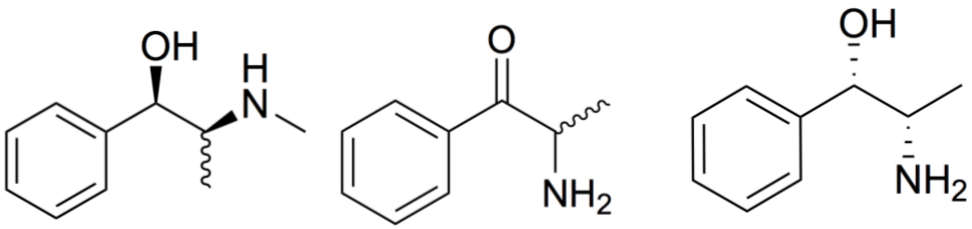

3 **4** **5**

Figure 1-5: (**3**) L-ephedrine; (**4**) Cathinone; (**5**) Cathine

Methcathinone and mephedrone were the first synthetic cathinones to be synthesised in 1928 and 1929 respectively.[13] Synthetic cathinones are considered to be central nervous system (CNS) stimulants, releasing the effect of anorectics and antidepressants. However, these drugs were removed from clinical use due to complications with misuse and addiction. While the *R*-cathinone enantiomer triggers dopamine release in the CNS, this makes it three times more effective than *S*-cathinone.[14]

Methcathinone and diethylpropion, which are appetite suppressants, were initially prescribed as antidepressant and anorectic drugs respectively, but

they were removed due to their abuse and dependence properties.[15] Bupropion (Wellbutrin) is the effective substituted cathinone as well as substituted amphetamine, which is used as an antidepressant and smoking cessation. [16]

Since 2004, the number of synthetic cathinones in different regions of the world has been growing rapidly, by decreasing the purity and accessibility of other stimulating substances such as MDMA (3,4-methylenedioxy-*N*-methylamphetamine) and cocaine. As with other NPS, the epidemiologic data for synthetic cathinones is very limited. Although, they first emerged in Europe in 2005, the uptake has been such that presently, they are the major category of NPS with over 80 different synthetic cathinone derivatives in the drug market.[13]

1.2.1 Chemistry of cathinone

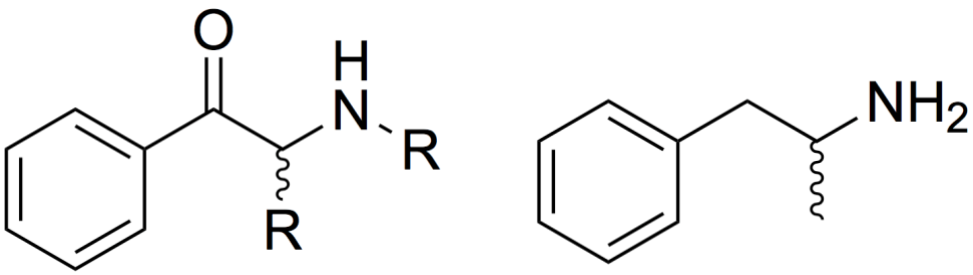

6 **7**

Figure 1-6: (**6**) Cathinone; (**7**) Amphetamine

The structure of cathinone (**6**), (Fig. 1-6), is very similar to amphetamine (**7**). Both are substituted phenethylamines with cathinone having a ketone group at the β-carbon site. Changing the R-groups attached to the cathinone

structure and/or altering the substitutions attached to the benzene ring, results in formation of different cathinone derivatives. The methyl group is present in all amphetamine and cathinone compounds in order to retain the β-carbon ketone moiety. Accordingly, replacing the CH_2 α to the aromatic ring with a ketone alters the structure of amphetamine to a cathinone. For instance, methamphetamine can be transformed to methcathinone, and MDMA (ecstasy) (**8**) can be altered to form methylone (**9**), this difference is demonstrated in figure 1-7. Hence, they're known as recreational substances due to their stimulating effect on the central nervous system.[13]

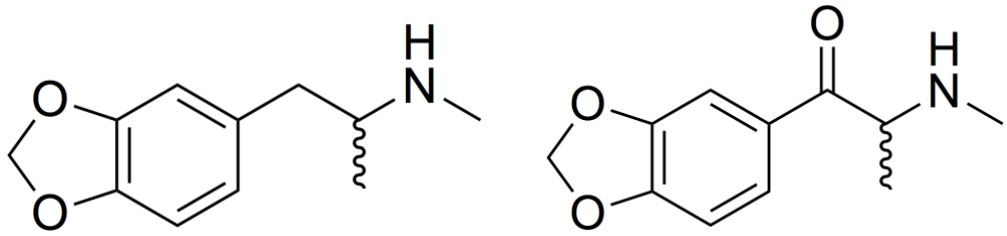

8 9

Figure 1-7: (**8**) MDMA (ecstasy); (**9**) Methylone

1.2.2 Ethcathinone

Ethcathinone (*N*-ethylcathinone) is a metabolite of diethylpropion (*N*,*N*-diethyl-2-amino-1-phenylpropan-1-one), but it is more powerful than diethylpropion. Researchers in Poland discovered that ethcathinone was the most commonly used NPS between 2012 and 2014, therefore resulting in it becoming categorized as a controlled drug. [11] Moreover, carbonyl reduction

of ethcathinone results in the production of different metabolites including ethylephedrine.

1.3 Ephedrine (1-phenyl-1-hydroxy-2-methylaminopropane)

Reduction of the ketone in substituted cathinone results in formation of ephedrine. Ephedrine is a commonly abused psychostimulant and it was first synthesised by Eberhard Späth.[17] Späth found that the methyl-substituted cathinone has a molecular formula of $C_{10}H_{15}NO$.[18] Furthermore, it was deduced that the benzene ring possessed a single side chain because it forms an oxidised benzoic acid upon oxidation. It was suggested that it's a secondary amine compound because when it reacts with nitrous acid it forms a nitroso-compound. [18]

Ephedrine comprises of two asymmetric chiral centres and accordingly results in four isomers. Freudenberg was the first to describe the configuration of the pairs of enantiomers. He implied that the isomers of ephedrine are categorised into two classes depending on their symmetry: (+)-ephedrine (**10**) and (-)-ephedrine (**11**) are from the *erythro* enantiomer of "alpha-[1-(methylamino)ethyl]benzene-methanol" 2) *threo* or pseudoephedrine comprises the (+)-pseudoephedrine (**12**) and (-)-pseudoephedrine (**13**) (Fig. 1-8). Reduction of (+)-pseudoephedrine forms S-methamphetamine, which is a form of psychoactive substance.[1, 19]

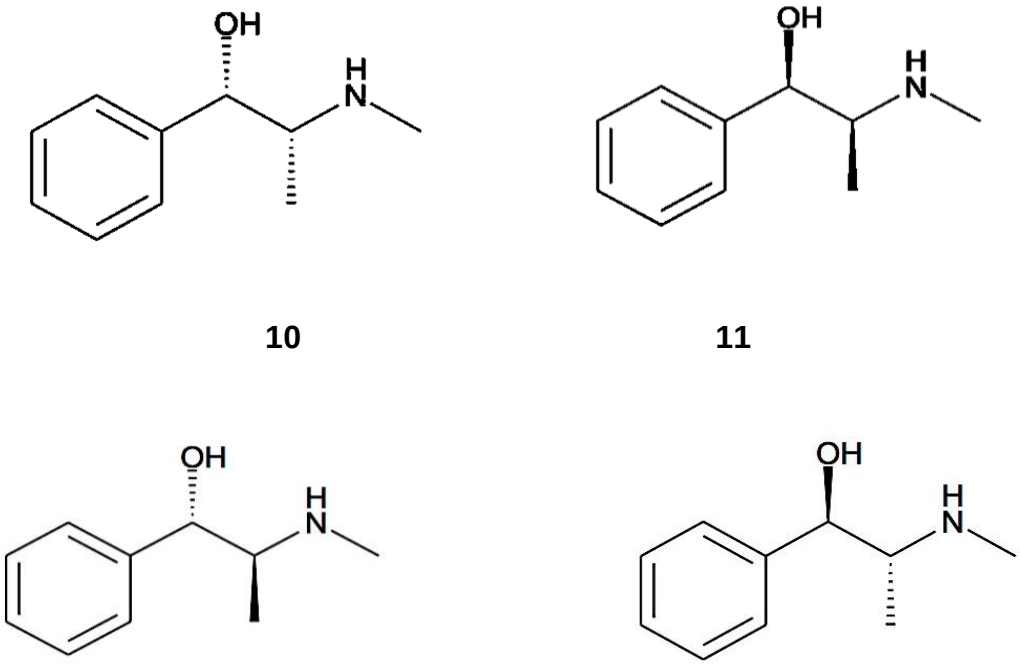

Figure 1-8. (**10**) (+)-ephedrine; (**11**) (-)-ephedrine; (**12**) (+)-pseudoephedrine; (**13**) (-)-pseudoephedrine

Ephedrine's effect is similar to that of amphetamine; it results in a rise in systemic arterial pressure, cardiac output as well as increasing the heart rate. It is assumed that it increases the blood pressure by changing constriction of the blood vessels by noradrenaline from adrenergic terminals; this action is known as the pressor response. Additionally, ephedrine alkaloid was the key ingredient in weight loss supplements, although in 1997 the Food and Drug Administration (FDA) had set rules on the amount of ephedrine alkaloid in these substances. However, in 2001, the FDA banned the synthesis and sale of ephedrine containing supplements.[20]

1.4 Gas Chromatography-Mass Spectrometry (GC-MS)

Gas Chromatography-Mass Spectrometry (GC-MS) is one of the most commonly applied analytical techniques in different branches of science; it is an extremely reliable confirmation test. Gas Chromatography (GC) is an essential technique in separating the components of a mixture according to their chemical properties as well as determining the quantity of each component of the mixture. However, in order to fully characterize the chemical structure, it requires a spectroscopic detection method. Hence, a mass spectrometric detector (MSD) is employed to establish physical properties, by generating small ions that have specific relative abundances for each compound and, therefore, allows information to be acquired about molecular mass and elemental structure, to create a fragmentation pattern for each molecule in the compound mixture. High-resolution mass spectrometry (HRMS) also provides information regarding the existing functional groups as well as the geometry and spatial isomerism of the molecule. Chemists and forensic scientists apply this knowledge to detect the structure of known compounds as well as elucidating the structure of an unknown compound mixture. Predominantly, GC-MS is used for the detection of various NPSs, in particular cathinones, in street samples and biological substances.[21]

Once the sample is injected at the split/ split-less injection port, the inert carrier gas (commonly usually argon, helium, hydrogen, nitrogen and carbon dioxide) is needed to vaporise the sample and carries the sample along the

column while ensuring that it does not react with the sample at the same time. The type of polarity of the stationary phase depends on the type of analyte. For example, polar molecules, such as cathinone derivatives require a polar stationary phase. Furthermore, the inert gas passes through the stationary phase that is located in an oven, which controls the temperature of the gas; therefore, the rate at which the sample elutes through the column is equal to the oven temperature. In addition, the oven temperature can be adjusted for a particular compound in order to maximise separation.

Subsequently, the separated sample is transferred into the mass spectrometer, which is under vacuum. Electrons bombard the compounds, in order to generate positive ions. As a result of this high-energy ionization, various ion fragments are formed. Afterwards, the ions pass through a magnetic field and are separated depending on their mass-to-charge ratio by an electron multiplier device.

Although GC-MS is a widely used separation technique, it is limited to volatile compounds. Therefore, for some samples, such as cathinone, there is a need for derivatization prior to analysis. However, derivitized cathinone compounds are unstable and degrade at high temperature, therefore resulting in considerable deformation of the peaks. Some examples of cathinone derivatizations analyzed using GC-MS were reported by Alsenedi *et al*.[22]

1.5 Presumptive tests

Colour presumptive testing is an analytical procedure used in forensic science as a colour test for detection of controlled drugs. This technique involves reaction of a series of reagents with the particular sample either as a powder or in solution, which if a reaction occurs, leads to an immediate or fast colour change. The main advantages of this technique are the simplicity and ease of use of the method. It does not require complex equipment and does not consume too much time to train analysts. These reactions can produce positive or negative results; a negative result helps to eliminate a drug or class of drugs, subject to the type of colour test.[23]

Primary presumptive observations reported by Smith *et al*. stated that cathinone derivatives test positive with Zimmerman's reagent. Therefore, these are the most effective test methods for these compounds.[1, 24] However, Nagy *et al*. reported that the Chen Kao test is specific for ephedrine compounds.[25] Thus, presumptive tests can be used to screen drug samples based on their derivative class.

1.6 Introduction to Nuclear Magnetic Resonance Spectroscopy (NMR)

Nuclear Magnetic Resonance (NMR) spectroscopy is one of the fundamental and important analytical techniques. The first measurements of nuclear magnetic moments were made using magnetic resonance absorption of molecular beams back in 1935, whereas Nuclear Magnetic Resonance (NMR) spectroscopy was first established in 1946 and has been

awarded several Nobel prizes (Felix Bloch (1905-1983), Edward M. Purcell (1912-1997) and Richard Robert Ernst (1991)). NMR spectroscopy has developed drastically since its first development. [26]

Nuclear Magnetic Resonance (NMR) spectroscopy is an important analytical technique. The results from an NMR analysis supplements the results obtained from other spectroscopic methods. It delivers quantitative information about the identification of small molecules such as controlled substances (i.e. NPS) without major requirements for a lot of sample preparation or sample derivatisation which is needed in GC-MS. NMR spectroscopy is able to distinguish between regioisomers of substances such as NPSs.

NMR spectra provides information about the identity, through structural characterisation, as well as evidence to ascertain the purity of chemical substances. Crucially, it enables the atom connectivity to be deciphered (through the use of *J*-couplings and 2D techniques), which facilitates a route to elucidate the structure of the molecule being analysed.

1.6.1 Nuclear Magnetic Resonance analysis

In NMR spectroscopy, NMR occurs when a sample is immersed in a homogeneous magnetic field. The nuclear spins within the sample will align either with or against the magnetic field. When a radiofrequency (RF) radiation photon bombards the sample, it absorbs the energy and triggers a nuclear spin transition, from the ground state to an excited state. Upon

relaxation, RF energy is released which is indicative of the nuclei's environment. The radiation frequency required for absorption, known as the Larmor frequency, depends on the nucleus type (e.g. ^{1}H or ^{13}C, ^{14}N) as well as its chemical environment. A signal is produced from the emitted nuclei; this is called free induction decay (FID), which is a superimposition of all the frequencies of the excited nuclei present in the sample. The FID is processed using a Fourier transformation that is performed computationally.[27]

1.6.2 Pulsar benchtop NMR

Pulsar is a high-resolution, 60 MHz benchtop NMR spectrometer. Benchtop NMR utilises a low-field instrument and is mainly appropriate for smaller molecules that provide unambiguous spectra; it is able to produce high quality heteronuclear and 1D, 2D spectra of 1H, ^{13}C, ^{19}F as well as ^{31}P. It is cryogen-free (a cryogen-free system retains magnetism without the requirement of cryogenic liquids), because it uses a permanent magnet. Benchtop NMR does not require extensive training and can be sited in any laboratory without special requirements that are necessary in a high-field NMR spectrometer. [28]

However, there are some disadvantages associated with low-field ^{1}H NMR specifically when analysing a mixture; the peaks in the ^{1}H NMR spectra can often overlap due to having similar chemical shifts that result from homo-nuclear spin couplings. High-field NMR does not experience this strong

coupling effect due to increasing the frequency between the multiplets. High-field NMR, therefore, has better resolution than its low-field counterparts. [28]

1.6.3 *J*-resolved (*J*-RES) NMR spectroscopy

As previously stated, although ^{1}H NMR is able to acquire fast spectral data in order to characterise a molecule, sometimes in biological metabolites and drugs, it can lead to the formation of a complex spectrum with overlapping signals or spectral crowding that would make them problematic for identification and quantification. Thus, the 2D *J*-resolved (2D *J*-RES) overcomes this setback by completely separating the complicated chemical shifts and *J*-couplings along two definite dimensions. [29]

1.6.4 Heteronuclear correlation (HETCOR)

Heteronuclear correlation (HETCOR) allows for the unambiguous assignment of both carbon and proton spectra by determining which hydrogen is attached to each carbon in a 2D NMR spectrum. Likewise, HETCOR can also be proposed to present information about correlations between protons and carbons through multiple bonds and *J*-couplings. Although heteronuclear correlation spectroscopy was traditionally used for carbon and proton nuclei, it has now been applied to determine the correlation between atoms containing different nuclei (i.e. ^{15}N nuclei).

Chapter 2 Aims

2.1 Aims of the project

This project aims to synthesise fluorinated *N*-ethylcathinones (**16**), and their principal metabolites (**17**) as the reduced form of fluoroethcathinone, as illustrated in Scheme 2-1. There are no reference materials available for any of the target compounds, so the primary objective of this project will be to prepare the target compounds and carry out structural characterisation of the materials. The regioisomers of the cathinone derivatives will be characterised by GC-MS, LC-MS, melting point, TLC and IR techniques. The forensic issue of rapid, selective and sensitive field-screening of the molecules will be addressed using a low-field NMR detector. The samples will be studied both in their pure form and in the presence of common adulterants and other isomeric fluorinated NPSs to determine the selectivity of the proposed methodology. Low-field NMR spectroscopy has significant benefits including affordability, portability and no requirement for dedicated locations or staff to perform routine maintenance. Recent developments in permanent magnet technology have better positioned low-field NMR instruments and facilitated their use for rapid analysis. However, their application to forensic screening of drug samples has not been exploited to the same extent as other approaches. Moreover, high field ^{1}H NMR, ^{13}C NMR and ^{19}F{^{1}H} NMR spectra of all the isomers will be generated in order to compare with the corresponding low-field data.

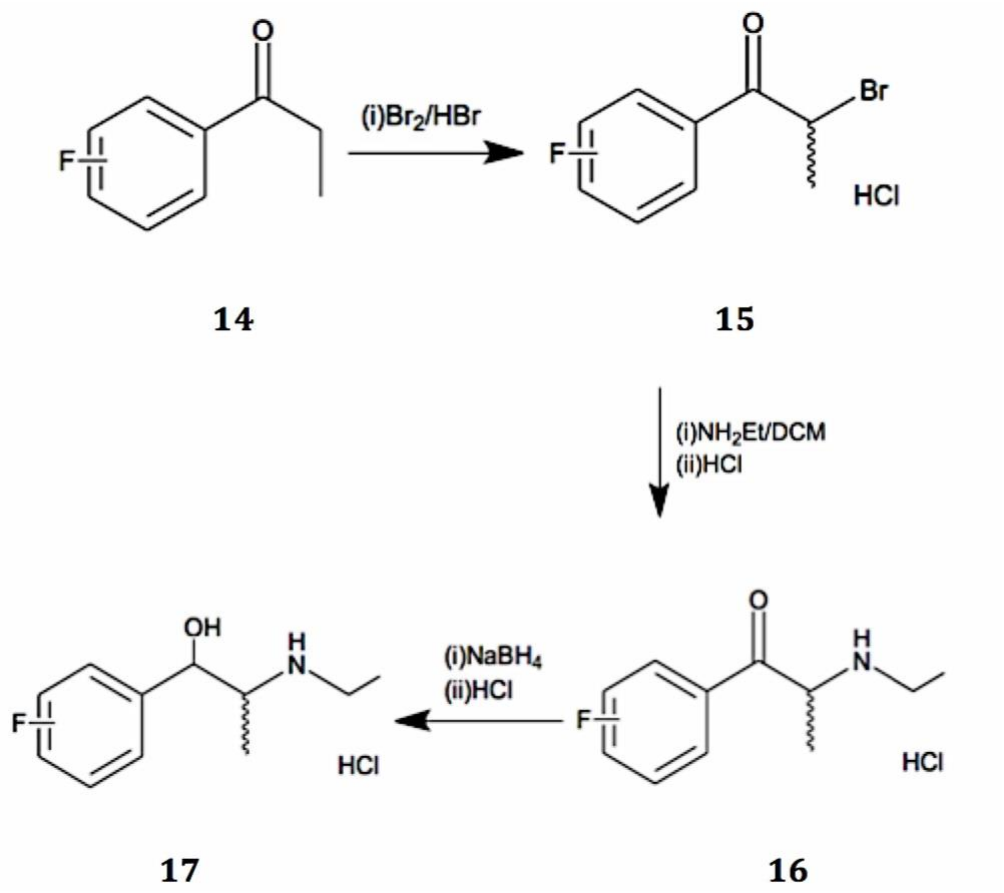

Scheme 2-1. Synthetic overview for the synthesis of the regioisomeric FEC (16) and their principle metabolites (17)

Isomeric FEC (**18**) is structurally similar to FMC (**19**) isomers (Fig. 2-1), as the structures only differ by a methyl group in the side-chain component. Therefore, *J*-RES and HETCOR spectroscopy will be employed to resolve the positional regioisomers using low-field bench top NMR (Pulsar).

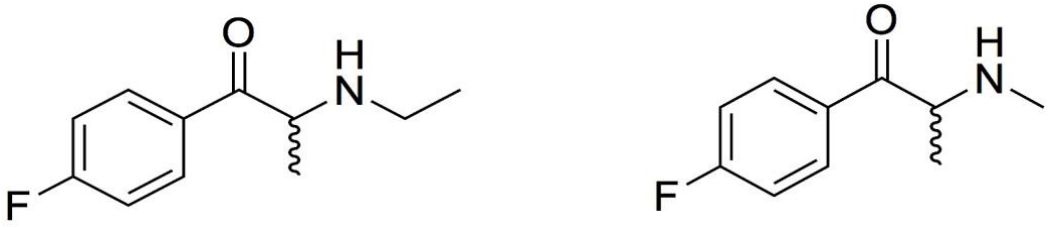

18 **19**

Figure 2-1. (18) FEC; (19) FMC

Chapter 3 Experimental

3.1 Materials and Methods

The synthetic cathinone hydrochloride salts and their metabolites were prepared using the methods reported by Santali *et al*.[30] All reagents were of commercial quality (obtained from Sigma–Aldrich, Gillingham, UK or Alfa-Aesar, Heysham, UK) and used without further purification. Solvents were dried, where required, using standard methods.[31] The synthesised compounds were fully characterised and their purity were deduced. All compounds were purified before experimental analysis. ^{1}H, ^{13}C, ^{1}H-^{1}H COSY, HMQC and HMBC NMR (10-20 mg/600 μL in D_2O containing 0.1% TSP (trimethylsilylpropanoic acid) as a reference standard) were obtained on a JEOL AS-400 (JEOL, Tokyo, Japan) NMR spectrometer functioning at a proton resonance frequency of 400 MHz and referenced to residual solvent peak, TSP ($\delta^{1}H$ (0 ppm)). $^{19}F\{^{1}H\}$ NMR spectra (10 mg/600 μL in D_2O containing 0.03% *v/v* trifluoroacetic acid (TFA)) were acquired and referenced to TFA (^{19}F (-76.55 ppm)). Infrared spectra were obtained in the range 4000– 400 cm^{-1} using a Thermo Scientific Nicolet iS10ATR-FTIR instrument (Thermo Scientific, Rochester, USA). GC–MS analysis was performed, and the data was collected using an Agilent 6890N GC and mass selective detector (MSD). The separation was carried out by manual, split linear injection, over a capillary column and helium was used as the carrier gas at a constant flow rate of 1.0 mL min^{-1}. Thin-Layer Chromatography (TLC) was conducted on aluminum-backed SiO_2 plates (Merck, Darmstadt,

Germany) and spots were envisaged using ultra-violet light (254 nm) and Ninhydrin dip (Ninhydrin (100 mg) with 0.5 mL acetic acid dissolved in 100 mL acetone**)**. Melting points were determined using a Gallenkamp melting point apparatus (Gallenkamp-Sanyo, UK). *J*-RES and HETCOR NMR spectra (20 mg/600 μL in D_2O and reference standard (TSP or TFA), in addition to 20 mg benzocaine where required) were obtained using an Oxford Instruments low-field Pulsar bench-top NMR (1.4 T).

3.2 Overall experimental synthesis

X-Fluoro-*N*-ethylcathinone hydrochloride and their metabolites were prepared as detailed below. An example of the reaction scheme is presented for 2-fluoroethcathinone (2-FEC) in Scheme 3-1.

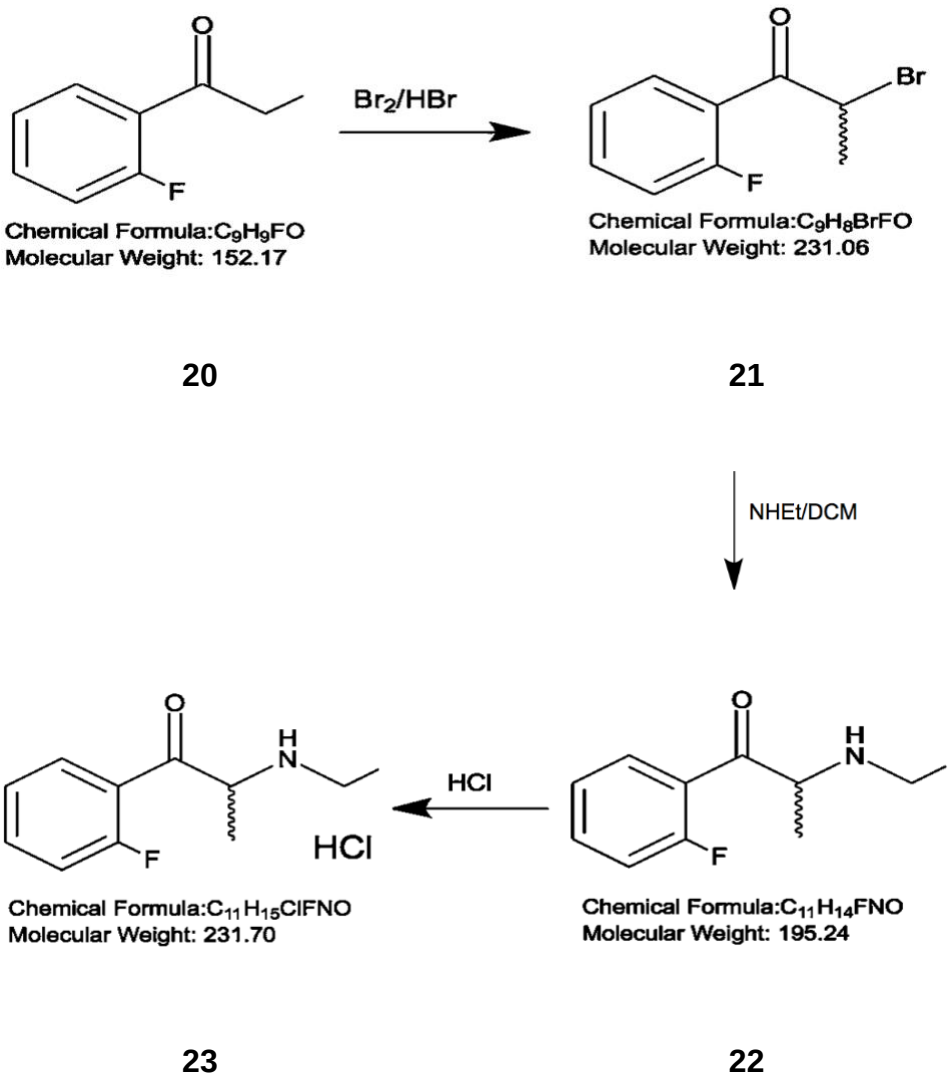

Scheme 3-1. Synthetic overview for the synthesis of 2-Fluoro-*N*-ethylcathinone hydrochloride

2.1 Synthesis of 2'-bromo-x-fluoropropiophenone (where X = 2,3 or 4)

α–Bromination: To a solution of x-fluoropropiophenone (3.04 g, 20mmol) in dichloromethane (20 mL), was added one drop of hydrobromic acid (48% aqueous solution) and one drop of bromine. The solution was stirred at room temperature until the colour faded. Additional bromine (1.02 mL, 20 mmol total including the original drop) was added dropwise over a period of 10 minutes with constant stirring for 1 hour. Subsequently, the solvent was removed *in vacuo* to yield a dark orange oil (or white depending on the isomer).[31] 2'-Bromo-2-fluoropropiophenone (**21**) is an example of the FEC intermediate (Fig. 3-1).

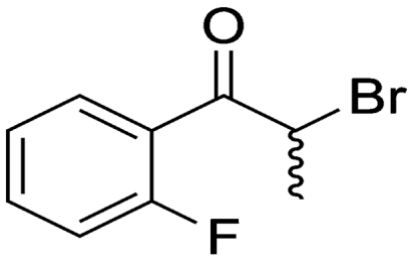

21

Figure 3-1. Structure of 2'-Bromo-2-fluoropropiophenone

3.2.2 Synthesis of X-fluoro-N-ethylcathinone hydrochloride

The 2-bromo-x-fluoropropiophenone (20 mmol) in dichloromethane (40 mL) was reacted with ethylamine solution (2 M in THF, 40 mmol). The mixture was stirred for 30 minutes at room temperature after which time precipitate was formed. The solution was concentrated *in vacuo* and the resultant solid residue was dissolved in hydrochloric acid (6 M, 50-75 mL) and the aqueous

solution was washed with dichloromethane (3 × 50 mL). Then, with stirring, the aqueous acidic solution was basified by slow addition of solid potassium bicarbonate until effervescence stopped forming. The aqueous solution was re-extracted with dichloromethane (3 × 50 mL). The combined organic fractions were dried using magnesium sulfate ($MgSO_4$) and the solvent was removed *in vacuo* to give a viscous yellow oil. The resultant oil was suspended in acetone (4 mL), and hydrochloric acid (4 M) solution in dioxane (5 mL, 20 mmol) and it was stirred at room temperature for 15 minutes. The solvent was removed *in vacuo* and the crude product co-evaporated three times with acetone. The solid was then recrystallised from acetone to give X-fluoro-N-ethylcathinone (X-FEC) hydrochloride as a colourless powder.

2-Fluoro-*N*-ethylcathinone hydrochloride (23): Yield (22%); ^{1}H NMR (D_2O, 400 MHz, 298 K) δ (ppm) **C3** = 7.35 (ddd, $^{3}J_{HH}$ = 8.2 Hz, $^{4}J_{HH}$ = 0.9 Hz, $^{3}J_{HF}$ =11.8 Hz, 1H, Ar-H), **C4** = 7.76 - 7.82 (m, 1H, Ar-H), **C5** = 7.98 (td, $^{3}J_{HH}$ = 7.6 Hz, $^{5}J_{HF}$ = 1.7 Hz, 1H, Ar-H), **C6** = 7.42 (td, $^{3}J_{HH}$ = 8.1 Hz, $^{4}J_{HH}$ = 1.0 Hz, 1H, Ar-H), **C8** = 4.98 (q, $^{3}J_{HH}$ = 7.3 Hz, 1H, CH), **C9** = 3.14-3.30 (m, 2H, CH_2), **C10** = 1.60 (d, $^{3}J_{HH}$ = 7.3 Hz, 3H, CH_3) **C11** = 1.38 (t, $^{3}J_{HH}$ = 7.3 Hz, 3H, CH_3); ^{19}F{^{1}H} NMR (D_2O, 376 MHz, 298 K) δ (ppm) -111.75; ^{13}C {^{1}H} (D_2O, 100 MHz, 298K) δ (ppm) 123.9 (ArC, $^{2}J_{CF}$ = 11.5, C1), 165.8 (ArC, $^{1}J_{CF}$ = 254.3, C2), 120.3 (ArC, $^{2}J_{CF}$ =23.4, C3), 140.3 (ArC, $^{3}J_{CF}$ = 9.9, C4), 133.8 (ArC, C5), 128.1 (ArC, C6), 198.0 (C=O, C7), 63.9 (**CH**CH_3, C8), 44.2 (NH**CH_2**CH_3, C9), 17.2 (CH**CH_3**, C10), 13.6 ($NHCH_2$**CH_3**, C11); MP: 149°C; IR (ATR–FTIR): 3140.00 (NH), 1693.55 (C=O), 1606.81 cm^{-1} (C=C); LC-MS

m/z = 196.1131 (0.01%, $[M+H]^+$); R_f [SiO_2, EtOAc: methanol (25%): aqueous ammonia (0.82. 85:10:5 %v/v) = (0.82)

3-Fluoro-*N*-ethylcathinone hydrochloride (24): Yield (19%); ^{1}H NMR (D_2O, 400 MHz, 298 K) δ (ppm) **C2** = 7.54 (td, $^3J_{HF}$ = 8.2, $^4J_{HH}$ = 2.3 Hz, 1H, Ar-H), **C4** = 7.78 (dt, $^3J_{HF}$ = 9.2, $^4J_{HH}$ = 1.9 Hz, 1H, Ar-H), **C5** = 7.62-7.68 (m, 1H, Ar-H), **C6** = 7.87 (d, $^3J_{HH}$ = 7.8 Hz 1H, Ar-H), **C8** = 5.14 (q, $^3J_{HH}$ = 7.3Hz, 1H, CH), **C9** = 3.29- 3.11 (m, 2H, CH_2), **C10** = 1.63 (d, $^3J_{HH}$ = 7.3 Hz, 3H, CH_3), **C11** = 1.38 (t, $^3J_{HH}$ 7.20 Hz, 3H, CH_3); ^{19}F{^{1}H} NMR (D_2O, 376 MHz, 298 K) δ (ppm) -113.44; ^{13}C {^{1}H} (D_2O, 100 MHz, 298K) δ (ppm) 137.2 ($^3J_{CF}$ = 6.8, d, ArC, C1), 125.1 ($^2J_{CF}$ = 21.5, d, ArC, C2), 165.5 ($^1J_{CF}$ = 247, d, ArC, C3), 118.2 ($^2J_{CF}$ = 22.9, d, ArC, C4), 134.1 ($^3J_{CF}$ = 7.6, d, ArC, C5), 127.9, ($^4J_{CF}$ = 2.2, d, ArC, C6), 199.3 (C=O, C7), 61.0 (**CH**CH_3 , C8), 44.2 (NH**CH_2**CH_3 , C9), 18.3 (CH_2**CH_3** , C10), 13.59 ($NHCH_2$**CH_3** , C11); MP: 196°C; IR (ATR–FTIR): 3050.00 (NH), 1698.37 (C=O), 1491.79 cm^{-1} (C=C); LC-MS m/z = 196.1136 (0.04%, $[M+H]^+$); R_f [SiO_2, EtOAc: methanol (25%): aqueous ammonia (0.82. 85:10:5 %v/v) = (0.71)

4-Fluoro-*N*-ethylcathinone hydrochloride (25): Yield (47%); ^{1}H NMR (D_2O, 400 MHz, 298 K) δ (ppm) **C2/6** = 8.11 (dd, $^3J_{HH}$ = 8.9, $^4J_{HH}$ = 5.3 Hz, 2H, AA′BB′, Ar-H), **C3/5** = 7.35 (t, $^3J_{HH}$ = 8.9, $^3J_{HF}$ = 2.3 Hz, 2H, AA′BB′, Ar-H), **C8** = 5.14 (q, $^3J_{HH}$ = 7.2 Hz, 1H, CH), **C9** = 3.19 (m, 2H, CH_2), C10 = 1.61 (d, $^3J_{HH}$ = 7.3 Hz, 3H, CH_3), **C11**= 1.36 (t, $^3J_{HH}$ = 7.3 Hz, 3H, CH_3); ^{19}F{^{1}H} NMR (D_2O, 376 MHz, 298 K) δ (ppm) -105.42; ^{13}C {^{1}H} (D_2O, 100 MHz, 298K) δ (ppm) 131.7 (ArC, C1), 134.9 (d, $^3J_{CF}$= 10.3, ArC, C2/6), 119.3

(d, $^{2}J_{CF}$= 22.2, ArC, C3/5), 169.6 (d, $^{1}J_{CF}$ = 255, ArC, C4), 198.9 (C=O, C7), 60.8 (**CH**CH_3 , C8), 44.2 (NH**CH_2**CH_3 , C9), 18.4 (CH_2**CH_3** , C10), 13.6 (NHCH_2**CH_3** , C11); MP: 256°C; IR (ATR–FTIR): 3170 (NH), 1684.97 (C=O), 1595.26 cm^{-1} (C=C); LC-MS m/z = 196.1131 (0.01%, $[M+H]^{+}$); R_f [SiO_2, EtOAc: methanol (25%): aqueous ammonia (0.82. 85:10:5 %v/v) = (0.66)

3.2.3 Reduced FEC synthesis (where X is 2,3 or 4)

X-FEC.HCl (1.600 g, 2.8 mM) was dissolved in 30 mL of anhydrous methanol and cooled in an ice-water bath; Sodium borohydride (2.65 g, 70 mM) was added slowly portion wise. Once no further effervescence was observed, the mixture was stirred for 24 hours under nitrogen. The reaction mixture was then concentrated *in vacuo* prior to dissolving in deionised water (100 mL). This aqueous solution was then extracted with DCM (3 x 75 mL). The organic fractions were combined, dried with magnesium sulphate ($MgSO_4$), filtered and washed with DCM (2 x 20 mL). The filtrate was then concentrated *in vacuo* to give a viscous yellow oil. The resultant oil was suspended in ethyl acetate (4 mL), and hydrochloric acid (4 M) solution in dioxane (2.2 mL, 20 mmol) and it was stirred at room temperature for 30 minutes. The solvents were removed *in vacuo* and triturated with acetone (3 x 20 mL), to produce an off-white powder, which was then filtrated and dried to give the final product.

2-(ethylamino)-1-(2-fluorophenyl)propan-1-ol hydrochloride (Reduced 2-FEC, 26): Yield (64%); ^{1}H NMR (D_2O, 400 MHz, 298 K) δ (ppm) **C3** = 7.19 (dd, $^{3}J_{HH}$ = 8.3 Hz, $^{3}J_{HF}$ = 11.0 Hz, 1H, Ar-H), **C4** = 7.44(m, 1H, Ar-H), **C5** =

7.57 (t, $^{3}J_{HH}$ = 7.7 Hz, 1H, Ar-H), **C6**= 7.31 (t, $^{3}J_{HH}$ = 7.5 Hz, 1H, Ar-H), **C7** = 5.45 (d, $^{3}J_{HH}$ = 3.1 Hz, 1H, CH), **C8** = 3.69 (d, $^{3}J_{HH}$ = 9.0 Hz, $^{3}J_{HH}$ = 6.0 Hz, 1H, CH), **C9** = 3.17 (m, $^{3}J_{HH}$ = 6.8, 6.3 Hz, 2H, CH_2), **C11** = 1.37 (t, $^{3}J_{HH}$ = 7.2 Hz, 3H, CH_3) **C10** = 1.15 (d, $^{3}J_{HH}$ = 6.8 Hz, 3H, CH_3); $^{19}F\{^{1}H\}$ NMR (D_2O, 376 MHz, 298 K) δ (ppm) -110.57; $^{13}C\ \{^{1}H\}$ (D_2O, 100 MHz, 298K) δ (ppm) 126.0 (d, $^{2}J_{CF}$ = 13.2 Hz, ArC, C1), 159.2 (d, $^{1}J_{CF}$ = 244 Hz, ArC, C2), 115.4 (d, $^{2}J_{CF}$ = 21.6 Hz, ArC, C3), 130.23 (d, $^{3}J_{CF}$ = 8.7 Hz, ArC, C4), 127.7 (d, $^{4}J_{CF}$ = 3.9 Hz, ArC, C5), 124.7 (d, $^{5}J_{CF}$ = 8.7 Hz, ArC, C6), 66.1 (C-O, C7), 56.7 (**CH**CH_3 , C8), 40.8 (NH**CH_2**CH_3 , C9), 9.6 (CH_2**CH_3** , C10), 10.5 (NHCH_2**CH_3** , C11); MP: 223-228°C; IR (ATR–FTIR): 1577.41 (N-H), 1107.35 (C-O), 3297.82 (O-H), 1482.05 cm^{-1} (C=C); LC-MS m/z = 198.1288 (0.01%, $[M+H]^{+}$); R_f [SiO_2, EtOAc: methanol (25%): aqueous ammonia (0.82. 85:10:5 %v/v) = (0.41).

2-(ethylamino)-1-(3-fluorophenyl)propan-1-ol hydrochloride (Reduced 3-FEC, 27): Yield (31%); ^{1}H NMR (D_2O, 400 MHz, 298 K) δ (ppm) **C5** = 7.14 (td, $^{3}J_{HF}$ = 8.7 Hz, $^{4}J_{HH}$ = 8.1 Hz, $^{5}J_{HH}$ 2.5 Hz, 1H, Ar-H), **C4** = 7.19 (t, $^{4}J_{HH}$ = 2.1 Hz, 1H, Ar-H), **C2** = 7.47 (td, $^{3}J_{HH}$ = 8.2, 6.0 Hz, 1H, Ar-H), **C6** = 7.22 (m, 1H, Ar-H), **C7** = 5.20 (d, $^{3}J_{HH}$ = 3.2 Hz, 1H, CH), **C8** = 3.65 (qd, $^{3}J_{HH}$ = 6.9 Hz, $^{4}J_{HH}$ = 3.2 Hz, 1H, CH), **C9** = 3.24 (m, 2H, CH_2), **C11** = 1.35 (t, $^{3}J_{HH}$ 7.3 Hz, 3H, CH_3), **C10** = 1.12 (d, $^{3}J_{HH}$ 6.9 Hz, 3H, CH_3); $^{19}F\{^{1}H\}$ NMR (D_2O, 376 MHz, 298 K) δ (ppm) -114.04; $^{13}C\ \{^{1}H\}$ (D_2O, 100 MHz, 298K) δ (ppm) 141.6 (d, $^{3}J_{CF}$ = 6.9 Hz, ArC, C1), 130.6 (d, $^{2}J_{CF}$ = 21.4 Hz, ArC, C2), 164.04 (d, $^{1}J_{CF}$ = 244 Hz, ArC, C3), 121.72 (d, $^{2}J_{CF}$ = 22.9 Hz, ArC, C4), 114.99 (d,

$^{3}J_{CF}$ = 8.3 Hz, ArC, C5), 112.89 (d, $^{4}J_{CF}$ = 8.3 Hz, ArC, C6), 70.65 (**C-O**, C7), 57.91 (**CH**CH_3 , C8), 40.70 (NH**CH_2**CH_3 , C9), 9.6 (CH_2**CH_3** , C10), 10.5 (NHCH_2**CH_3** , C11); MP: 229-233°C; IR (ATR–FTIR): 1612.79 (N-H), 1099.92 (C-O), 3332.51 (O-H), 1590.13 cm^{-1} (C=C); LC-MS m/z = 198.1287 (0.02%, $[M+H]^{+}$); R_f [SiO_2, EtOAc: methanol (25%): aqueous ammonia (0.82. 85:10:5 %v/v)= (0.33).

2-(ethylamino)-1-(4-fluorophenyl)propan-1-ol hydrochloride (Reduced 4-FEC, 28): Yield (49%); ^{1}H NMR (D_2O, 400 MHz, 298 K) δ (ppm) **C2/6** = 7.43 (ddt, $^{3}J_{HH}$ = 7.1, $^{4}J_{HH}$ = 5.0 Hz, $^{4}J_{HF}$ = 2.3 Hz, 2H, AA′BB′, Ar-H), **C3/5** = 7.21 (t, $^{4}J_{HH}$ = 7.1, $^{3}J_{HF}$ 2.3 = Hz, 2H, AA′BB′, Ar-H), **C7** = 5.17 (d, $^{3}J_{HH}$ = 3.3 Hz, 1H, CH), **C8** = 3.62 (dt, $^{4}J_{HH}$ = 6.4, 3.0 Hz, 1H, CH), **C9** = 3.23 (m, 2H, CH_2), **C11** = 1.34 (t, $^{3}J_{HH}$ = 7.2 Hz, $^{4}J_{HH}$ = 2.4, 3H, CH_3) **C10** = 1.14 (d, $^{3}J_{HH}$ = 6.8 Hz, $^{4}J_{HH}$ = 2.5, 3H, CH_3); $^{19}F\{^{1}H\}$ NMR (D_2O, 376 MHz, 298 K) δ (ppm) -115.78; $^{13}C\ \{^{1}H\}$ (D_2O, 100 MHz, 298K) δ (ppm) 134.6 (d, $^{4}J_{CF}$ = 1.9 Hz, ArC, C1), 127.9 (d, $^{3}J_{CF}$ = 8.5 Hz, ArC, C2/6), 115.5 (d, $^{2}J_{CF}$ = 21.5 Hz, ArC, C3/5), 163.6 (d, $^{1}J_{CF}$ = 244 Hz, ArC, C4), 70.87 (C-O, C7), 58.0 (**CH**CH_3 , C8), 40.7 (NH**CH_2**CH_3 , C9), 10.52 (CH_2**CH_3** , C10), 9.7 (NHCH_2**CH_3** , C11); MP: 236-241°C; IR (ATR–FTIR): 1604.93 (N-H), 1101.57 (C-O), 3351.11 (O-H), 1570.97 cm^{-1} (C=C); LC-MS m/z = 198.1291 (0.02%, $[M+H]^{+}$); R_f [SiO_2, EtOAc: methanol (25%): aqueous ammonia (0.82. 85:10:5 %v/v) = (0.26).

3.3 GC-MS Temperature Programming

The temperature programme was optimised so that the closely eluting, and almost baseline-separated derivatives are baseline resolved. 1 mL of the sample was injected into the column, with an oven temperature of 100-150°C ramped at a rate of 10 °C/min and then it was ramped up to 170˚C at a rate of 2 ˚C/min and followed by a temperature hold at 300 °C at a gradient rate of 100˚C/min for 2 minutes. This temperature setting is demonstrated in table 3-1.

Table 3-1. GC-MS Temperature setting

GC-MS Temperature setting		
Temperature (˚C)	Rate (˚C/min)	Hold Time (min)
100-150	10	0
150-170	2	0
170-300	100	2

3.3.1 Sample preparation for GC–MS analysis

Samples were prepared for GC–MS analysis by dissolving approximately 5–10 mg of the hydrochloride salt of each isomer in 1 mL methanol containing eicosane as a standard in a ratio of 1 mg mL^{-1}.

3.3.2 Derivitisation of samples

N-Acetylation was achieved by sequential addition of five drops of acetyl chloride and five drops of triethylamine to 5-10 mg of each isomer of

hydrochloride salt of FEC.[32] The reaction mixture was stirred for five minutes to allow complete consumption of the amine. 1 mL of this solution was then diluted with 2:1 methanol containing 1 mg mL^{-1} eicosane as an internal standard. The solutions were further diluted with methanol in a ratio of 0.5:1.5 in order to obtain maximum baseline separation. The mixture was injected directly into the GC–MS equipment.

3.4 Thin Layer Chromatography

The mobile phase was prepared using a ratio of 85:10:5 %v/v of ethyl acetate, methanol (25%) and aqueous ammonia (density of 0.880 g/cm^3). The plates were cut 10x10 cm; they were spotted accordingly and left in the mobile phase to develop over 30 minutes. Once the plates were developed they were viewed under UV light (254 nm) and the colour of the spots (if any) revealed were noted. The plates were then dipped into the pre-prepared ninhydrin solution and placed into an oven at 80°C until all spots were formed (~40 min). Once removed from the oven, the R_f value was calculated for each sample. Six repetitive tests of all compounds were conducted, and FMC negative control samples were used in all tests. All three FEC (**18**) and FMC (**19**) samples were run on the same plate in each case. The colours of the TLC spots were spotted to be dark pink on all the FEC and FMC samples. R_f values were recorded and %RSD was calculated.

The same mobile phase was used for running each of the reduced FEC compounds with the FECs (six replicates again). They were then visualised

under UV light (254 nm) but they did not show any response at this wavelength. Therefore, they were dipped into ninhydrin solution and left in an oven at 80°C for 40 minutes in order to visualise the components. R_f values were recorded and %RSD was calculated.

3.5 Presumptive tests

Presumptive tests were performed according to the United Nations recommended guidelines.[32] Solutions of 10 mg of each sample and 1 mL water were prepared, 1–2 drops were placed into a dimple well of a spotting tile, along with a reference blank of only water. Then the colour test reagent (1–2 drops) was added. The same procedure was repeated on the compounds as powders. Any immediate colour change, as well as the effect after 20 minutes were noted. The preparation of the reagents is described below: [33]

Zimmerman's Test: Reagent 1: 1% solution 1,3-dinitrobenzene in methanol (10 mL), Reagent 2: 15% aqueous potassium hydroxide solution (10 mL)

Chen Ko Test: Reagent 1: 10% v/v aqueous acetic acid (10 mL), Reagent 2: 1% aqueous copper (II) sulphate solution (10mL), Reagent 3: 8% aqueous sodium hydroxide solution (10mL)

Robadope Test: Reagent 1: 2% aqueous sodium carbonate solution (10 mL), Reagent 2:1% aqueous sodium nitroprusside solution (10 mL), Reagent 3: 50% ethanolic acetone solution (10 mL)

Liebermann's Test: 10% w/v sodium nitrile in sulphuric acid (10 mL)

Marquis test: Reagent 1: 1% formaldehyde (37% aqueous solution), Reagent 2: Concentrated sulphuric acid (10 mL, d = 1.86 g/cm^3)

Mandelin test: Reagent 1: 1% ammonium metavanadate, Reagent 2: Concentrated sulphuric acid (10 mL, d = 1.86)

Simon's test: Reagent 1: 2% aqueous sodium carbonate solution (10 mL), Reagent 2: 1% aqueous sodium nitroprusside solution (10 mL), Reagent 3: 50% ethanolic acetaldehyde solution (10 mL).

Scott's test: Reagent 1: 2% thiocyanate solution, glycerol, glacial acetic acid (5 drops); Reagent 2: hydrochloric acid (Until precipitate disappears); Reagent 3: chloroform (10 drops)

Chapter 4 Results and discussion of FEC isomers

4.1 Nuclear Magnetic Resonance (NMR) results of fluoroethcathinone

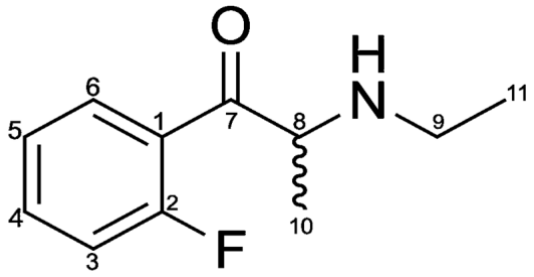

23

Figure 4-1. Chemical structure of 2-FEC (**23**)

The structure of all the FEC isomers were characterised using high field NMR and the results were compared with that of FMC reported in the paper by Khreit *et al* in order to verify the results obtained.[30] The structure of 2-FEC (**23**), shown in Fig. 4-1, possesses eight unique ^{1}H NMR environments and this is reflected in the ^{1}H NMR spectrum. The ^{1}H NMR spectrum of **23** is shown in Fig. 4-2. The presence of J_{HF} coupling in the aromatic ring enables the position of the ^{1}H nuclei to be located. For example, the proton located on carbon 3 possesses $^{3}J_{HF}$ of 11.8 Hz and $^{3}J_{HH}$ and $^{4}J_{HH}$ coupling of 8.2 and 0.9 Hz respectively, therefore the peak appears as a doublet of doublet of doublets. In the ^{1}H-^{1}H COSY spectrum a single cross-peak is observed which is due to the $^{3}J_{HH}$ coupling to the proton on carbon 4 (Fig. 4-3). The proton located on position 5 possesses a $^{5}J_{HF}$ coupling of 1.7 Hz in addition to a $^{3}J_{HH}$ coupling of 7.6 Hz to both protons located on carbons 4 and 6. This is why this peak appears with the multiplicity of a triplet of

doublets. The $^{3}J_{HH}$ coupling from the proton located on position 5 to the one located on position 4 ($^{3}J_{HH}$ coupling of 7.6 Hz) is reflected in the observation of a cross-peak in the ^{1}H-^{1}H COSY spectrum (Fig. 4-3). Furthermore, the second cross peak is not visible in the spectrum due to being weak. Moreover, the proton located on carbon 6 also appears at 7.42 with a triplet of doublets, therefore it consists of two *J*-couplings of $^{3}J_{HH}$ 8.1 Hz and coupling of $^{4}J_{HH}$ 1.0 Hz. The observations are presented in a cross peak in the ^{1}H-^{1}H COSY spectrum (Fig. 4-3).

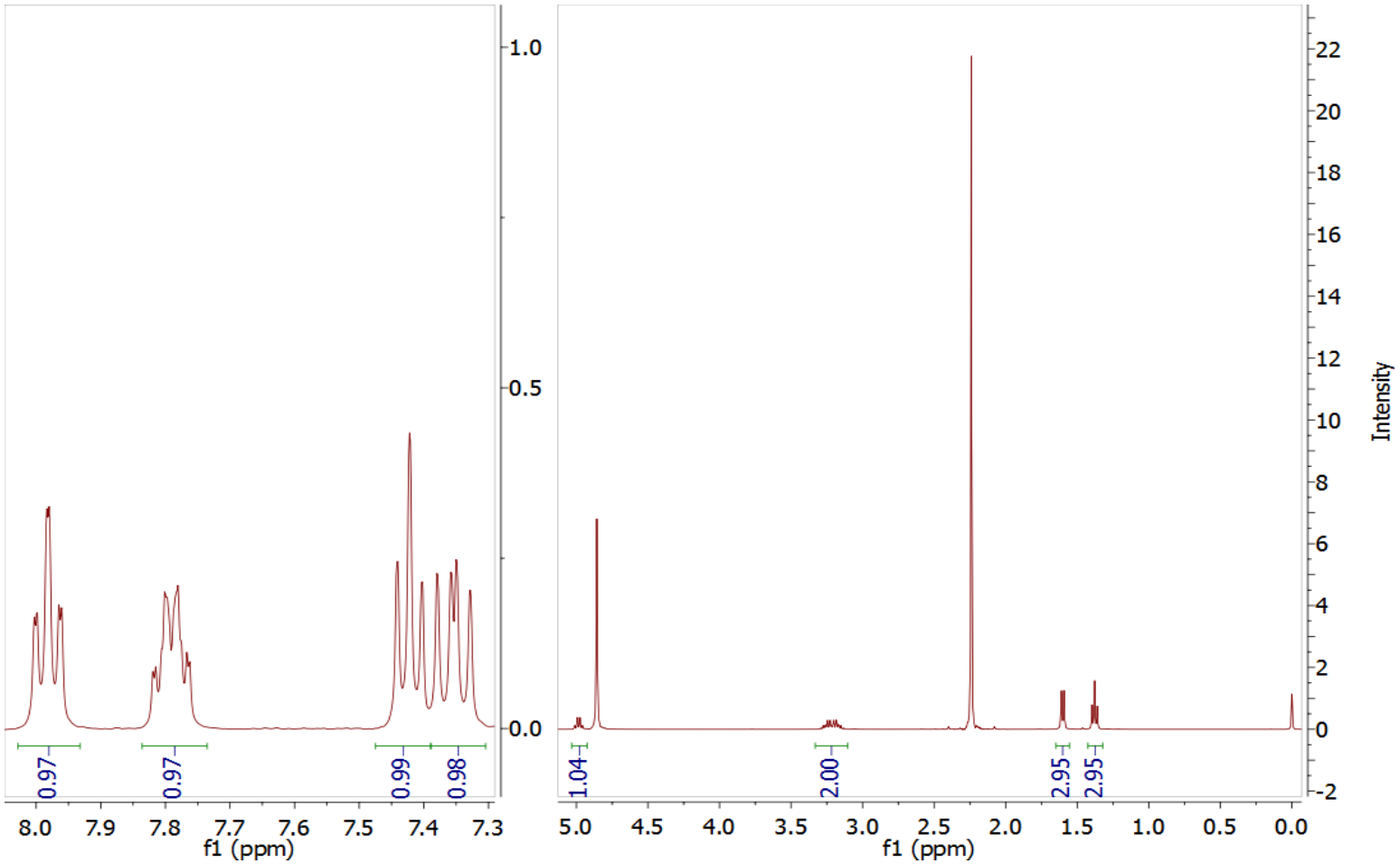

Figure 4-2. ^{1}H NMR spectrum of **23** collected in D_2O

A chiral centre is located at position 8 in **23**. This peak presents itself as a quartet with a $^{3}J_{HH}$ coupling of 7.3 Hz. This coupling is reciprocated by the methyl group protons, which are bound to this position. Furthermore, a cross peak links the chiral hydrogen to the methyl protons in the ^{1}H-^{1}H COSY NMR spectrum.

The methyl group of the ethyl moiety is located at δ 1.38. This is a triplet because it couples only with the 2 protons of the CH_2 group adjacent to it, and therefore, it possesses a $^{3}J_{HH}$ coupling of 7.3 Hz. Conversely, the CH_2 group presents as a multiplet. This is due to the proximity of the chiral centre, which these protons have a weak interaction with, and the methyl group. Again, a cross peak is seen for the interaction between the CH_2 and CH_3 protons in the ^{1}H-^{1}H COSY (Fig. 4-3). However, the cross-peak for the CH_2 protons and that of the chiral proton is not manifest in the ^{1}H-^{1}H COSY NMR spectrum, due to long range coupling.

The proton of the amine is not observed in the ^{1}H NMR spectrum. This is believed to be due to rapid exchange of hydrogen with that of the deuterated solvent (D_2O).

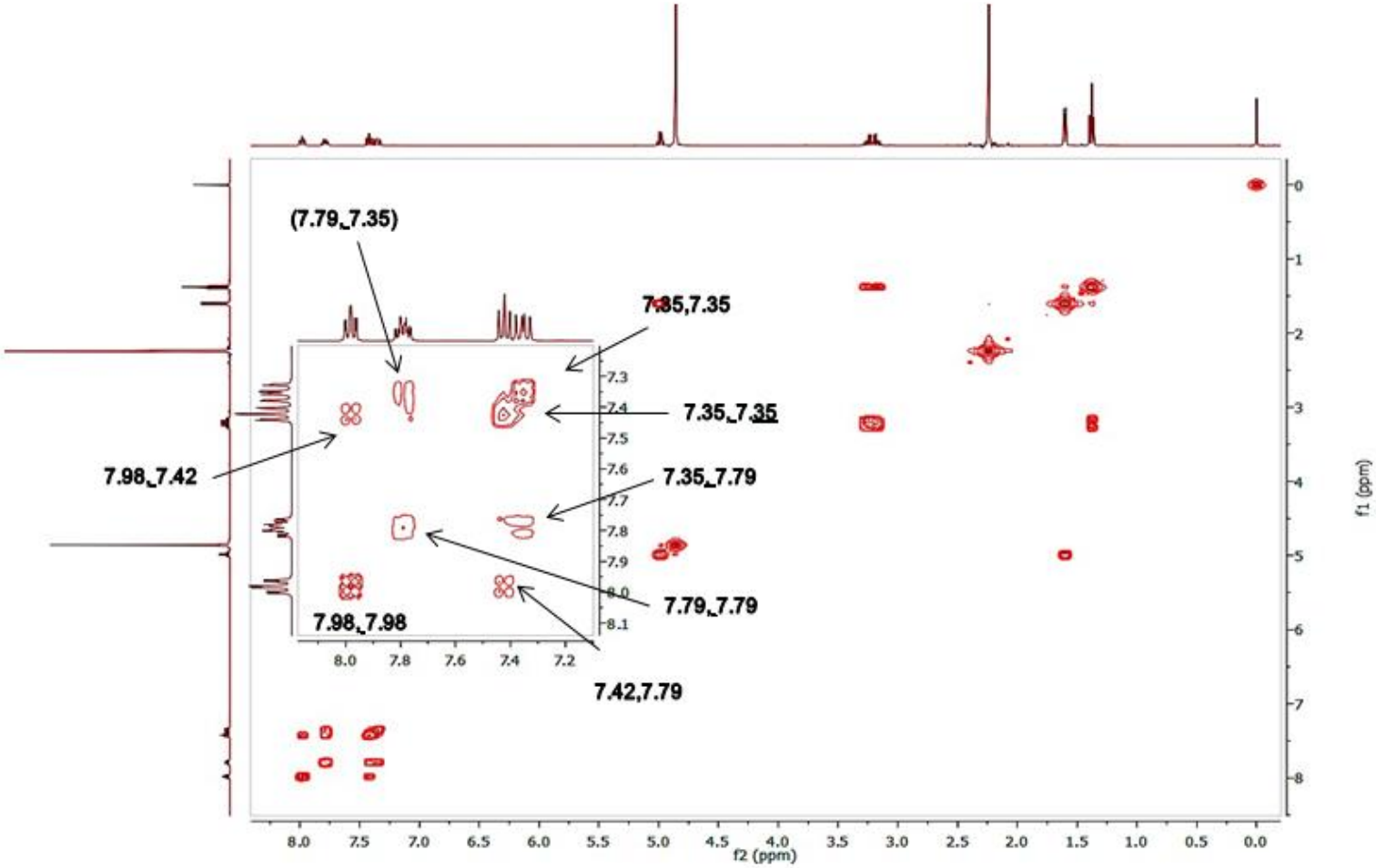

Figure 4-3. ^{1}H-^{1}H COSY NMR spectrum of **23** collected in D_2O

The $^{13}C\{^{1}H\}$ NMR spectrum of **23** (Fig. 4-4) reveals that 11 unique carbon environments exist. When the $^{13}C\{^{1}H\}$ DEPT-135 was collected, this simplified to eight environments. The carbonyl (δ 198.0) is not observed as well as the quaternary carbon of the aromatic ring (δ 123.9) in the $^{13}C\{^{1}H\}$ DEPT-135 spectrum (Fig. 4-5). Furthermore, the carbon located in the aromatic ring that possesses a one bond coupling to ^{19}F (carbon 2) is not observed, in the $^{13}C\{^{1}H\}$ DEPT-135, because the carbon centre is effectively "quaternary". The carbon located at position 5 is *para* to the fluorine substituted carbon (C2). Consequently, it appears as a singlet and does not possess a *J*-coupling constant. Moreover, carbon 6 possesses $^{4}J_{CF}$ coupling of 2.9 Hz.

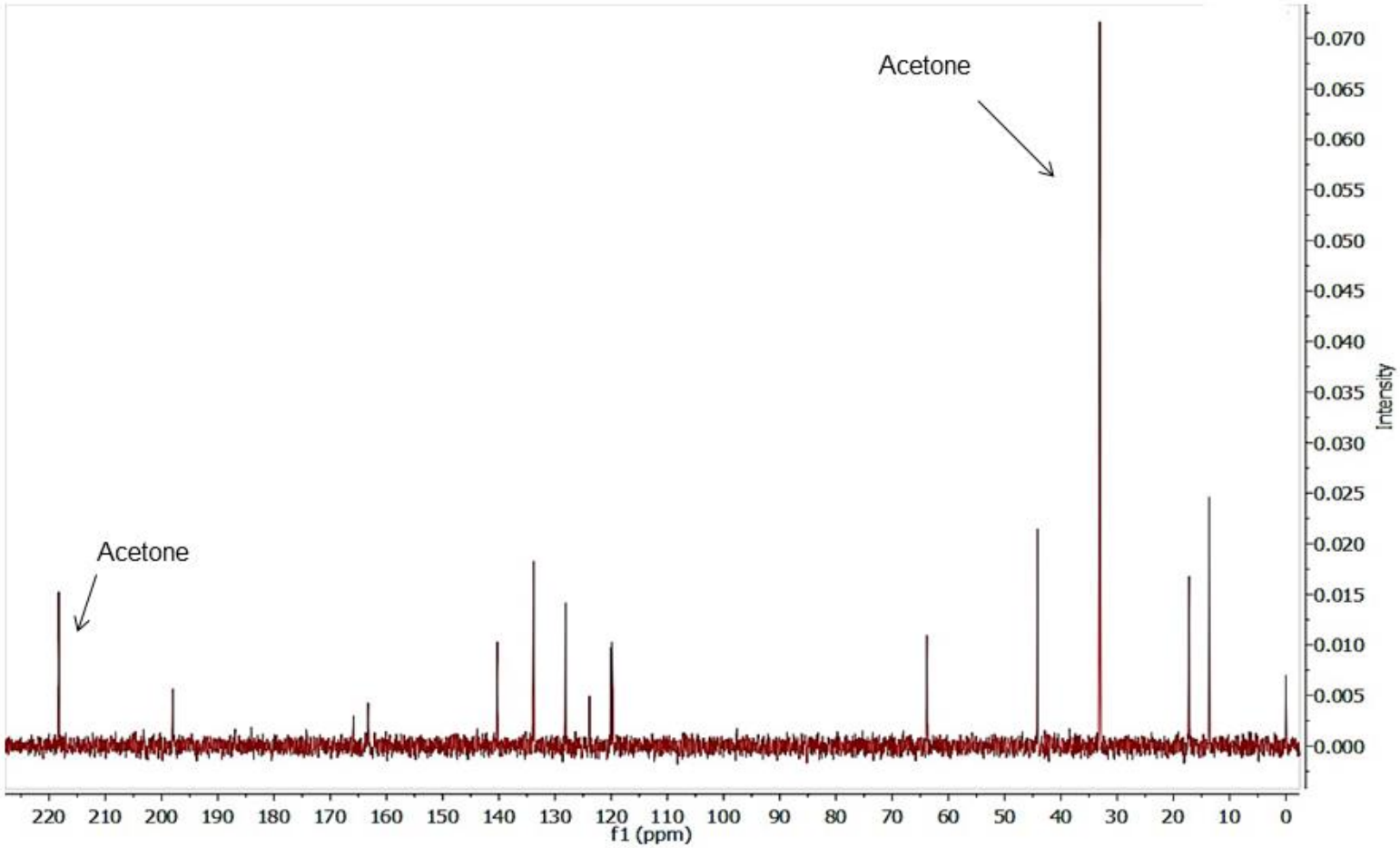

Figure 4-4. $^{13}C\{^{1}H\}$ NMR spectrum of **23** collected in D_2O

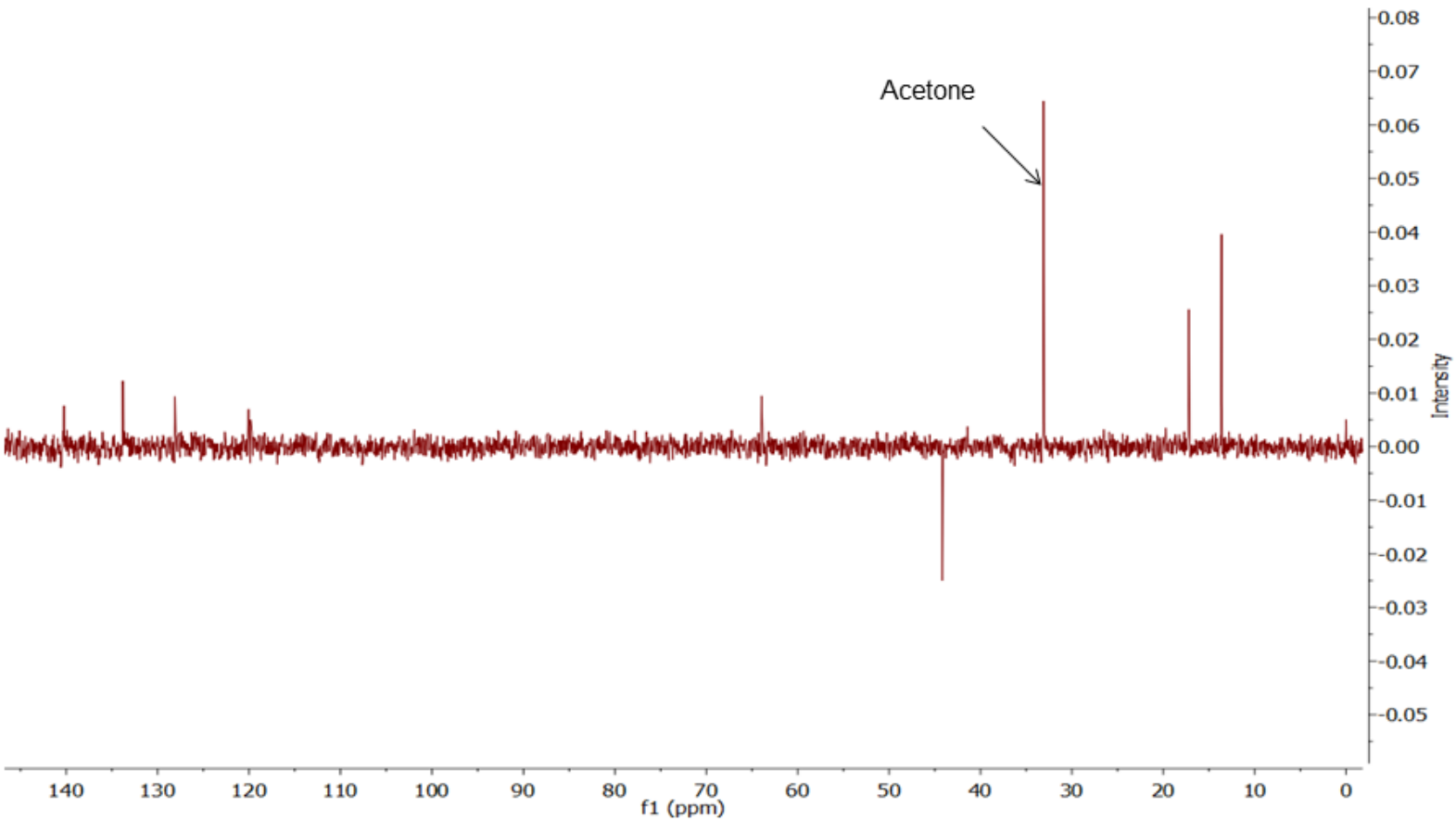

Figure 4-5. $^{13}C\{^{1}H\}$ DEPT-135 NMR spectrum of **23** collected in D_2O

The HMQC spectrum of **23** was used to connect the ^{1}H environments identified from the ^{1}H NMR spectrum to those of the ^{13}C domain. From the HMQC spectrum, it is seen that the proton located at position 3 (δ 7.35) is connected to the carbon at δ 120.3. Also, the chiral centre carbon at δ 63.9 links to one hydrogen in the ^{1}H domain at δ 4.98. The spectrum is shown in Fig. 4-6 and the results tabulated in table 4-1.

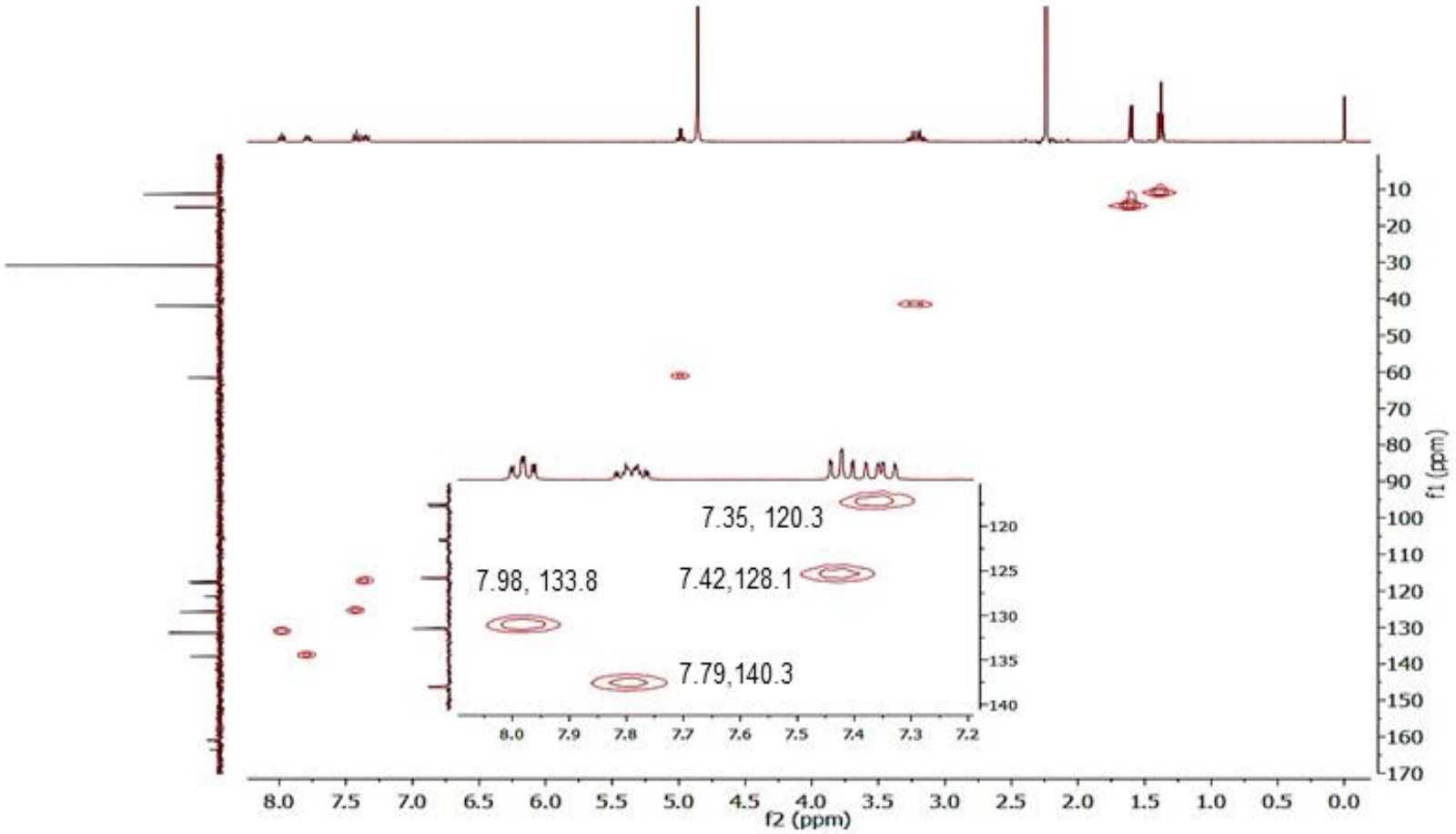

Figure 4-6. ^{1}H-^{13}C HMQC NMR spectrum of **23** collected in D_2O

The HMBC spectra were utilised to identify the two quaternary carbons due to their $^{2}J_{CH}$ interactions with proton nuclei in their local vicinity (Fig. 4-7). This spectrum confirms that the peaks at δ 123.9 and 198.0 correspond to positions 1 and 7 respectively.

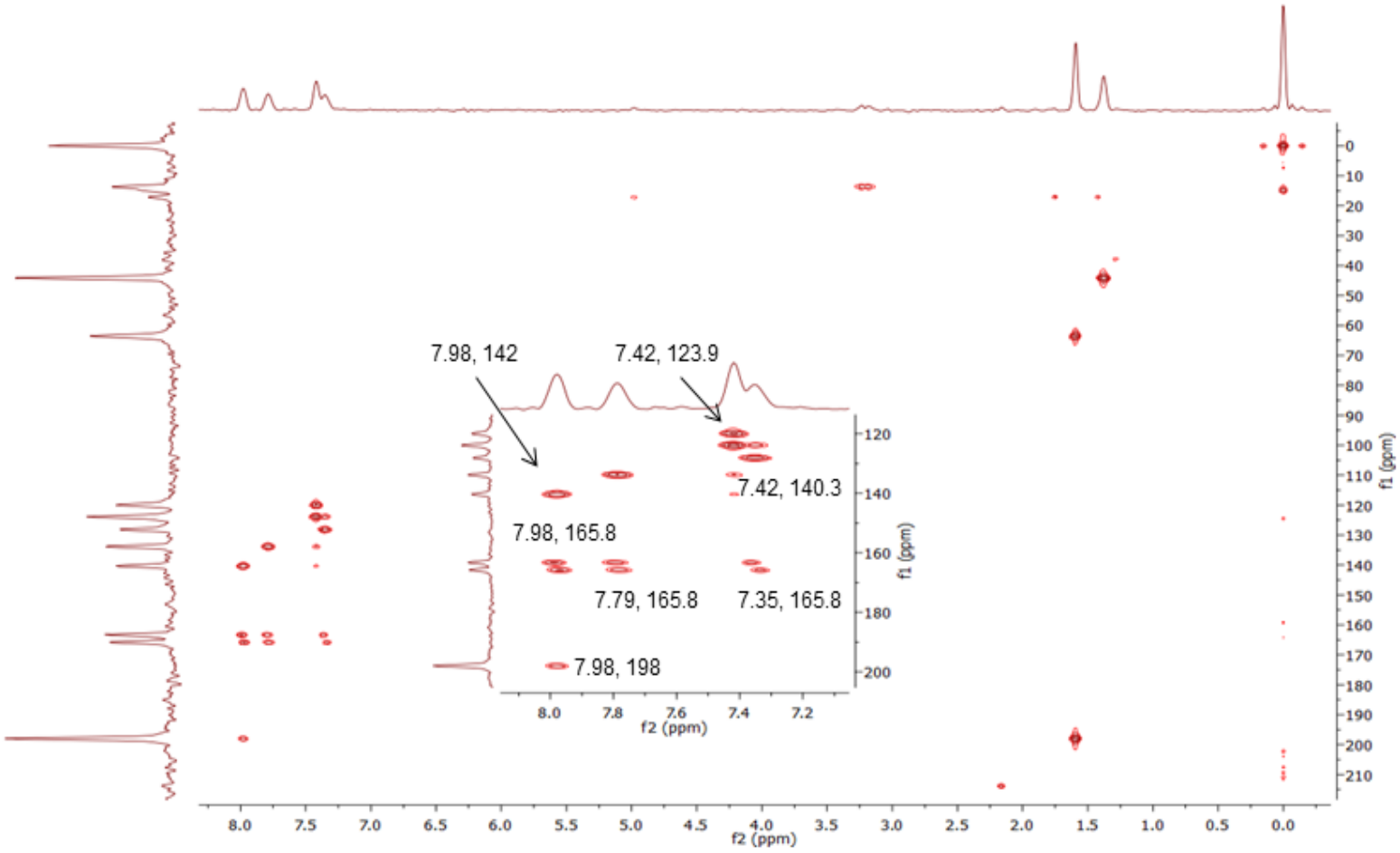

Figure 4-7. ^{1}H-^{13}C HMBC NMR spectrum of **23** collected in D_2O

23 possesses a single ^{19}F nucleus. The $^{19}F\{^{1}H\}$ NMR spectrum (Fig. 4-8) of **23** reveals a single peak thus confirming only one environment is present. In this spectrum, the peak located at δ -76.55 is TFA, which is used as an internal standard.

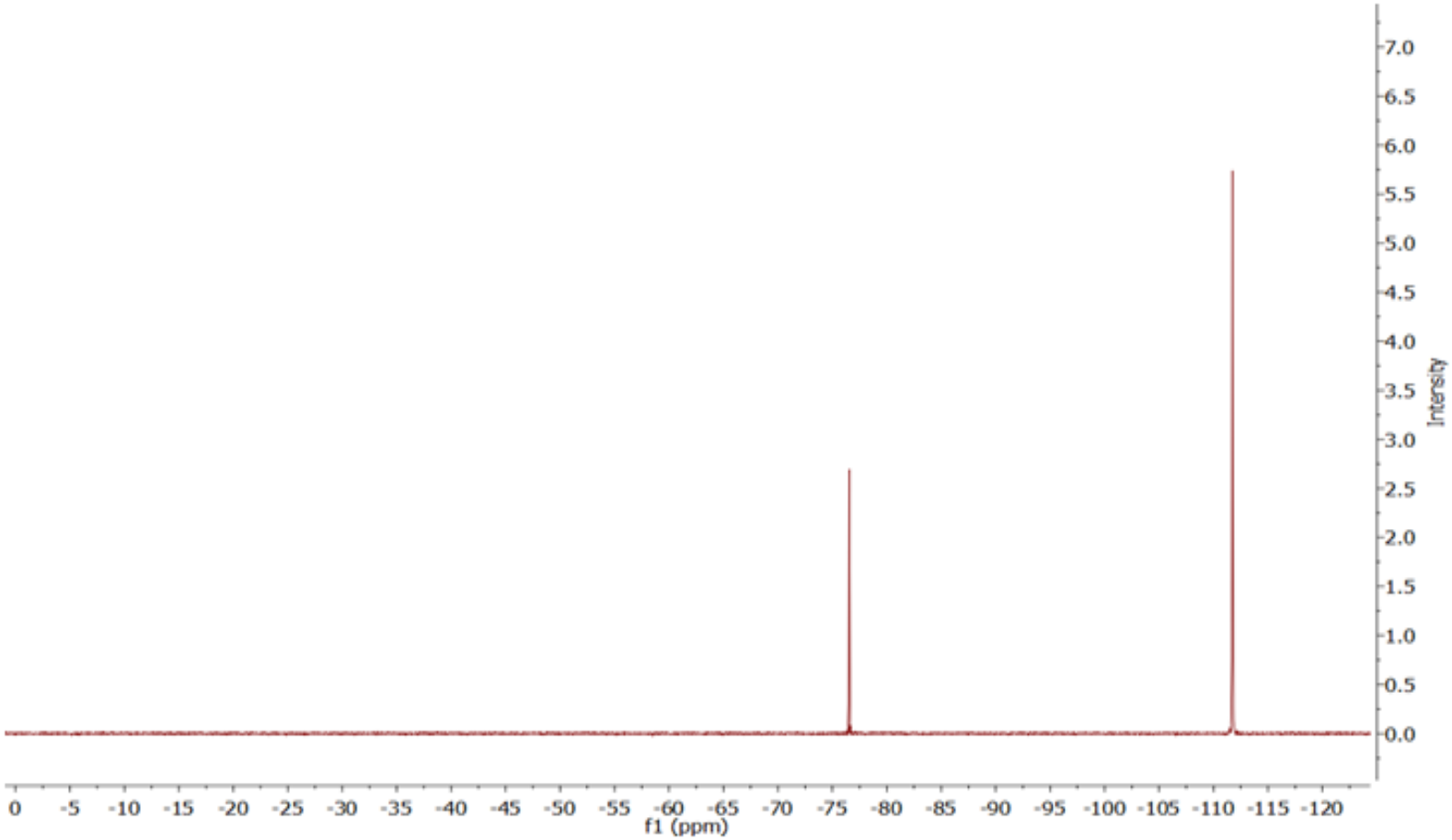

Figure 4-8.$^{19}F\{^{1}H\}$ NMR spectrum of **23** collected in D_2O. The peak at $\delta^{19}F$ -76.55 is TFA

Table 4-1. NMR results for **23**

2-FEC (23) NMR Results

C number	No. Of Hs	^{1}H NMR: δ / ppm, *J*-coupling (Hz)	^{13}C{^{1}H} NMR: δ / ppm, *J*-coupling (Hz)	^{19}F{^{1}H} NMR: δ / ppm
1	**0**	-	123.9, d, $^{2}J_{CF}$=11.5	
2	**0**	-	165.8, d, $^{1}J_{CF}$=254.3	-111.75, s
3	**1**	7.35, ddd, $^{3}J_{HH}$ = 8.2 Hz, $^{4}J_{HH}$ = 0.9 Hz, $^{3}J_{HF}$ = 11.8	120.3, d, $^{2}J_{CF}$=23.4	
4	**1**	7.76-7.82, m	140.3, d, $^{3}J_{CF}$=9.9	
5	**1**	7.98, td, $^{3}J_{HH}$ = 7.6 Hz, $^{5}J_{HF}$ = 1.7 Hz,	133.8, s	
6	**1**	7.42, td, $^{3}J_{HH}$ = 8.1 Hz, $^{4}J_{HH}$ = 1.0 Hz	128.1, s, $^{4}J_{CF}$=2.9	
7	**0**	-	198.0, s	
8	**1**	4.98, q, $^{3}J_{HH}$ = 7.3 Hz	63.9, s	
9	**2**	3.14-3.30, m	44.2, s	
10	**3**	1.60, d, $^{3}J_{HH}$ = 7.3 Hz	17.2, s	
11	**3**	1.38, t, $^{3}J_{HH}$ = 7.3 Hz	13.6,s	
Acetone		2.05 (CH_3)	31.0 (CH_3), 215.0 (C=O)	

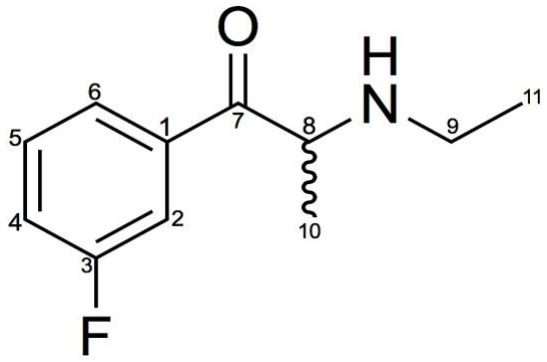

24

Figure 4-9.Chemical Structure of 3-FEC (24)

The ^{1}H NMR spectrum of 3-FEC (**24**) is shown in Fig. 4-9. **24** has the same number of chemical environments as **23**. Similar to **23**, **24** possesses similar chemical shifts in the side chain containing the chiral centre. In both isomers, the chiral centre sited at position 8 occurs as a quartet with a $^{3}J_{HH}$ coupling of ~7.3 Hz. This coupling is due to the presence of the methyl group located at the chiral centre. This methyl group is found at δ 1.63 for **24** and appears as a doublet due to the presence of one neighbouring proton on the chiral centre. Moreover, a cross peak is detected in the ^{1}H-^{1}H COSY NMR spectra of **23** and **24** (Fig. 4-11 and 4-19). The ^{1}H NMR spectrum of the rest of the chain (ethyl) in **24** is the same as **23** and they have identical cross peaks in the ^{1}H-^{1}H COSY NMR spectrum for this moiety.

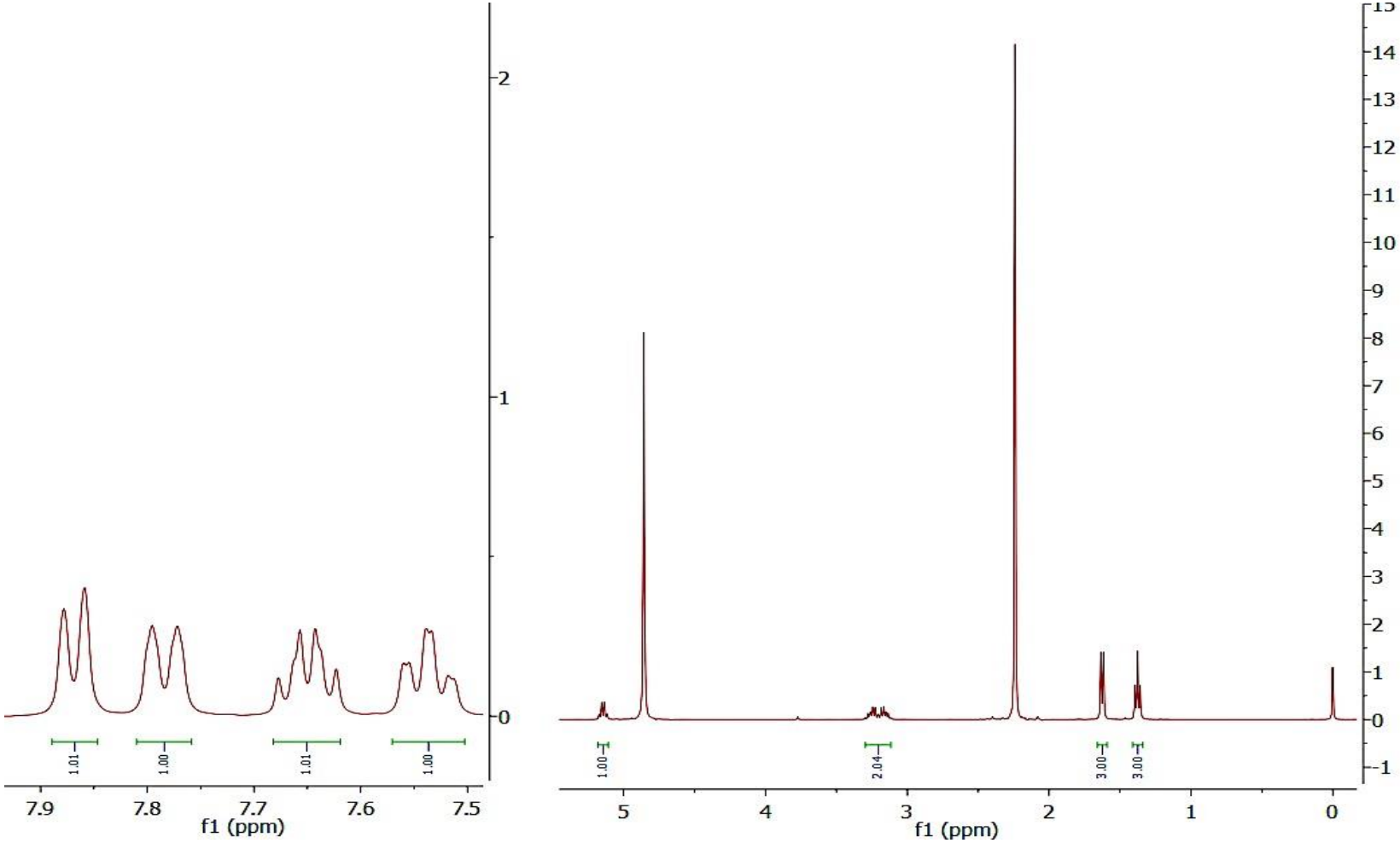

Figure 4-10. ^{1}H NMR spectrum of **24** collected in D_2O

The aromatic region of the ^{1}H NMR spectrum (Fig. 4-10) of **24** also contains four proton environments. However, due to the presence of the fluorine at the *meta* position, the chemical shifts are more down-field than the corresponding signals in **23**. Again, the location of the ^{1}H nuclei can be detected using J_{HF} coupling in the aromatic ring. For instance, the proton located on position 2 appears as a triplet of doublets and has a $^{3}J_{HF}$ coupling of 8.2 Hz and a much weaker $^{4}J_{HH}$ coupling of 2.3 Hz.

Moreover, the proton located on position 4 has a $^{3}J_{HF}$ coupling of 9.2 Hz in addition to a $^{3}J_{HH}$ coupling of 1.9 Hz and as a result this signal is present with the multiplicity of a doublet of triplets, the J_{HH} couplings to C6 and C2 are not detected due to being too small. The observation of a cross peak in the ^{1}H-^{1}H COSY spectrum illustrates the $^{3}J_{HH}$ coupling from the proton positioned on C4 to the one sited on C5 (Fig. 4-11).

Additionally, the proton located at position 6, also appears as a doublet since it's adjacent to the quaternary carbon and has a $^{3}J_{HH}$ coupling of 7.8 Hz. This interaction between the protons on carbons 5 and 6 is also observed as a cross peak in the ^{1}H-^{1}H COSY spectrum. Additionally, J_{HF} coupling is not observed because it's too small.

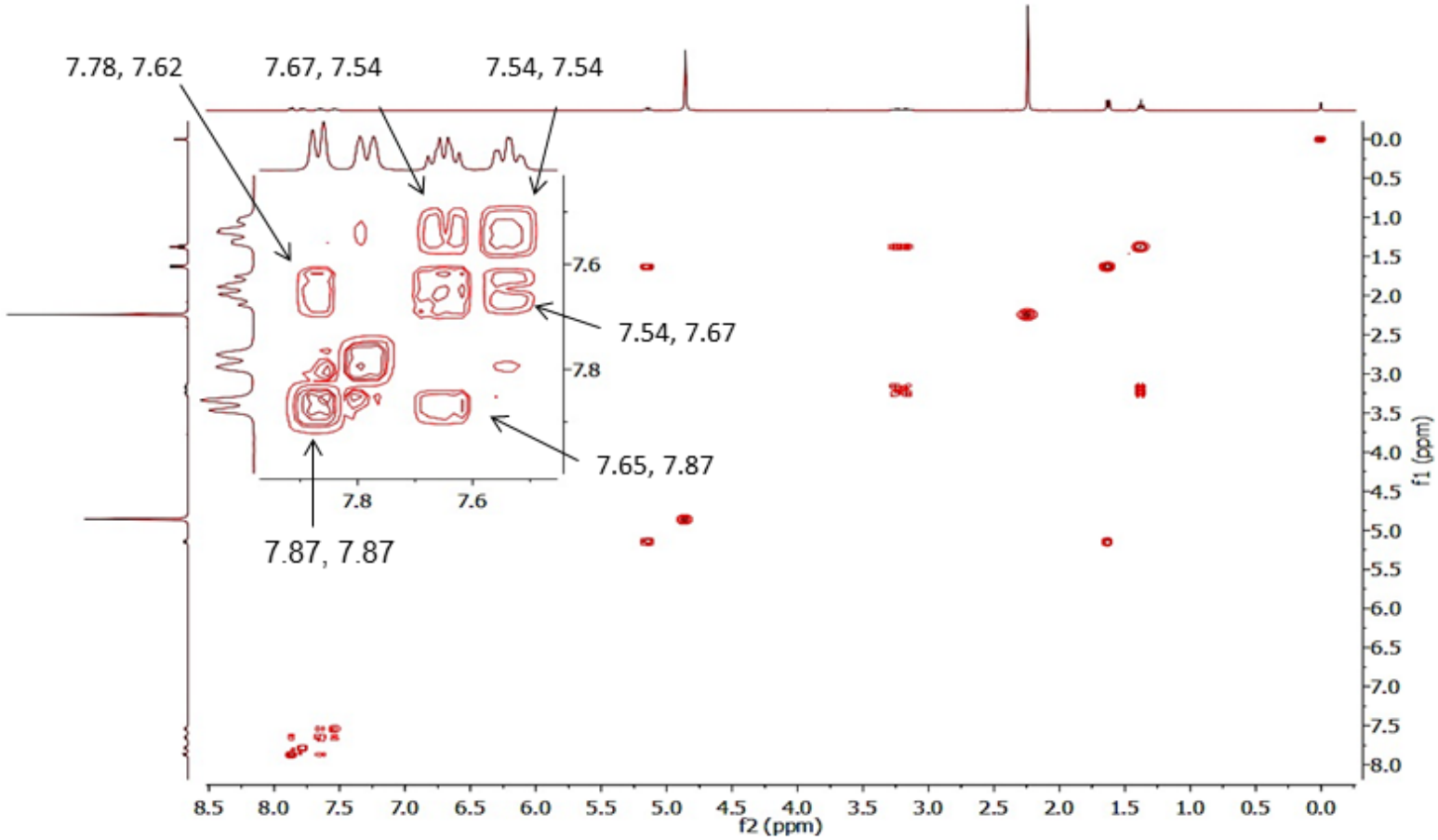

Figure 4-11. ^{1}H-^{1}H COSY spectrum of **24** collected in D_2O

Compared to **23**, the $^{13}C\{^{1}H\}$ NMR spectrum of **24** (Fig. 4-12) also possesses eleven unique carbon environments. When the $^{13}C\{^{1}H\}$ DEPT-135 spectrum was collected (Fig. 4-13), this also simplified to eight environments. The carbonyl (δ 199.3) and quaternary carbon (δ 137.2) have higher chemical shifts in comparison to **23** due to the position of the fluorine atom changing to the *meta* position (carbon number 3), causing the aforementioned positions to become more deshielded. These signals are not observed in the $^{13}C\{^{1}H\}$ DEPT-135 spectrum. Similar to **23**, the carbon possessing a fluorine atom located at C3 (δ 165.5) of the aromatic ring is not observed either, because the carbon centre is effectively “quaternary”. When comparing the $^{13}C\{^{1}H\}$ NMR spectrum of **24** to that of **23**, it is observed that the chemical shift of the chiral centre carbon has shifted up-field.

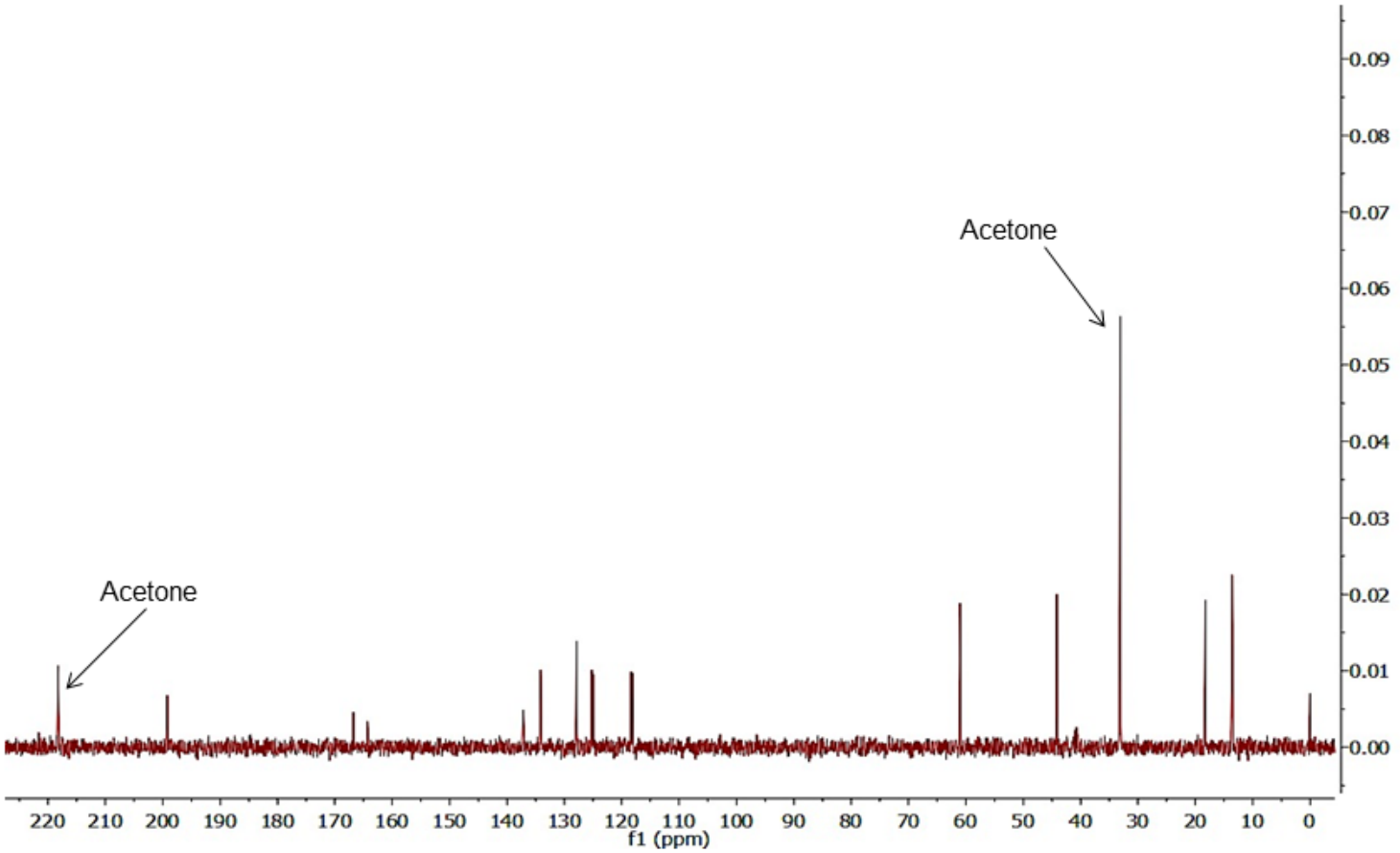

Figure 4-12. $^{13}C\{^{1}H\}$ NMR spectrum of **24** collected in D_2O

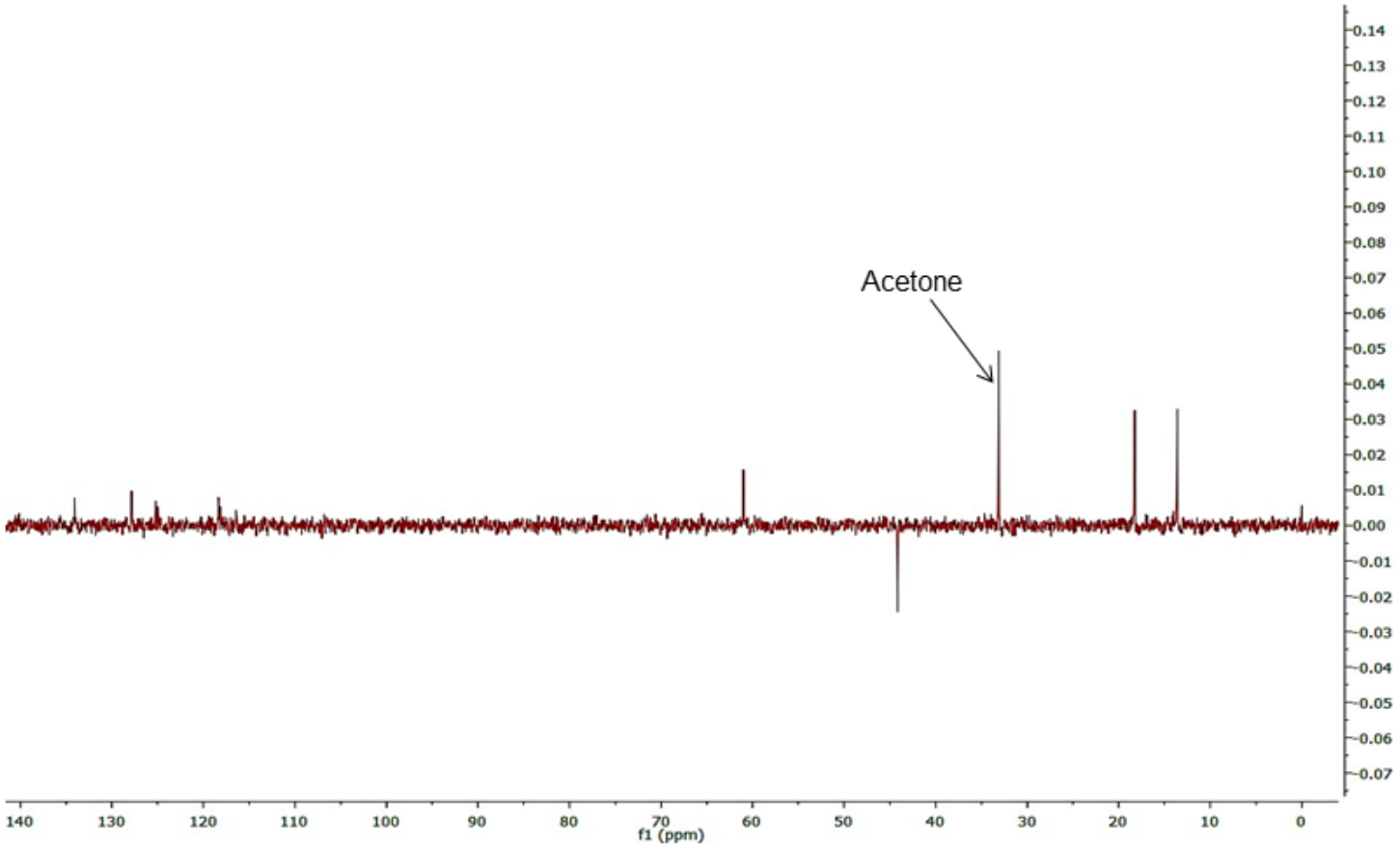

Figure 4-13. $^{13}C\{^{1}H\}$ DEPT-135 spectrum of **24** collected in D_2O

Similar to **23**, the HMQC spectrum of **24** was used to relate the ^{1}H environments identified from the ^{1}H NMR spectrum to those of the ^{13}C domain. The spectrum shown in Fig. 4-14, illustrates the correlation between the ^{1}H peak at δ 7.54 to the ^{13}C peak at δ 125.2; this correlation refers to the carbon located at position 2, while the carbon at location 4 has a ^{1}H-^{13}C correlation of δ 7.78 and δ 118.2 respectively.

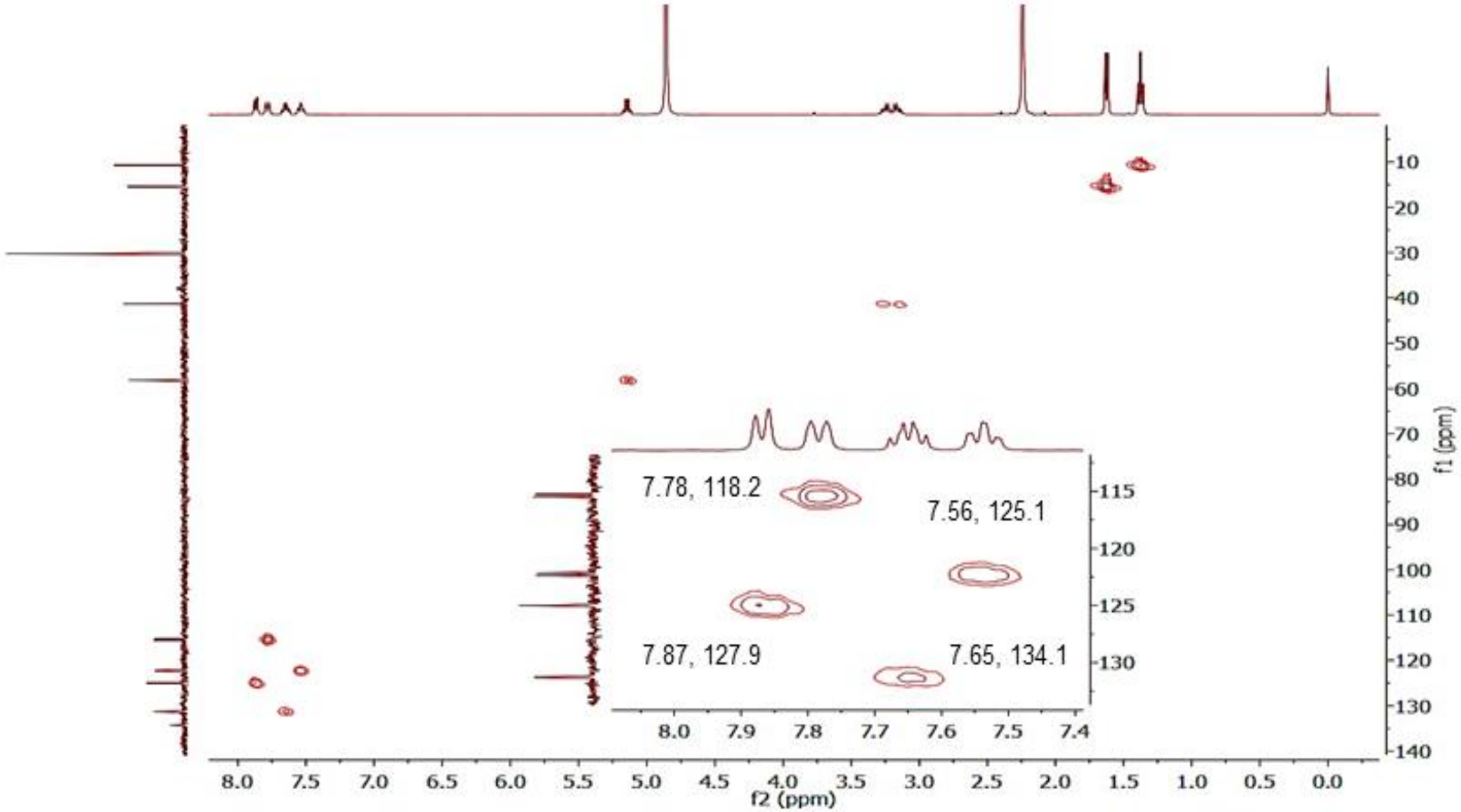

Figure 4-14. ^{1}H-^{13}C HMQC spectrum of **24** collected in D_2O

Moreover, the HMBC spectrum (Fig. 4-15) was acquired to identify the two quaternary carbons due to their $^{2}J_{CH}$ interactions with proton nuclei in their local vicinity. This spectrum validates that the peaks at δ 137.2 and δ 199.3 correspond to positions 1 and 7 respectively. Also, the HMBC spectrum allowed the position of each carbon on the side chain to be matched to its adjacent carbon by identifying the $^{2}J_{CH}$ and $^{3}J_{CH}$ interactions.

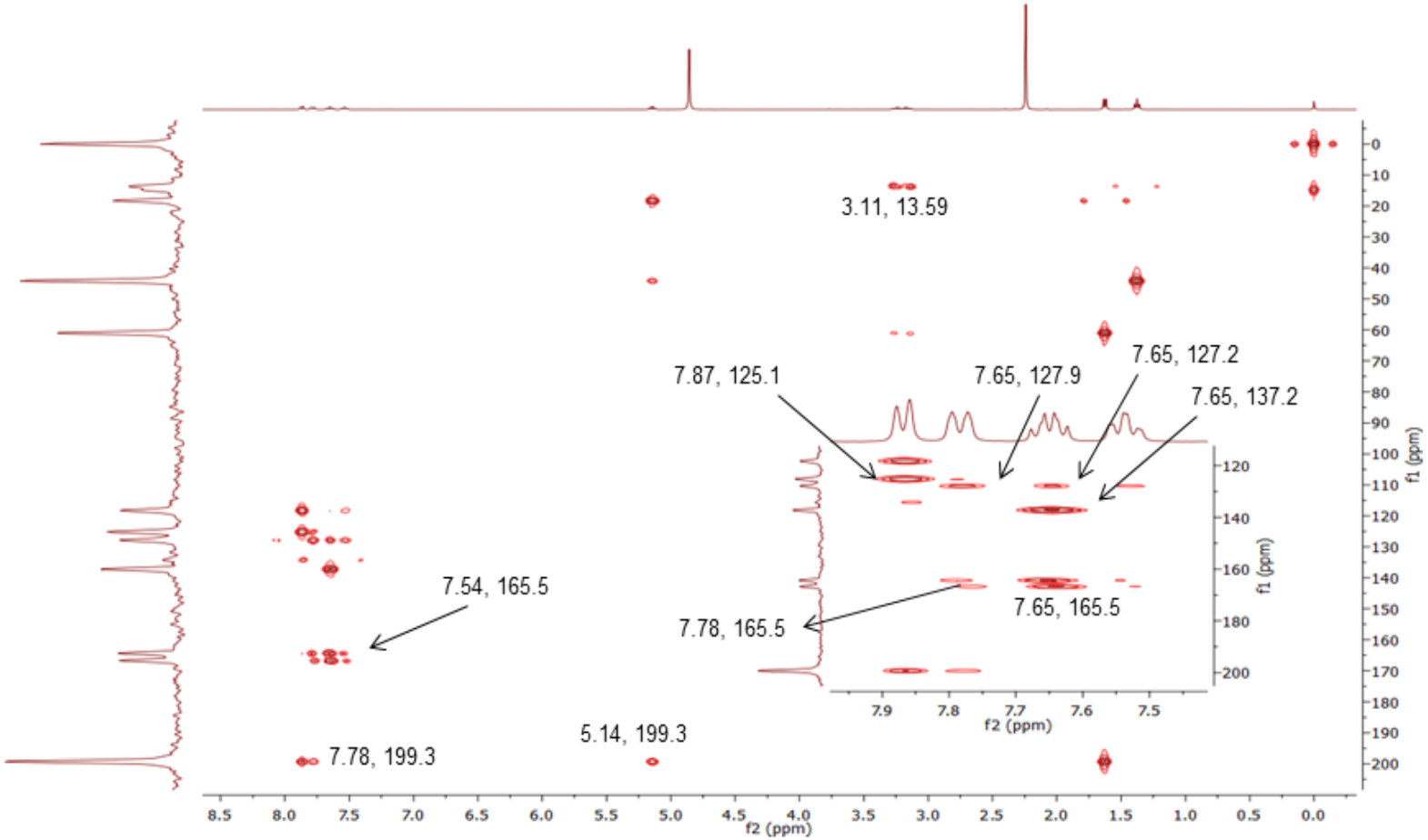

Figure 4-15. ^{1}H-^{13}C HMBC spectrum of **24** collected in D_2O

Again, similar to **23**, **24** possesses a single ^{19}F nucleus. The $^{19}F\{^{1}H\}$ NMR spectrum (Fig. 4-16) of **24** revealed a single peak at δ -113.44, which is very similar to that of **23**. Therefore, it is difficult to distinguish between the two isomers by only $^{19}F\{^{1}H\}$ NMR spectrum analysis. However, comparison of these results to $^{19}F\{^{1}H\}$ NMR results of 3-fluoromethcathinone (FMC), reported by Archer, in which the ^{19}F signal is at δ -114.23, confirms the *meta*-substituted position of the fluorine atom.[33] Subsequently, analogous to **23**, the peak located at δ -76.55 is TFA, which is used as an internal standard. The NMR data for **24** are displayed in table 4-2.

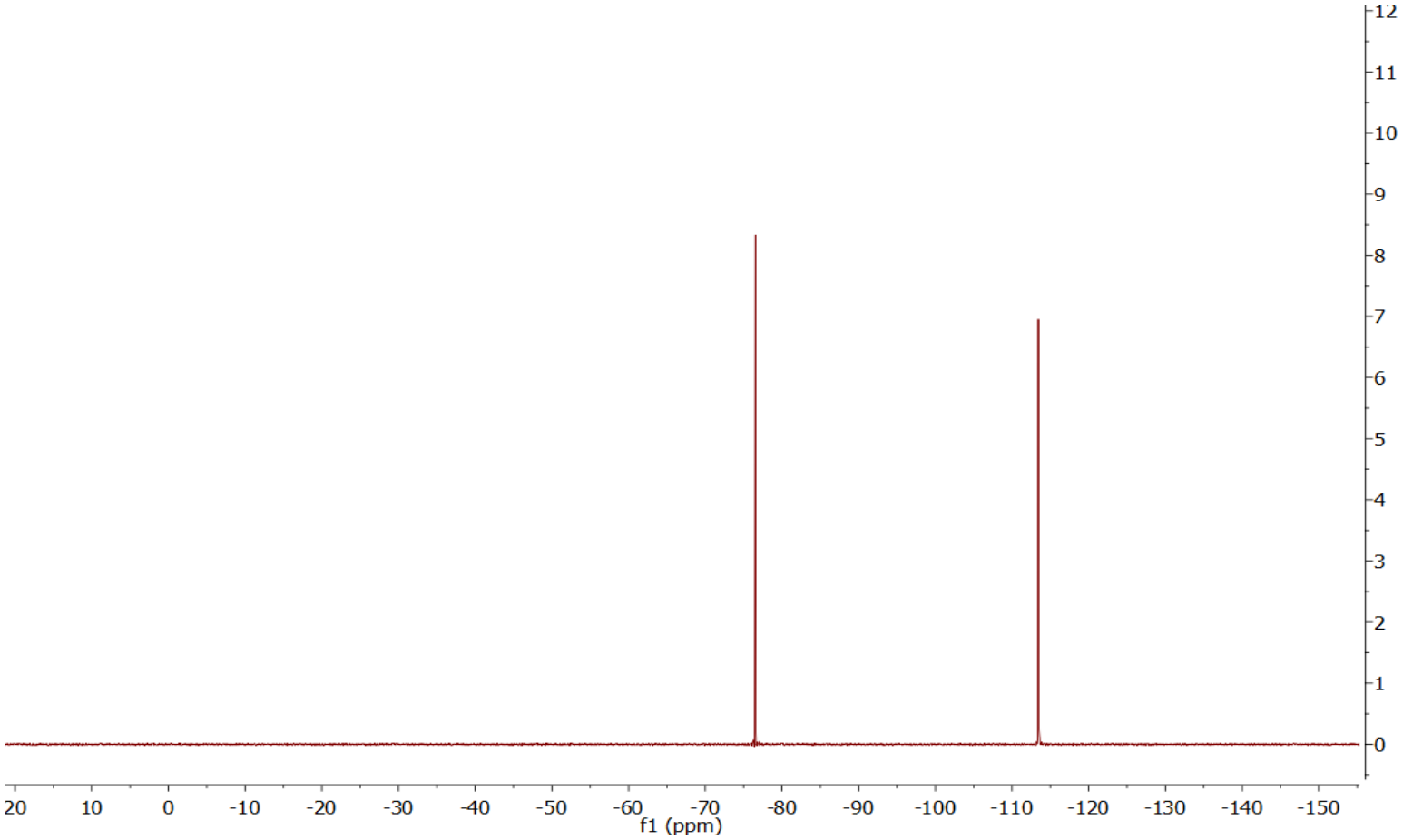

Figure 4-16. $^{19}F\{^{1}H\}$ NMR spectrum of **24** in D_2O. The peak at δ ^{19}F -76.55 is TFA

Table 4-2. NMR results for **24**

3-FEC (26)

C number	No. Of Hs	^{1}H NMR: δ / ppm, *J*-coupling (Hz)	^{13}C{^{1}H} NMR: δ / ppm, *J*-coupling (Hz)	^{19}F{^{1}H} NMR: δ / ppm
1	**0**	-	137.2, d, $^{3}J_{CF}$ =6.8	
2	**1**	7.54, td, $^{3}J_{HF}$ = 8.2, $^{4}J_{HH}$ = 2.3 Hz	125.1, d, $^{2}J_{CF}$ =21.5	
3	**0**	-	165.5, d, $^{1}J_{CF}$=247	-113.44
4	**1**	7.78, dt, $^{3}J_{HF}$ = 9.2, $^{4}J_{HH}$ = 1.9 Hz	118.2, d, $^{2}J_{CF}$ =22.9	
5	**1**	7.62- 7.68, m,	134.1, d, $^{3}J_{CF}$ =7.6	
6	**1**	7.87, d, $^{3}J_{HH}$ = 7.8 Hz	127.9, d, $^{4}J_{CF}$ =2.2	
7	**0**	-	199.3, s	
8	**1**	5.14 q, $^{3}J_{HH}$ = 7.3Hz	61.0, s	
9	**2**	3.29-3.11, m	44.2, s	
10	**3**	1.63, d, $^{3}J_{HH}$ = 7.3	18.3, s	
11	**3**	1.38, t, $^{3}J_{HH}$ = 7.3	13.59, s	
Acetone		2.24 (CH_3)	33.1 (CH_3), 218.0 (C=O)	

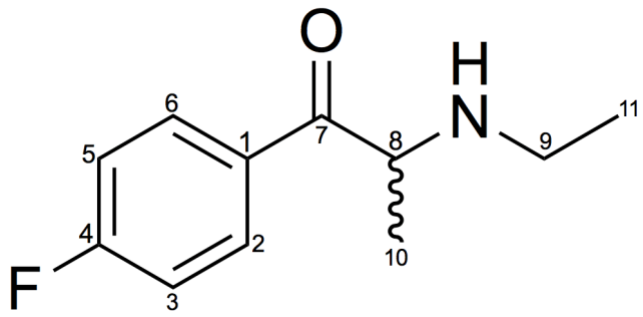

25

Figure 4-17. Chemical structure of 4-FEC (**25**)

The ^{1}H NMR spectrum of 4-FEC (**25**) is shown in Fig. 4-17. In contrast to **23** and **24** only seven unique ^{1}H NMR environments are observed in the ^{1}H NMR spectrum. Upon inspection of the aromatic region of the ^{1}H NMR spectrum of **25** reveals characteristics of a *para*-substituted aromatic system. In addition, presence of J_{HF} coupling in the aromatic ring enables the position of the ^{1}H nuclei to be located. Dissimilar to **23** and **24**, there are only two chemical signals present in the aromatic region, each integrating to two ^{1}H nuclei, resulting in two $^{3}J_{HH}$ couplings. The $^{3}J_{HH}$ coupling from the proton located on position 2 to the one located on position 3 as well as $^{3}J_{HH}$ coupling of the proton located at position 5 and 6, are reflected in the observation of cross-peaks in the ^{1}H-^{1}H COSY spectrum (Fig. 4-19)

.

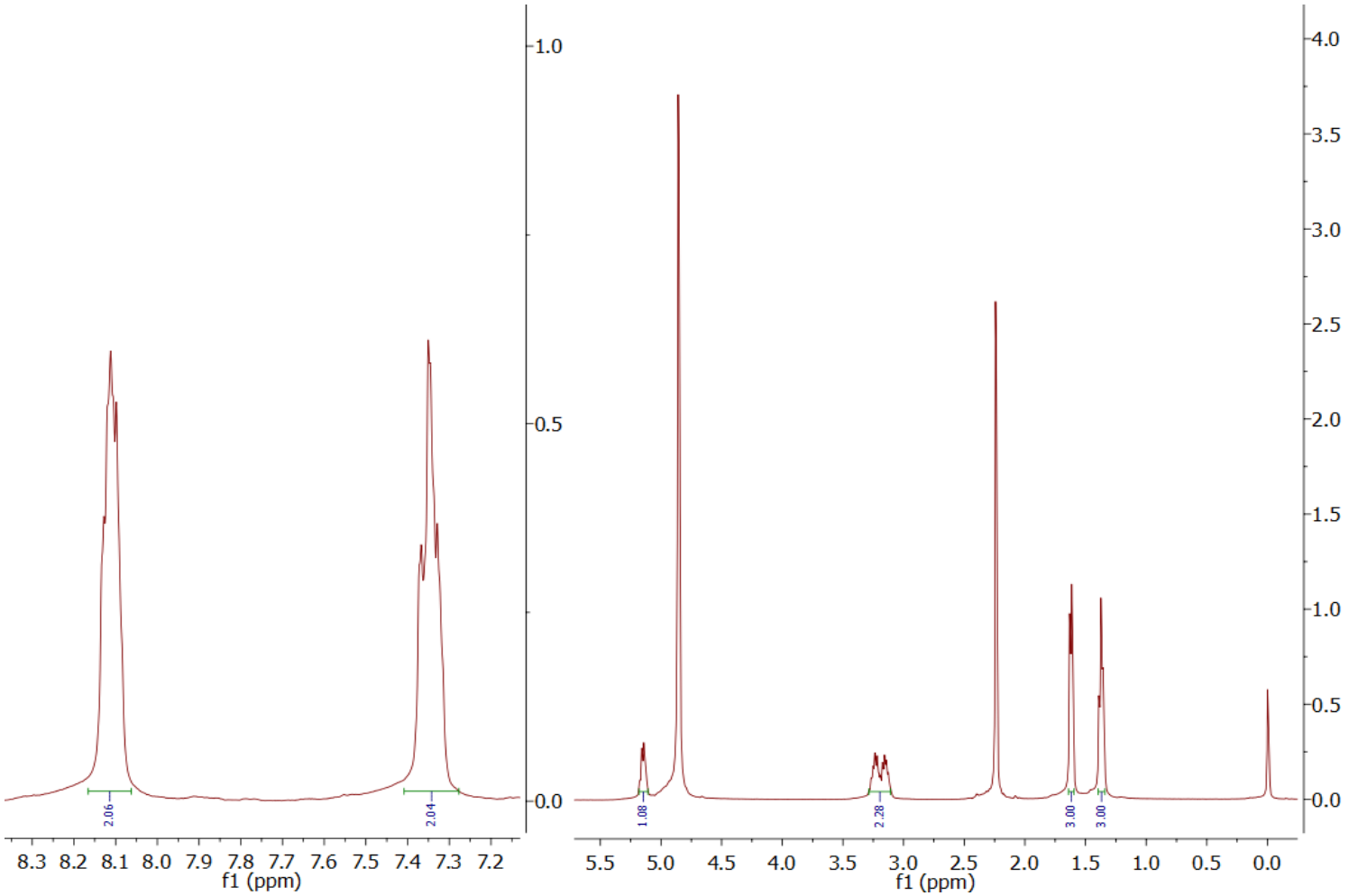

Figure 4-18. ^{1}H NMR spectrum of **25** collected in D_2O

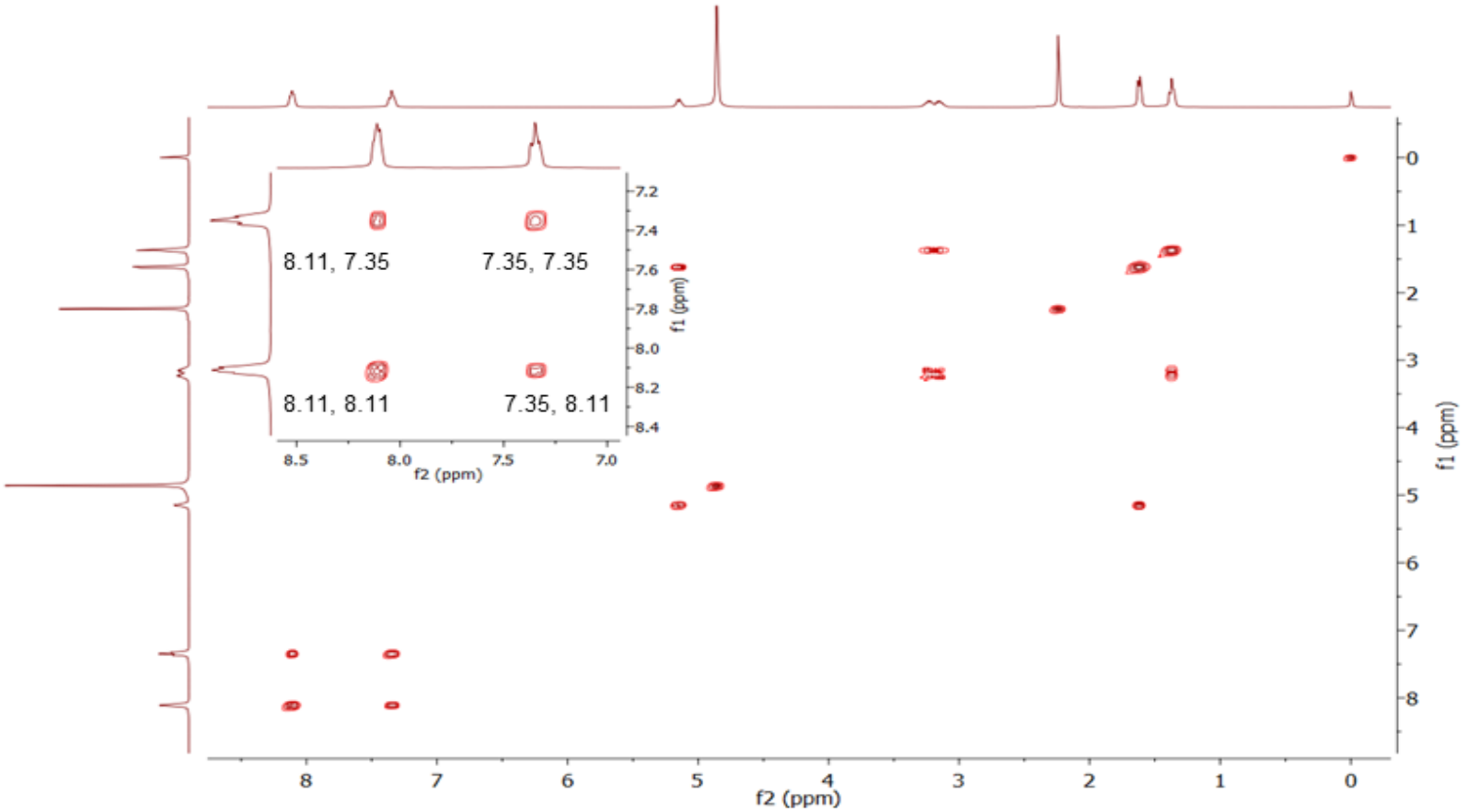

Figure 4-19. ^{1}H-^{1}H COSY NMR spectrum of **25** collected in D_2O

The $^{13}C\{^{1}H\}$ NMR spectrum (Fig. 4-20) of **25** reveals 9 unique carbon environments. When the $^{13}C\{^{1}H\}$ DEPT-135 spectrum was collected (Fig. 4-21), this simplified to six environments. The number of ^{13}C environments in the aromatic region is only four; this is less than **23** and **24** due to the *para*-substituted system in **25**. The peaks at δ 134.9 with $^{3}J_{CF}$ coupling of 10.3 Hz and δ 119.3 with $^{2}J_{CF}$ coupling of 22.2 Hz represent carbons 2/6 and 3/5 respectively, these peaks are also observed in the $^{13}C\{^{1}H\}$ DEPT-135 spectrum at their respective chemical shifts.

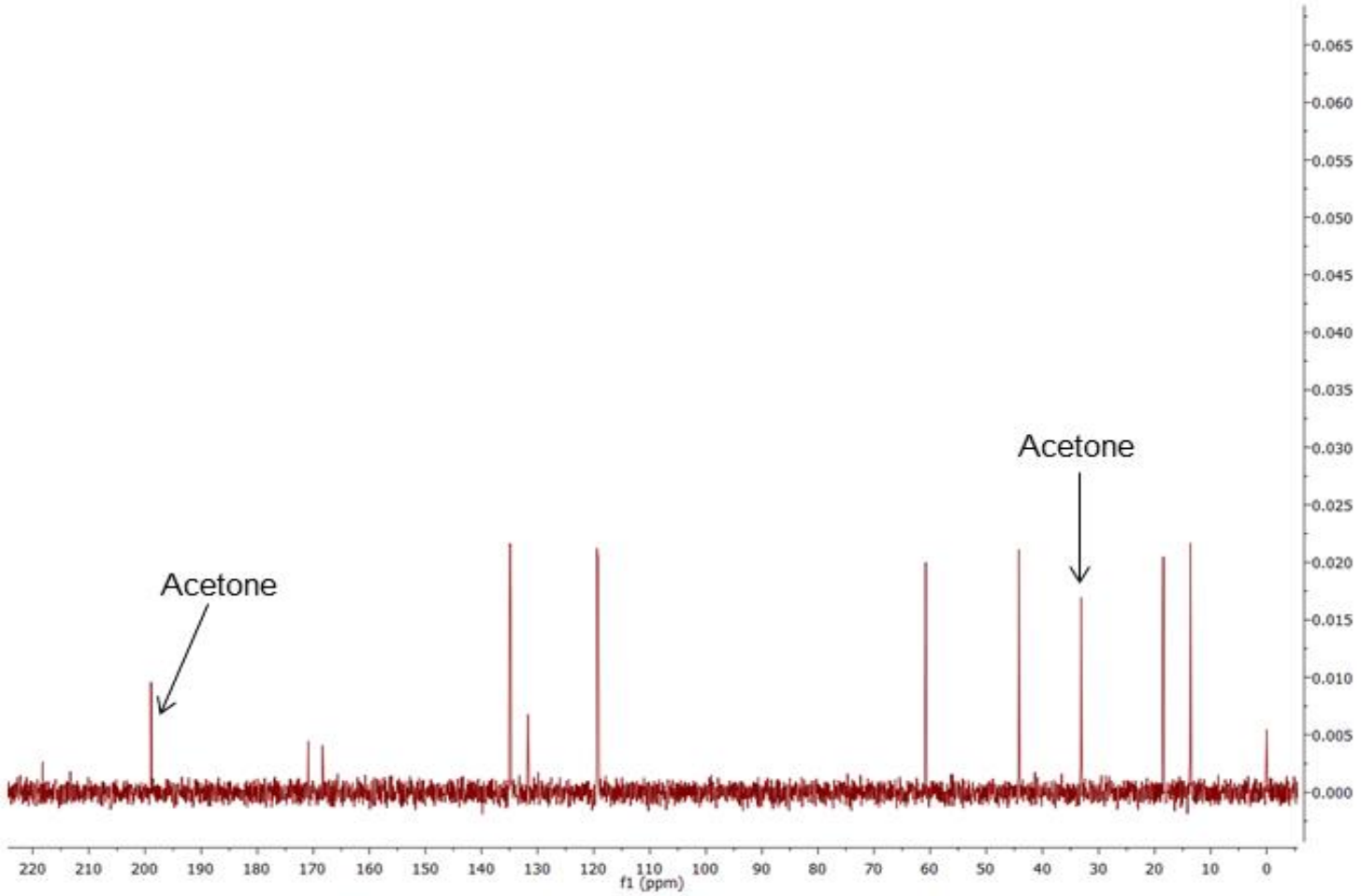

Figure 4-20. $^{13}C\{^{1}H\}$ NMR spectrum of **25** collected in D_2O

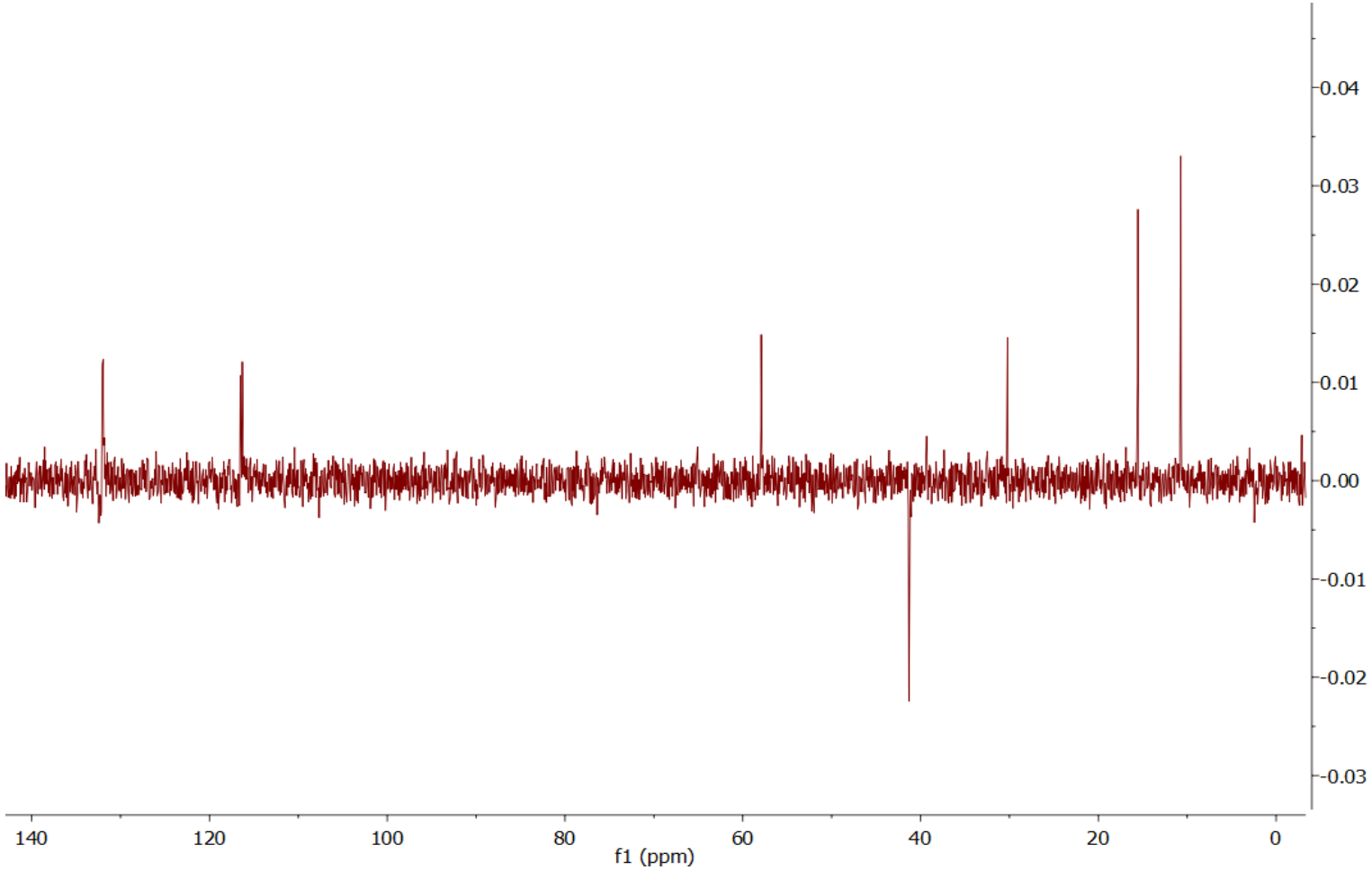

Figure 4-21.$^{13}C\{^{1}H\}$ DEPT-135 NMR spectrum of **25** collected in D_2O

The HMQC spectrum of **25** was also utilised to correlate the ^{1}H environments identified from the ^{1}H NMR spectrum to those of the ^{13}C domain. From the HMQC spectrum, it can be seen that there are only two ^{1}H-^{13}C correlations in the aromatic region. The correlation between ^{1}H δ 7.35 and ^{13}C δ 119.3 and the correlation between δ 8.11 and δ 134.9 relate to C3/C5 and C2/C6 respectively. This reflects characteristics of a *para*-substituted aromatic system. The spectrum is shown in Fig. 4-22 and the results tabulated in Table 4-3.

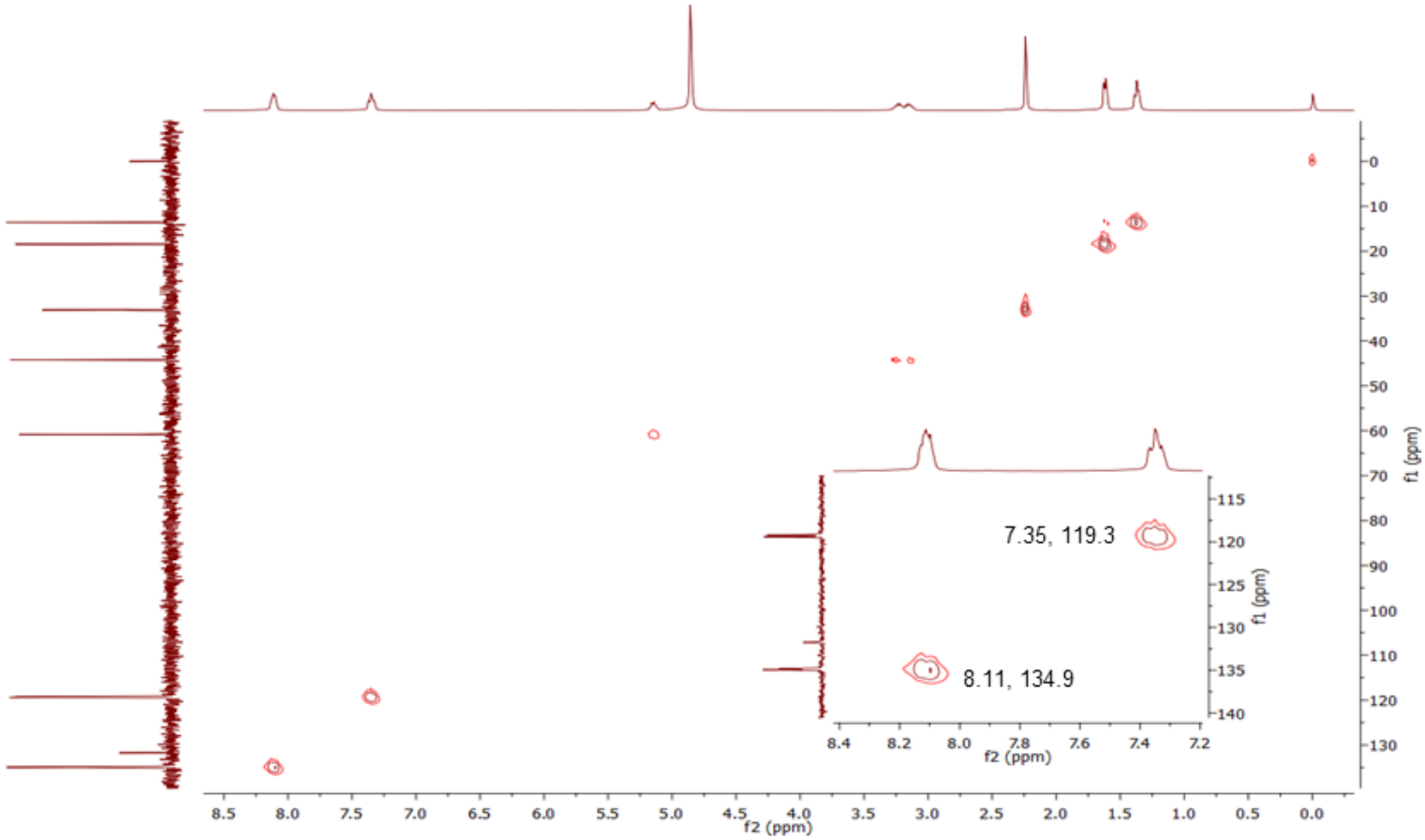

Figure 4-22. ^{1}H-^{13}C HMQC NMR spectrum of **25** in D_2O

Moreover, the ^{1}H-^{13}C HMBC spectrum (Fig. 4-23) was utilised to further identify couplings, namely between H2 /H6 and C7 ($^{3}J_{HC}$) to verify the assignment of the propan-1-one substituted side chain at C1 on the aromatic centre (between C2 and C6).

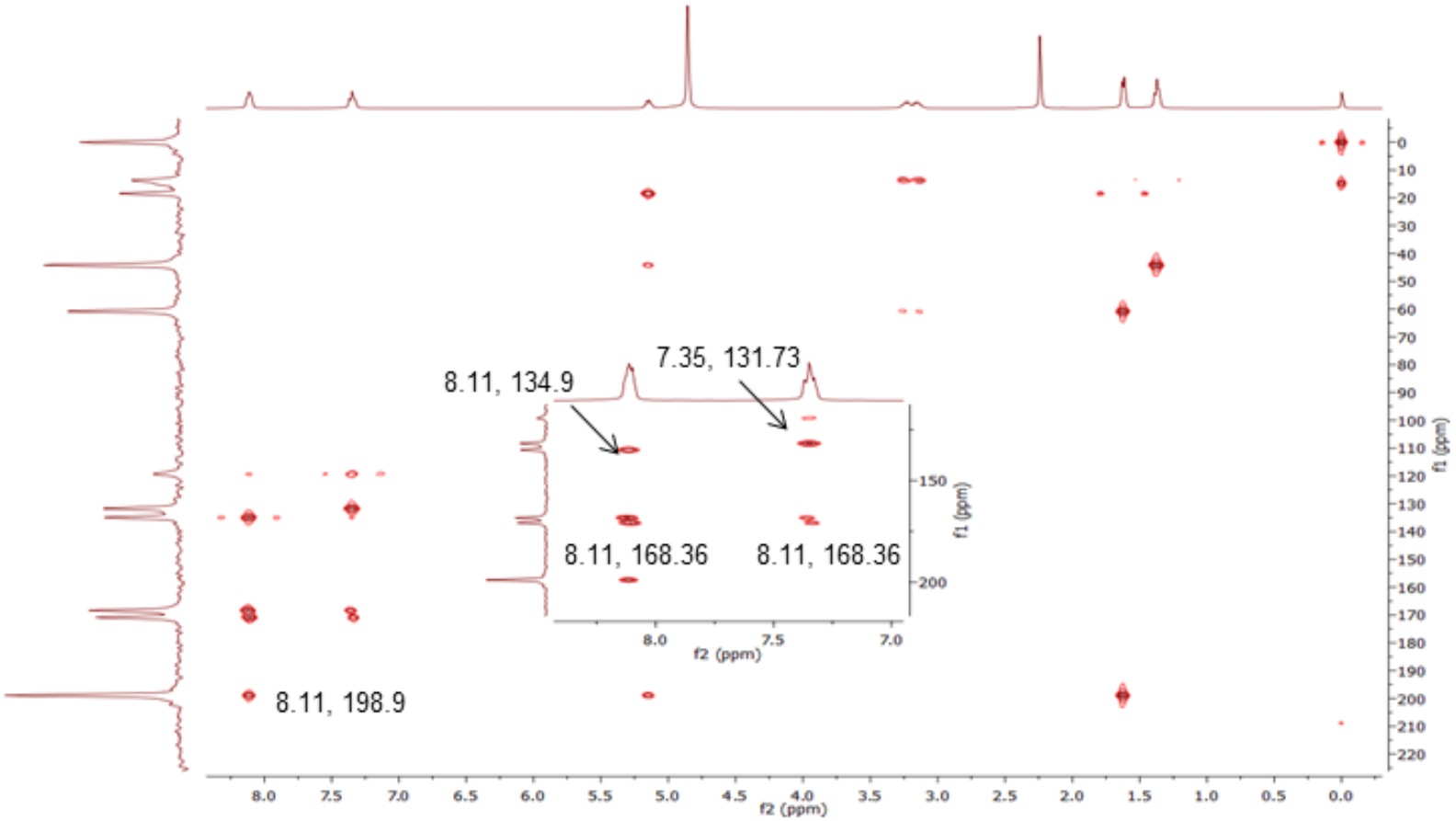

Figure 4-23. ^{1}H-^{13}C HMBC spectrum of **25** in D_2O

Identical to the two other isomers, **25** possesses a single ^{19}F nucleus. The $^{19}F\{^{1}H\}$ NMR spectrum (Fig. 4-24) revealed a single peak for **25** at δ -105.42, which is significantly lower than the ^{19}F chemical shift in **23** and **24**. Comparison of this result to the $^{19}F\{^{1}H\}$ NMR spectrum of 4-FMC (δ -104.53), reported by Archer, confirms the *para*-substituted aromatic system.[33]

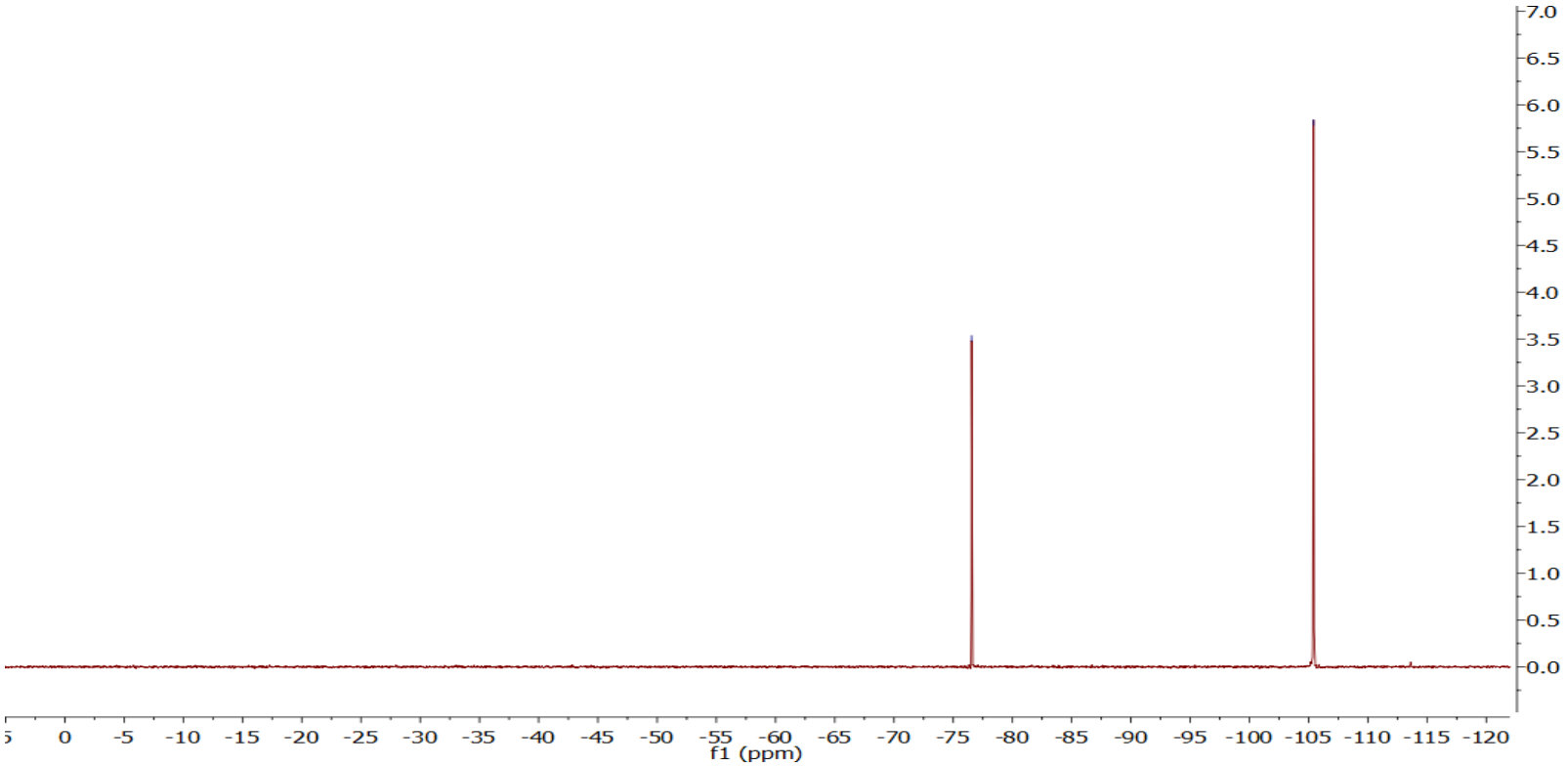

Figure 4-24. $^{19}F\{^{1}H\}$ NMR spectrum of **25** collected in D_2O. The peak at $\delta^{19}F$ -76.55 is TFA

Table 4-3 NMR results for **25**

		4-FEC (25)		
C number	**No. Of Hs**	**^{1}H NMR:** δ / ppm, *J*-coupling (Hz)	**^{13}C{^{1}H} NMR:** δ / ppm, *J*-coupling (Hz)	**^{19}F{^{1}H} NMR:** δ / ppm
1	0	-	131.7, s	
2	1	8.11, dd, $^{3}J_{HH}$ = 8.9, $^{4}J_{HH}$ = 5.3	134.9, d, $^{3}J_{CF}$= 10.3	
3	1	7.35, t $^{3}J_{HH}$ = 8.9, $^{3}J_{HF}$ = 2.3	119.3, d, $^{2}J_{CF}$ = 22.2	
4	0	-	169.6, d, $^{1}J_{CF}$ = 255	-105.42, s
5		Same as 3		
6		Same as 2		
7	0	-	198.9, s	
8	1	5.14, q, $^{3}J_{HH}$ = 7.2	60.8, s	
9	2	3.19, m	44.2, s	
10	3	1.61, d, $^{3}J_{HH}$ = 7.3	18.4, s	
11	3	1.36, t, $^{3}J_{HH}$ = 7.3	13.6, s	
Acetone		2.25 (CH_3)	33.1 (CH_3), 218.0 (C=O)	

4.2 Melting point analysis

Melting points of **23**-**25** are 149°C, 196°C and 256°C, respectively. Melting points of **23**-**25** are comparable to the literature value of the fluoromethcathinone, reported on swgdrug.[34] Although FMC is a very similar cathinone derivative, with only the methyl group changing to an ethyl group, the melting point of the FEC derivatives were considerably higher than 2-FMC, 3-FMC and 4-FMC isomers. These compounds have melting points of 129°C, 169.3°C and 230°C, respectively.

4.3 Thin layer chromatography (TLC)

TLC was used to identify and determine the purity of cathinone compounds; visualization analysis of the TLC plates of fluoroethcathinone compounds produced bright pink coloured spots, when observed with ninhydrin solution. The analysis of the retention factors (R_f) indicated some separation of the compounds; predominantly **23**-**25** have R_fs of 0.82, 0.71 and 0.66 respectively. Comparison of the R_f values of the FEC isomers with the reference FMC isomers (R_f = 0.49, 0.40, 0.35 for 2-FMC, 3-FMC and 4-FMC respectively) indicate that the FEC isomers elute quicker, using the conditions described. The order of regioisomer elution remains the same, with each FEC regioisomer possessing a R_f value that is ~0.31 higher than the corresponding FMC regioisomer.

The TLC test was repeated six times and its percentage relative standard deviations (%RSD) was measured. %RSD determines the partial error

associated with the test, following six TLC measurements **23**, **24** and **25** produced %RSD of 2.24%, 2.09% and 2.38% respectively. This signifies that the error associated with the test is minimal because the error associated with the test is about 2%.

4.4 Attenuated Total Reflectance Fourier Transform infrared spectroscopy (ATR-FTIR)

Table 4-4 confirms the results of the infrared spectroscopy analysis. **23**, **24** and **25** displayed strong C=O absorption bands at 1693.55, 1698.37, 1684.97 cm^{-1} respectively. The samples also exhibit additional broad C-C absorptions at 1606.81, 1491.79 and 1595.26 cm^{-1} respectively, indicative of an aromatic nucleus in all compounds, and peaks at 3140, 3050, 3170 cm^{-1} due to the NH stretch. The spectrum of each of the samples is shown in figures 4-25, 4-26 and 4-27 respectively.

Table 4-4 Infrared analysis of the three isomeric FEC

Infrared Spectroscopy (IR) Results

STRETCH	**23 / cm^{-1}**	**24 / cm^{-1}**	**25 / cm^{-1}**
N-H	3140.00	3050.00	3170.00
C-H	2937.40	2967.71	2968.21
CH_2	2732.08	2790.33	2787.49
C=O	1693.55	1698.37	1684.97
C=C aromatic	1606.81	1491.79	1595.26
C-N	1223.34	1202.15	1284.89
C-C	1047.37	1042.04	1044.68
C-H	765.39	748.48	756.98

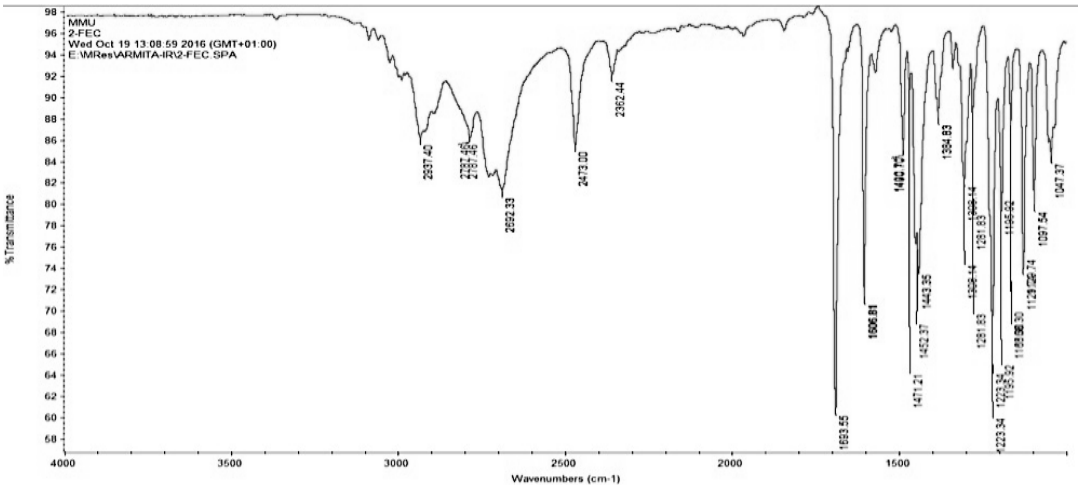

Figure 4-25. Infrared spectrum of **23**

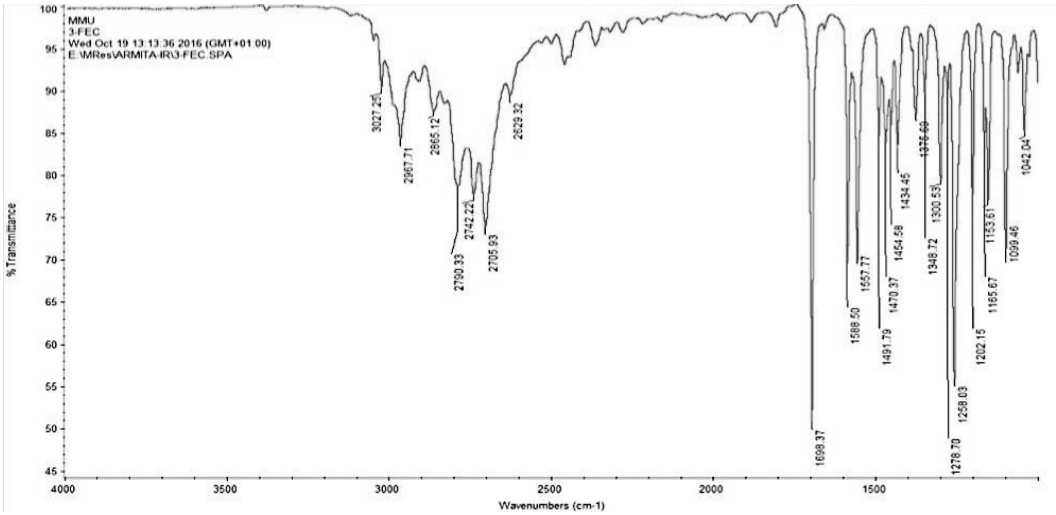

Figure 4-26. Infrared spectrum of **24**

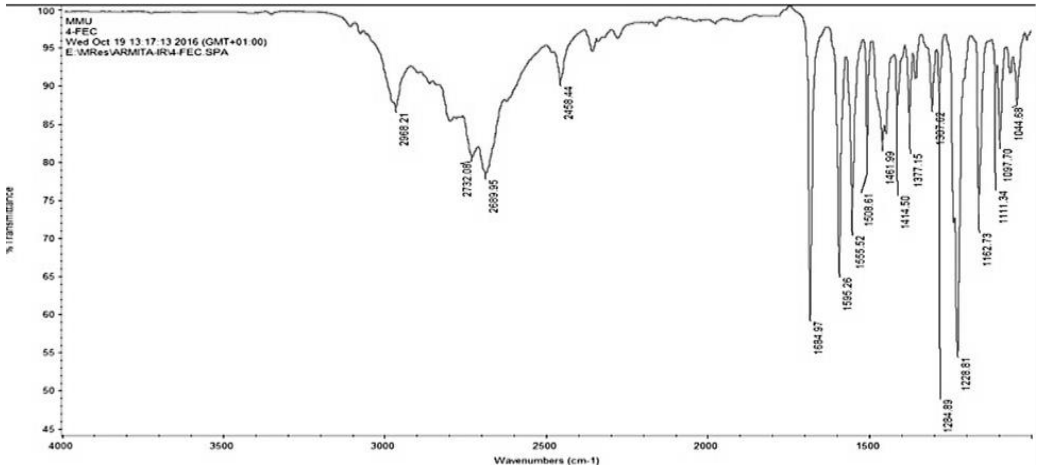

Figure 4-27. Infrared spectrum of **25**

4.5 Colour presumptive tests

Marquis test: Used for the identification of amphetamine, morphine and heroin. The test utilises formaldehyde in glacial acetic acid and concentrated sulphuric acid. An orange intermediate that slowly turns brown signifies the presence of amphetamine. Development of the orange-brown colour is due to formation of the carbenium ion from the reaction between formaldehyde and an aromatic compound in the acidic conditions by electrophilic

substitution. The carbenium ion formed reacts with the aromatic ring of drugs (i.e. amphetamine and methamphetamine form an orange color) to produce alcohol and further reaction with a second molecule of the drug results in formation of a dimer.

Marquis did not result in any colour change when **23**-**25** were tested, due to the deactivation of the aromatic ring by the electron withdrawing effect of the ketone moiety. This inhibits the reaction of the Marquis reagent with the amine group. Therefore, it does not form an orange colour, which is representative of the reaction of the Marquis reagent with amines.

Mandelin test: The Mandelin's test presumptive reagent is made up of ammonium vanadate in concentrated sulfuric acid; it is used for identification of opiates (codeine), phenylethylamines, MDMA and MDA. When Mandelin's reagent reacts with any of these drugs vanadate ions form a conjugated system with different oxidation states, leading to different colours. Thus, the reduction of the vanadium(V) (dark yellow) with the drug in the presence of sulfuric acid, results in the formation of different colour changes, depending on the oxidation state of vanadium. Upon reduction to vanadium (IV) and vanadium (III), in the presence of an alkaloid, the colour of solution changes to blue and then green, respectively.[35] The reaction mechanisms of the Mandelin reagent with these drugs acting as a ligand is unknown. Darsigny *et al* stated that morphine and methamphetamine do not react with Mandelin's reagent. This could be due to the absence of an *O*-methyl group and a methylenedioxy bridge in these drugs respectively,

because the presence of an *O*-methyl group and a methylenedioxy bridge is necessary for a reaction to occur between Mandelin's reagent and the drugs of abuse.[36]

Mandelin's reagent formed an orange colour upon reaction with isomers of FEC. However, this colour change was not persistent as the FEC isomers turned light yellow after 20 minutes. Conversely, the same compounds did not experience any colour change when tested as powders in reactions. The orange color acquired is not a result of change in the oxidation state of vanadate. Darsigny *et al* also implies that it may be due to side-reactions with the reagent.[36]

Simon's test: Simon's test is typically used for identification of the secondary amines (methamphetamine and other N-substituted amphetamine substances). When Simon's reagents react with secondary amines it produces a deep blue Simon-Awe complex.[35] The reaction between amine and acetaldehyde forms the enamine, which then reacts with the sodium nitroprusside to form an immonium salt. Finally, the hydrolysed immonium salt yields the Simon-Awe complex. The Simon reagent does not react with the cathinone and ephedrine derivatives; this could be due to the electron withdrawing effects of the ketone group, which weakens the nucleophilicity of the amine functionality, this essentially prevents enamine production at the first step.[37]

Robadope's Test: Similar to the Simon reaction, this test involves the reduction of the amine with a carbonyl compound to yield an iminium salt, which then results in formation of an enamine. If the amine is tertiary or quaternary, the iminium salt cannot form, although the nucleophilic addition of the amine at the carbonyl may still occur after the first step, for tertiary amines. However, this is impossible for the quaternary amines since they do not possess a lone pair of electrons. The iminium salt is produced in the second step by elimination of a water molecule involving an electron pair on the nitrogen. However, the second step is impossible for tertiary amines. Therefore, Robadope and Simon's reagents are not able to identify derivatives containing tertiary amines nor quaternary ammonium salts.

Scott's test: Scott's test is typically used for the detection of cocaine and crack cocaine. The reaction mechanism is based on the insoluble complex of the cobalt thiocyanate ion with a free nitrogen base of cocaine. Nonetheless, this reaction mechanism can produce false positive results. Therefore, alternative modified reagents are also used to obtain accurate results. The original reaction solution can be first basified prior to adding ethylene glycol, for example; this method is particularly useful for the detection of ketamine hydrochloride that consists of lignocaine and cocaine. The reaction mechanism involves the formation of an octahedral structure for the cocaine-cobalt (II) thio-cyanate complex with two thiocyanate ligands and two *bis*-chelating cocaine ligands.[36]

The Scott test is a three-step reaction. Step 1: blue crystals (i.e. precipitates)

are formed upon addition of cobalt thiocyanate, in the presence of cocaine. Step 2: the blue crystal will fade after addition of hydrochloric acid, in the presence of cocaine. Step 3: addition of chloroform, will produce two layers, of which the lower layer is blue. The anticipated colour changes are representative of cocaine.

Zimmerman's Test: The Zimmermann reaction is facilitated by a carbonyl group that is in close proximity to a methyl group in the same molecule. The methylene group, which is activated through oxidation under alkaline conditions, then reacts with 2′,4′- dinitrobenzene to form a reddish-purple colour upon formation of a Meisenheimer complex. This reaction can be further oxidised to form a Zimmerman mixture. Subsequently, Zimmerman reaction with cathinone derivatives is always positive, therefore, this was the most efficient test method.[35]

Liebermann's Test: Liebermann color test reacts with phenols. The nitrous acid, present in the Liebermann color test, converts the phenol into nitrosophenol, through formation of carbocations with primary amine and N-nitrosamines with secondary amines.[35] The substituents present on the benzene ring will affect the color observed, and occasionally it is suggested to perform the test at 100°C to acquire further coupling between nitrosophenol and phenol. The reaction of methcathinone derivatives with Liebermann's reagent give yellow coloured products, whereas no colour change was observed when Liebermann's reagent was applied to FEC and FMC derivatives.[24]

Chen Ko Test: Copper sulfate and sodium hydroxide solution, which are the main reagents in the Chen Kao test, tend to react with proximate amino- and hydroxyl-groups. This results in the formation of a violet-coloured chelate complex. Since cathinone derivatives do not contain a hydroxyl group it does not react with the Chen Kao reagent. A blue precipitate is formed in the presence of cathinone. However, employment of the Chen Kao reagent results in the appearance of a violet colour due to the formation of a symmetrical chelate with ephedrine isomers. Nonetheless, the stability and solubility of this reagent is affected by the structural and steric differences of the alkylamine part of the molecule.[25]

Overall, various presumptive tests of cathinone derivatives were carried out and the results are summarised in Tables 4-5 and 4-6. As a result of these colour tests, Mandelin, Scott and Zimmerman reagents demonstrated immediate colour changes for all the three isomers. Further colour change observations were noted again after 20 minutes (Tables 4-7 and 4-8), where the major changes occurred when employing Mandelin, Simon (in particular **23** which turned khaki from peach), Scott, and Zimmermann (**24** and **25**).

Table 4-5 Immediate colour changes of the FEC regioisomers using *Marquis*, *Mandelin*, *Simon*, and *Robadope's* tests.

	Immediate Colour Presumptive Test			
	Marquis	***Mandelin***	***Simon***	***Robadope***
Blank	Very pale yellow	Yellow	Dark Peach	Dark Orange
23	-	Light Orange	-	-
24	-	Light Orange	-	-
25	-	Light Orange	-	-

Table 4-6 Immediate colour changes of the FEC regioisomers using *Scott*, *Zimmerman*, *Liebermans*, and *Chen Kao* tests.

	Immediate Colour Presumptive Test			
	Scott	***Zimmerman***	***Liebermans***	***Chen Kao***
Blank	Bright red	Colourless	Colourless (Cloudy)	Light blue
23	Orange	Light pink	-	-
24	Orange	Light pink	-	-
25	Orange	Light pink	-	-

Kovar *et al.* states that the Zimmerman test reacts only if a carbonyl group and an alkyl group are present in order to form a Meisenheimer complex. This complex produces a reddish-purple colour upon reaction of 2,4-dinitrobenzene. This reaction can be further oxidised to form a Zimmerman mixture. Subsequently, the Zimmerman test for cathinone derivatives is always positive, therefore, this was the most efficient test method. [37]

Marquis did not result in any colour change, due to the deactivation of the aromatic ring by the electron withdrawing effect of the ketone moiety. This inhibits reaction of the Marquis reagent with the amine group. Therefore, it does not form an orange colour, which is representative of the reaction of Marquis reagent with amines.[31] In some cases, ambiguous colour changes resulted from the reaction of fluoroethcathinone isomers with the colour test reagents. For example, Mandelin reagent turned orange from yellow upon application to the isomers of FEC. However, this colour change was not persistent as the FEC isomers turned lime after 20 minutes. Conversely, the same compounds did not experience any colour change when tested as powders in reactions.

Table 4-7 Colour changes of the FEC regioisomers using *Marquis*, *Mandelin*, *Simon*, and *Robadope's* tests after 20 minutes

Colour presumptive test results after 20 minutes

	Marquis	***Mandelin***	***Simon***	***Robadope***
Blank	Colourless	Intense yellow	Peach	Light brown
23	-	Lime	-	-
24	-	Lime	-	-
25	-	Lime	-	-

Table 4-8 Colour changes of the FEC regioisomers using *Scott*, *Zimmerman*, *Liebermans*, and *Chen Kao* tests, after 20 minutes

Colour presumptive test results after 20 minutes

	Scott	***Zimmerman***	***Liebermans***	***Chen Kao***
Blank	Peach	Colourless (Cloudy)	Colourless (Cloudy)	Blue
23	Light Orange	Cloudy	-	-
24	Light Orange	Brown	-	-
25	Light Orange	Brown	-	-

4.6 Gas chromatography–mass spectrometry

GC-MS was used for identifying the compounds and the impurities in the samples. The underivitized GC-MS analysis of the mixture of the three isomers resulted in overlap of the peaks. Since the GC-MS method is only limited to volatile compounds, the fluoro*eth*cathinone derivatives required derivitisation with acetyl chloride in order to resolve and separate the three FEC isomers from each other, prior to the analysis. However, as mentioned in Section 1.4, the derivitised FEC isomers are unstable and degrade at high temperature, therefore resulting in considerable deformation of the peaks. The samples remain stable for 24 hours; this allows enough time to analyse the compounds throughout a day. Moreover, eicosane was employed as a reference in all cases.

Analysis of spectra of both non-derivitised and derivitised compounds demonstrated that derivatisation is the way forward for these compounds, as the three derivatised compounds are very close to being baseline separated. The GC-MS spectra of all the non-derivitised and derivitised compounds revealing their Retention times (R_t) are presented in figures 4-28 to 4-35.

Table 4-9 Retention times (R_t) of the non-derivitised and derivitised compounds

Analyte	Retention times (R_t) of Non-derivitised/ min	Retention times (R_t) of Derivitised/ min
Eicosaine	12.53	16.57
23	5.86	13.75
24	5.99	12.99
25	6.05	12.67

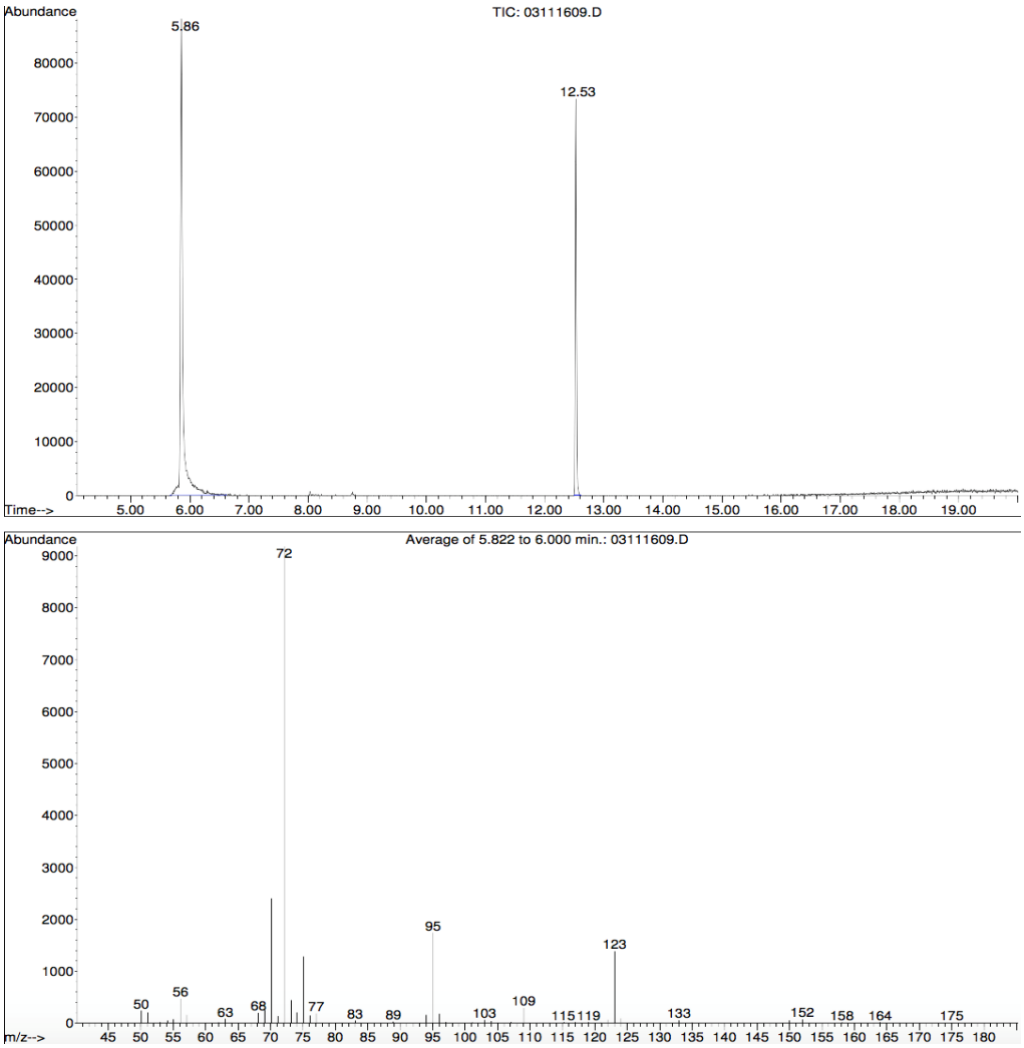

Figure 4-28. GC-MS spectrum of underivitised **23** in the presence of eicosane at R_t = 12.53 min

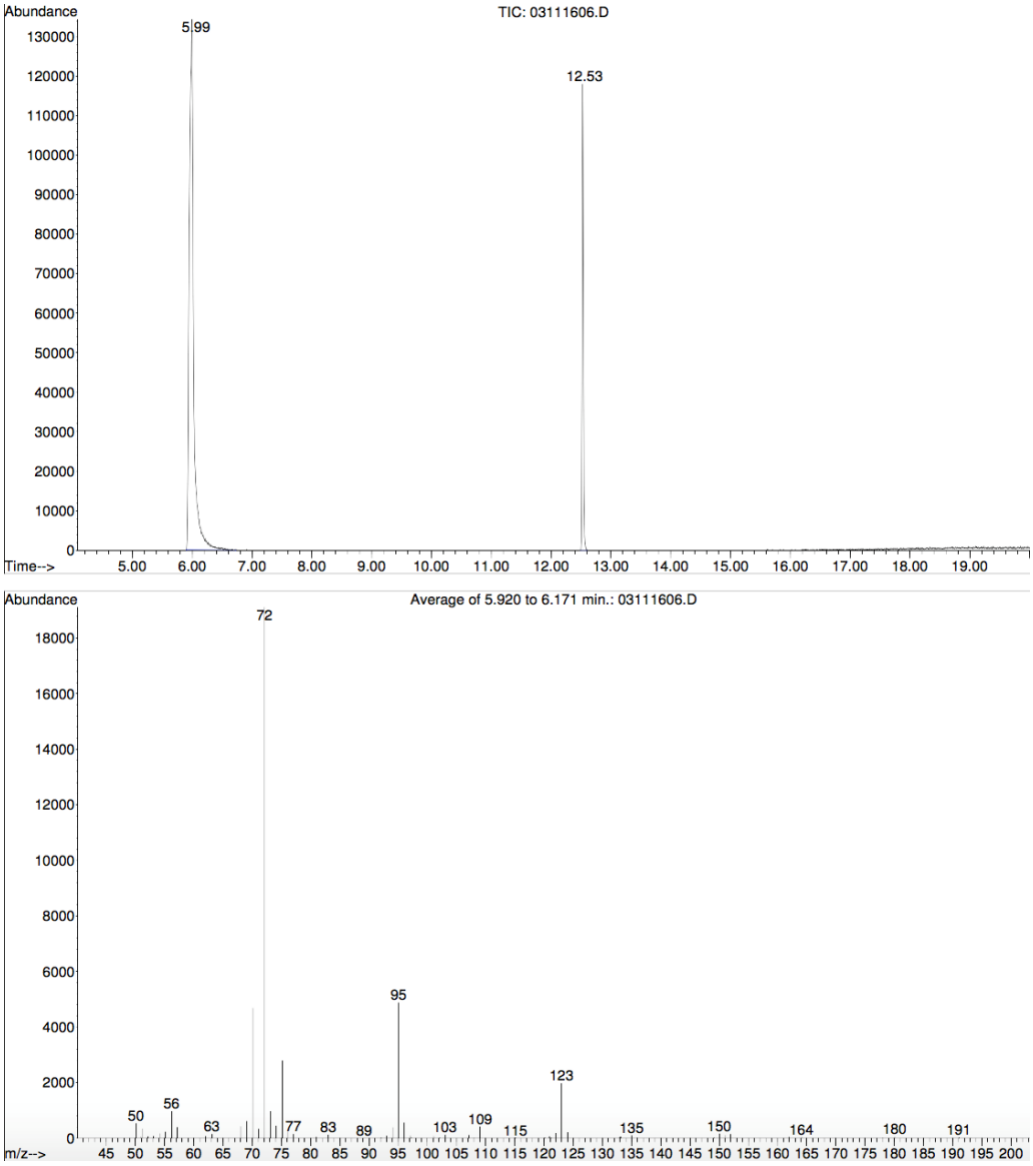

Figure 4-29. GC-MS spectrum of underivitised **24** in the presence of eicosane at R_t = 12.53 min

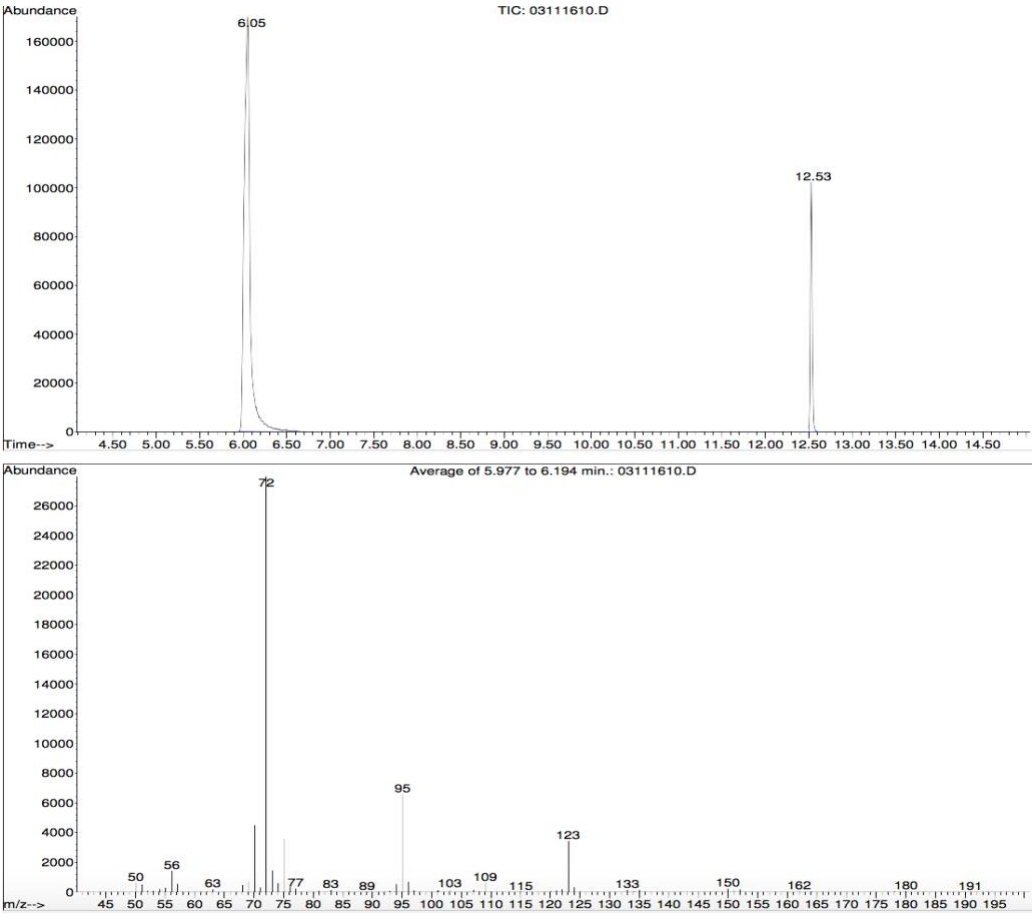

Figure 4-30. GC-MS spectrum of underivitised **25** in the presence of eicosane at R_t = 12.53 min

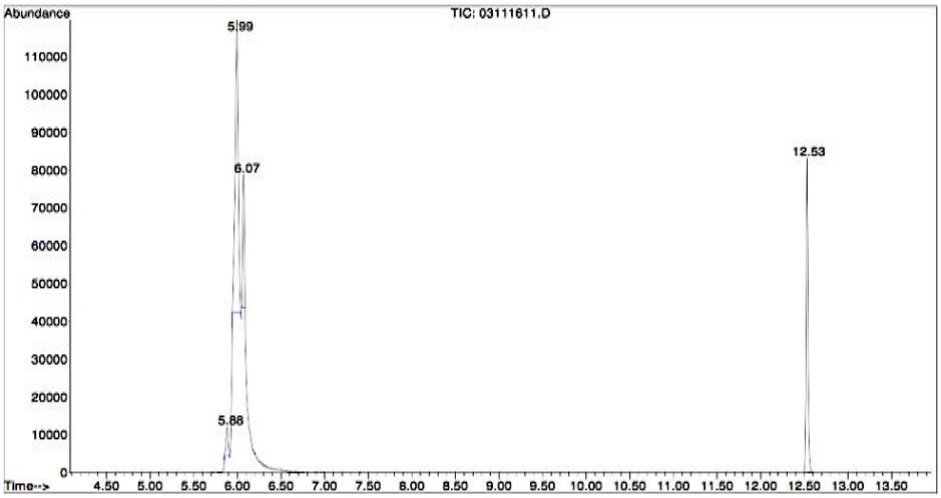

Figure 4-31. GC-MS spectrum of underivitised mixture of FEC isomers in the presence of eicosane. Peak at 12.53 min is eicosane

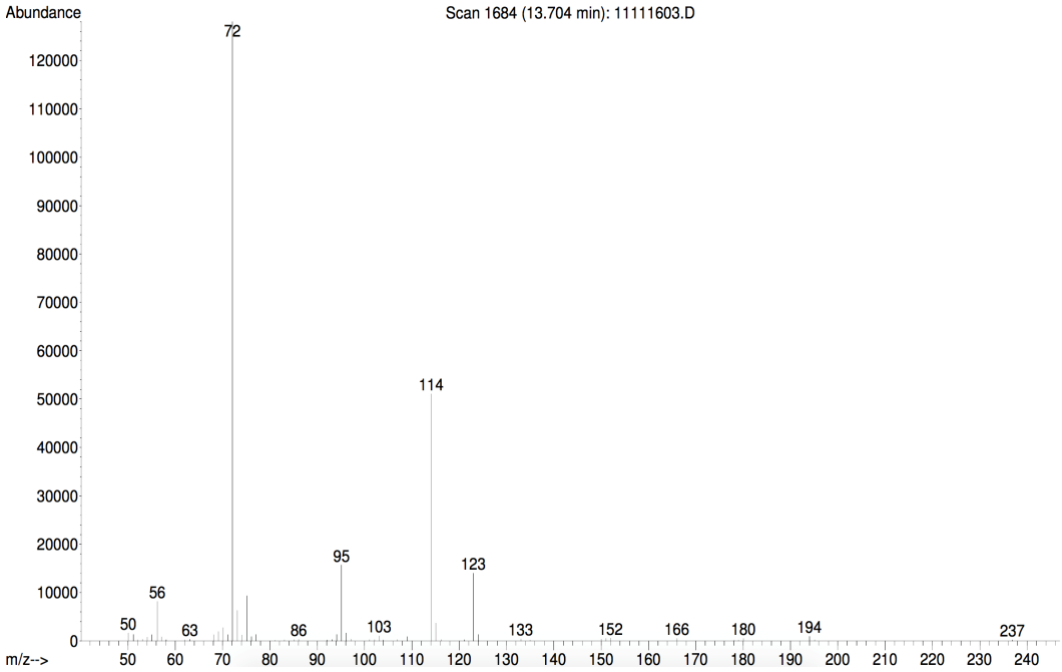

Figure 4-32. MS traces of derivitised **23** in the presence of eicosane at R_t = 16.57 min

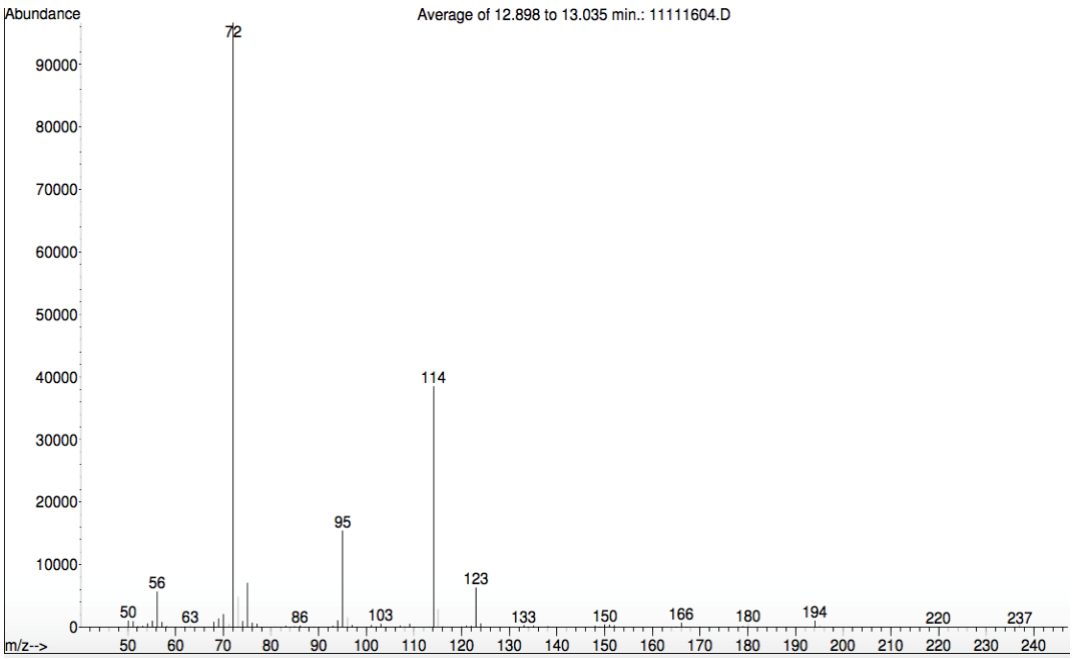

Figure 4-33. MS traces of derivitised **24** in the presence of eicosane at R_t = 16.57 min

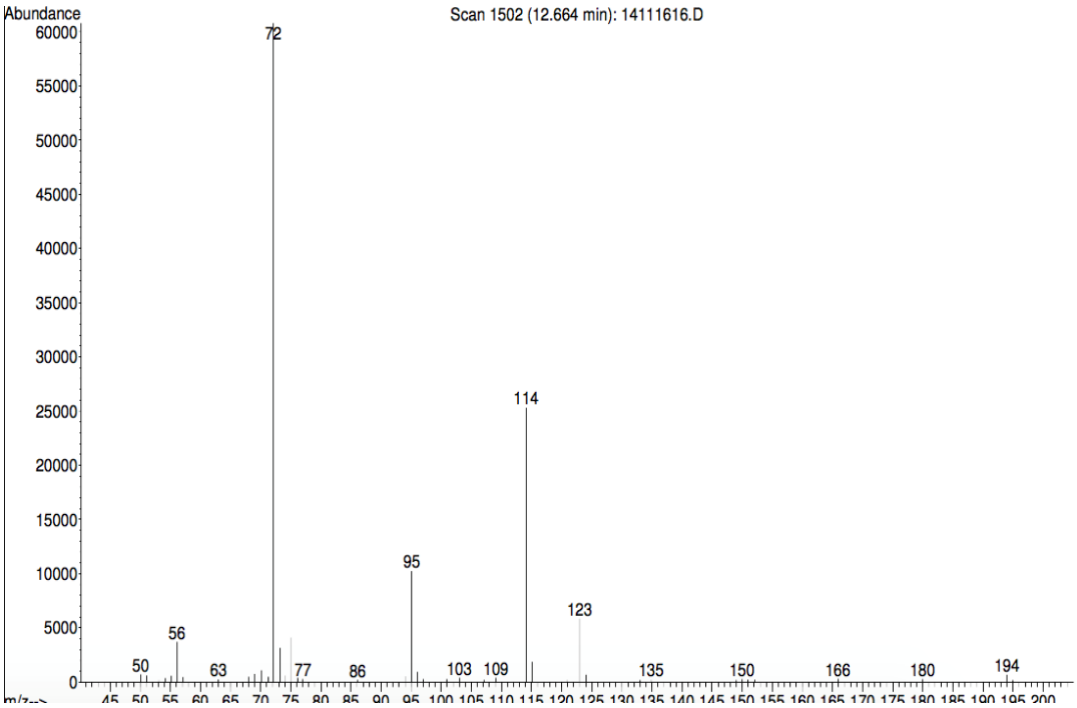

Figure 4-34. MS traces of derivitised **25** in the presence of eicosane at R_t = 16.57 min

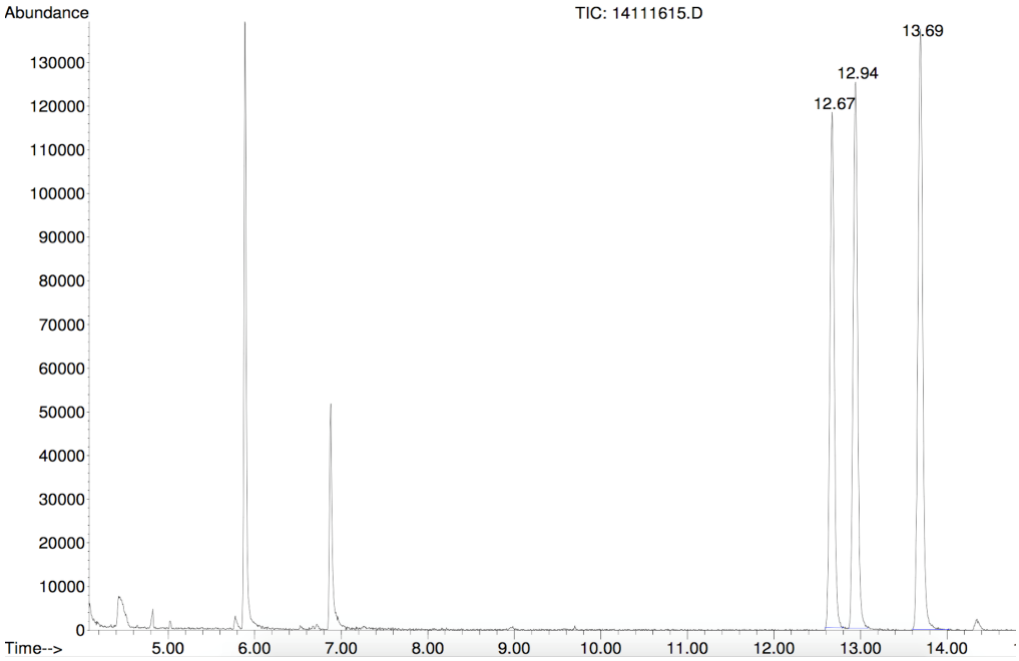

Figure 4-35. GC-MS chromatogram of derivitised mixture of FEC isomers in the presence of eicosane at R_t = 16.57 min which has been truncated

Chapter 5 Results and discussion of reduced FEC compounds

5.1 Nuclear Magnetic Resonance (NMR) results of reduced fluoroethcathinone (ethylephedrine)

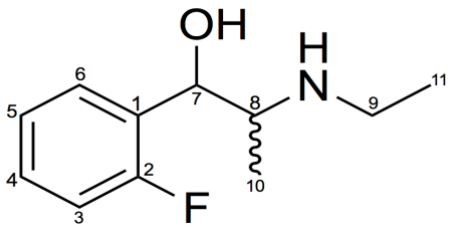

26

Figure 5-1. Structure of reduced 2-FEC (**26**)

The carbonyl group of the regioisomers of FEC was reduced to an alcohol to produce ethylephedrine using anhydrous methanol and sodium borohydride. The ^{1}H NMR spectrum of reduced 2-FEC (**26**) is shown in Fig 5-2. The structure of **26** possesses nine unique ^{1}H NMR environments and this is reflected in the ^{1}H NMR spectrum. The amine and alcohol hydrogen nuclei are not observed, most likely due to exchange with deuterium. Similar to **23**, the presence of J_{HF} coupling in the aromatic ring enables the position of the ^{1}H nuclei to be located. For instance, in comparison to **23**, the proton located on position 6 retains a $^{3}J_{HH}$ coupling of 7.5 Hz and appears as a triplet. The proton located on carbon 3 also forms a $^{3}J_{HH}$ coupling to the proton located on carbon 4 and a $^{3}J_{HF}$ to the fluorine located on carbon 2. As a result, it appears as a multiplicity of a doublet of doublets. The $^{3}J_{HH}$ coupling from the proton on carbon 3 to the one on position 4 is reflected in the observation of a cross peak in the ^{1}H-^{1}H COSY spectrum (Fig. 5-3).

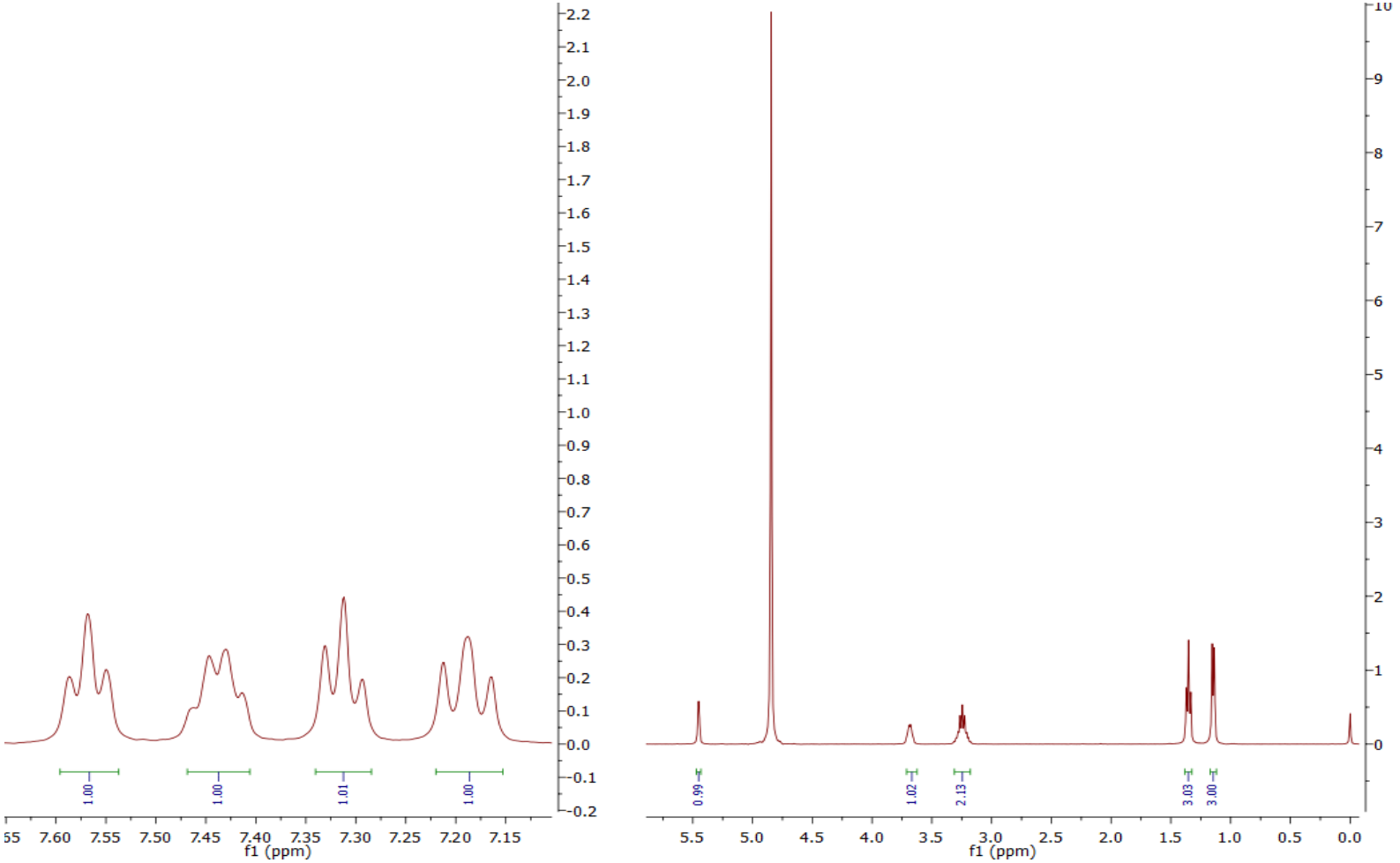

Figure 5-2. ^{1}H NMR spectrum of **26** collected in D_2O

Major changes are observed in **23** compared to **26** with respect to the side chain possessing the alcohol group instead of the carbonyl moiety. An additional signal is present due to the formation of a CH group between the aromatic ring and the chiral centre. This peak presents itself as a doublet with a $^{3}J_{HH}$ coupling of 3.4 Hz, due to coupling to the proton residing on the chiral centre. Moreover, a cross peak is observed in the ^{1}H-^{1}H COSY NMR spectrum.

Due to the change from carbonyl moiety to the alcohol group, the peak multiplicity of the chiral centre changed; this peak was observed at δ 3.68 in the ^{1}H NMR as a doublet with two $^{3}J_{HH}$ couplings of 9.1 and 6.0 Hz. A cross peak is observed in the ^{1}H-^{1}H COSY NMR spectrum; the chiral centre has a cross peak to the protons located on the adjacent carbon atom at δ 1.15. The rest of the peaks related to the side chains are unaffected in the reduced form.

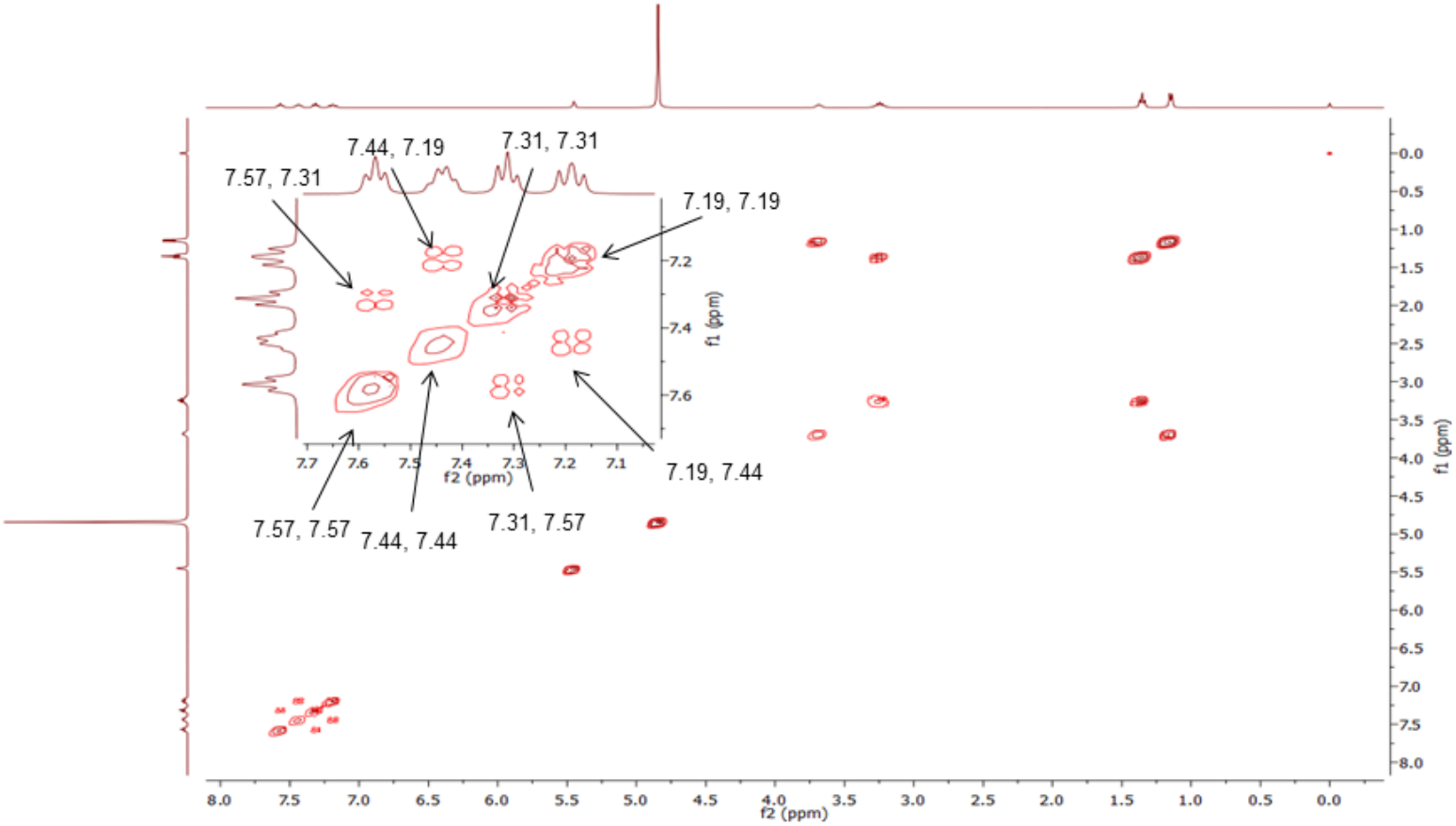

Figure 5-3. ^{1}H-^{1}H COSY NMR spectrum of **26** collected in D_2O

Similar to **23**, the $^{13}C\{^{1}H\}$ NMR spectrum of **26** (Fig. 5-4) reveals 11 unique carbon environments, because the numbers of carbons are unaltered. When the $^{13}C\{^{1}H\}$ DEPT-135 spectrum was collected (Fig. 5-5), this simplified to nine environments. The carbon located in the aromatic ring that possesses a one-bond coupling to ^{19}F (carbon 2) is not observed because the carbon centre is effectively “quaternary”. In **26**, the carbonyl carbon (located at δ 198.0 in **23**) was not observed since it has been reduced. The corresponding CH group appears at δ 66.1. In addition, the hydrogen located on carbon 7 is now visible in the DEPT NMR spectrum as an absorptive peak; in the analogous FEC compound this was a quaternary and so was not observed. Furthermore, the quaternary carbon of the aromatic ring (δ 126.0) is not detected in the $^{13}C\{^{1}H\}$ DEPT-135 spectrum.

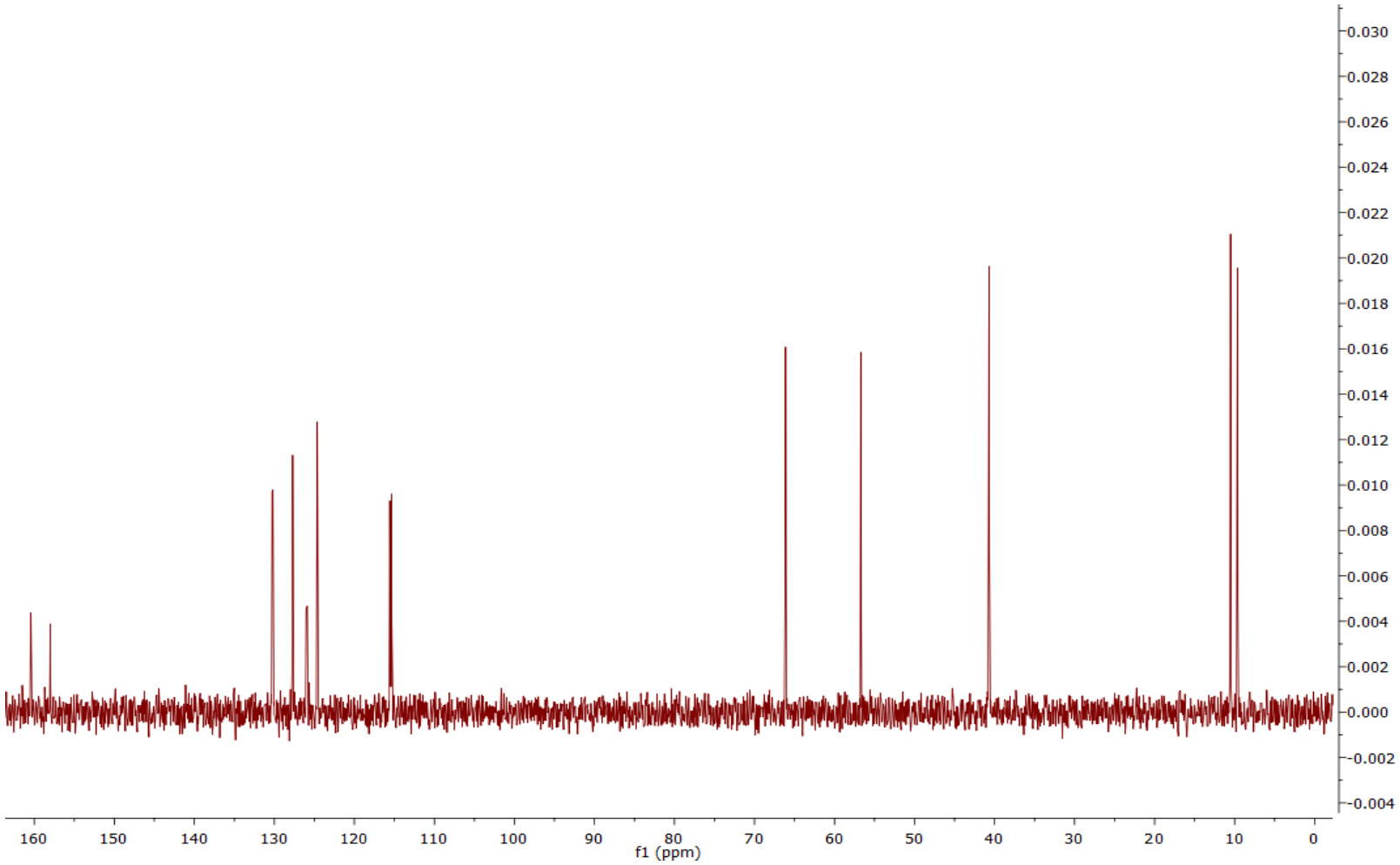

Figure 5-4. $^{13}C\{^{1}H\}$ NMR spectrum of **26** collected in D_2O

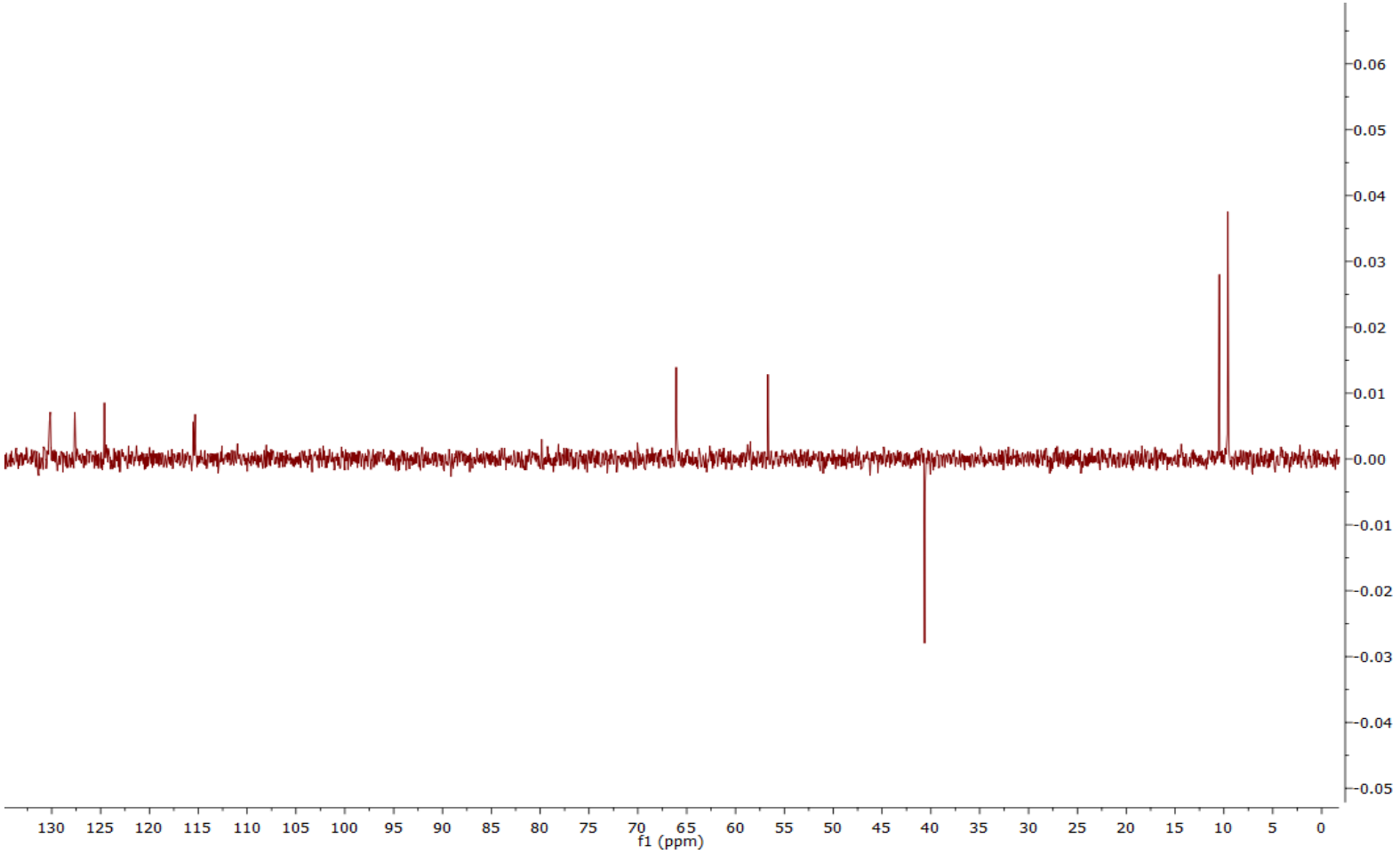

Figure 5-5. $^{13}C\{^{1}H\}$ DEPT-135 NMR spectrum of **26** collected in D_2O

The HMQC spectrum of **26** was used to connect the ^{1}H environments identified from the ^{1}H NMR spectrum to those of the ^{13}C domain. The spectrum is shown in Fig. 5-6 and the results tabulated in Table 5-1. Comparing this spectrum to the one from **23,** it is very noticeable that the only change detected is the presence of the new CH crosslinking signal. The correlations between the ^{1}H peak at 7.19 ppm and the ^{13}C peak at 115.4 ppm as well as the ^{1}H peak at 7.31 ppm and the ^{13}C peak at 124.7 ppm, relates to carbons 3 and 6 respectively.

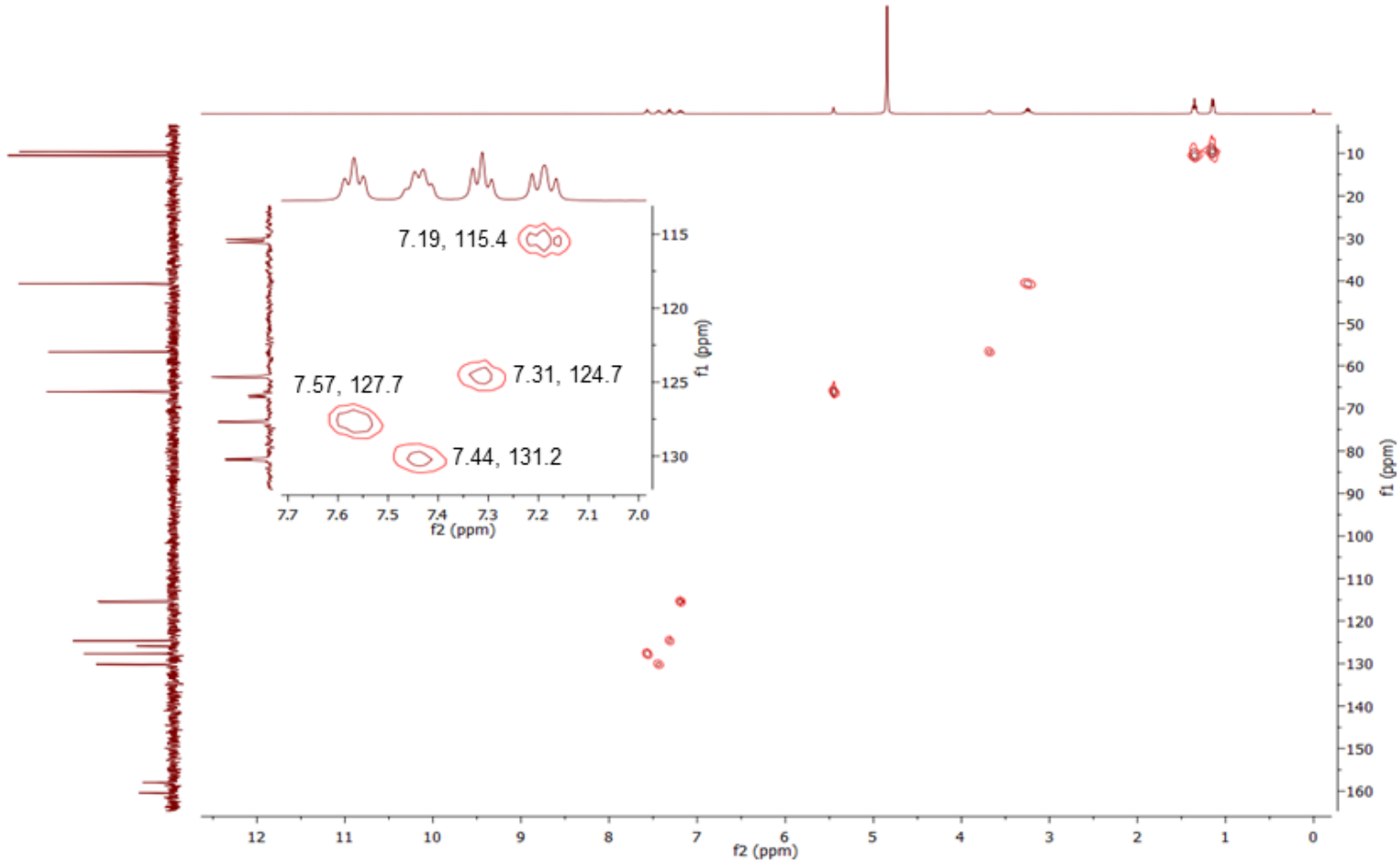

Figure 5-6. ^{1}H-^{13}C HMQC NMR spectrum of **26** collected in D_2O

Comparable to **23**, the HMBC spectrum (Fig. 5-7) of **26** identifies only one quaternary carbon at δ 126.0, which corresponds to carbon position 1, due to $^{2}J_{CH}$ interaction with proton nuclei in their local vicinity.

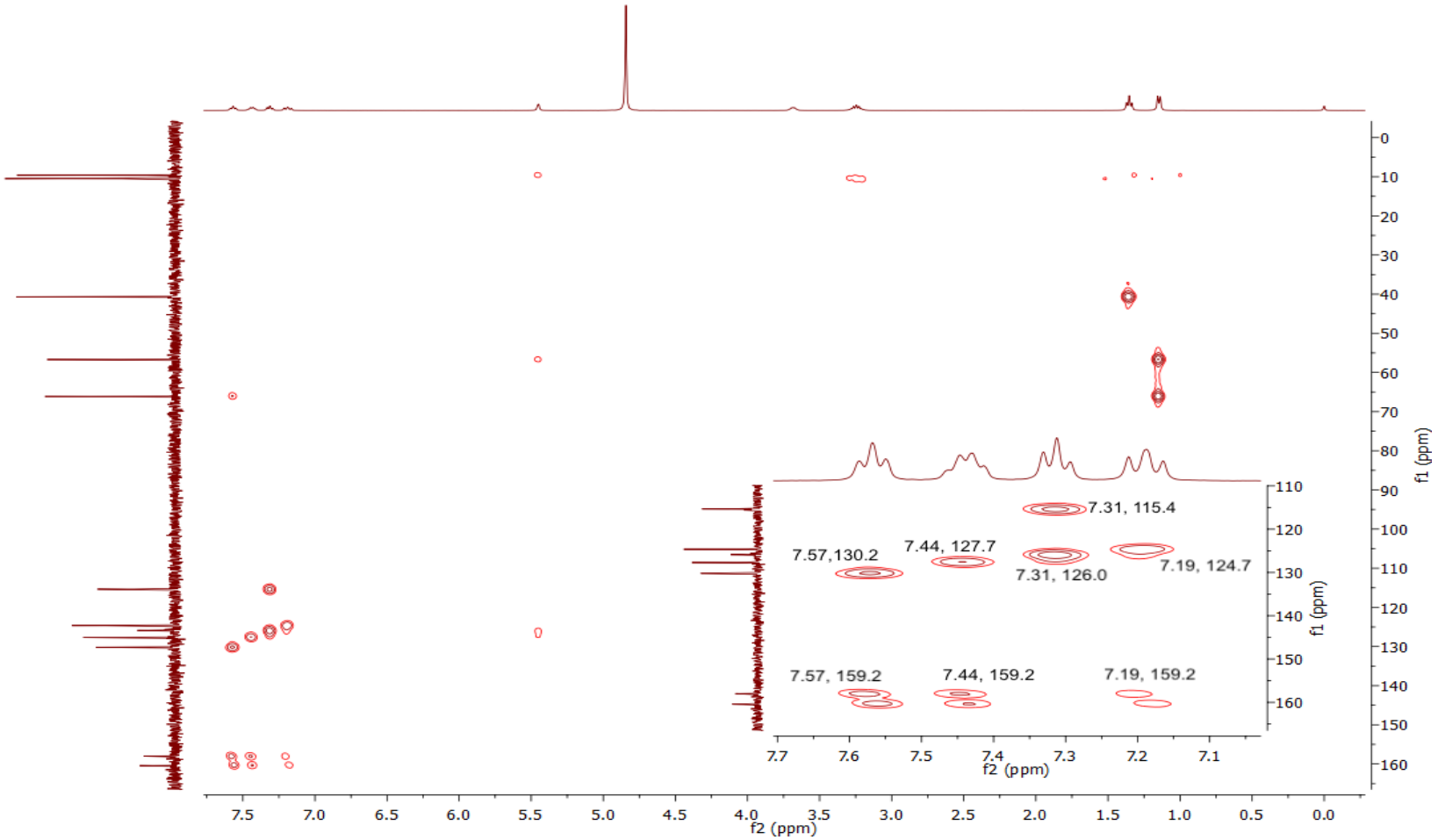

Figure 5-7. ^{1}H-^{13}C HMBC NMR spectrum of **26** collected in D_2O

26 also possesses a single ^{19}F nucleus. The $^{19}F\{^{1}H\}$ NMR spectrum (Fig. 5-7) of **26** reveals a single peak (δ -110.57). This signal is very close to the one of **23** (δ -111.75), so that they are unlikely to be distinguishable by only $^{19}F\{^{1}H\}$ NMR.

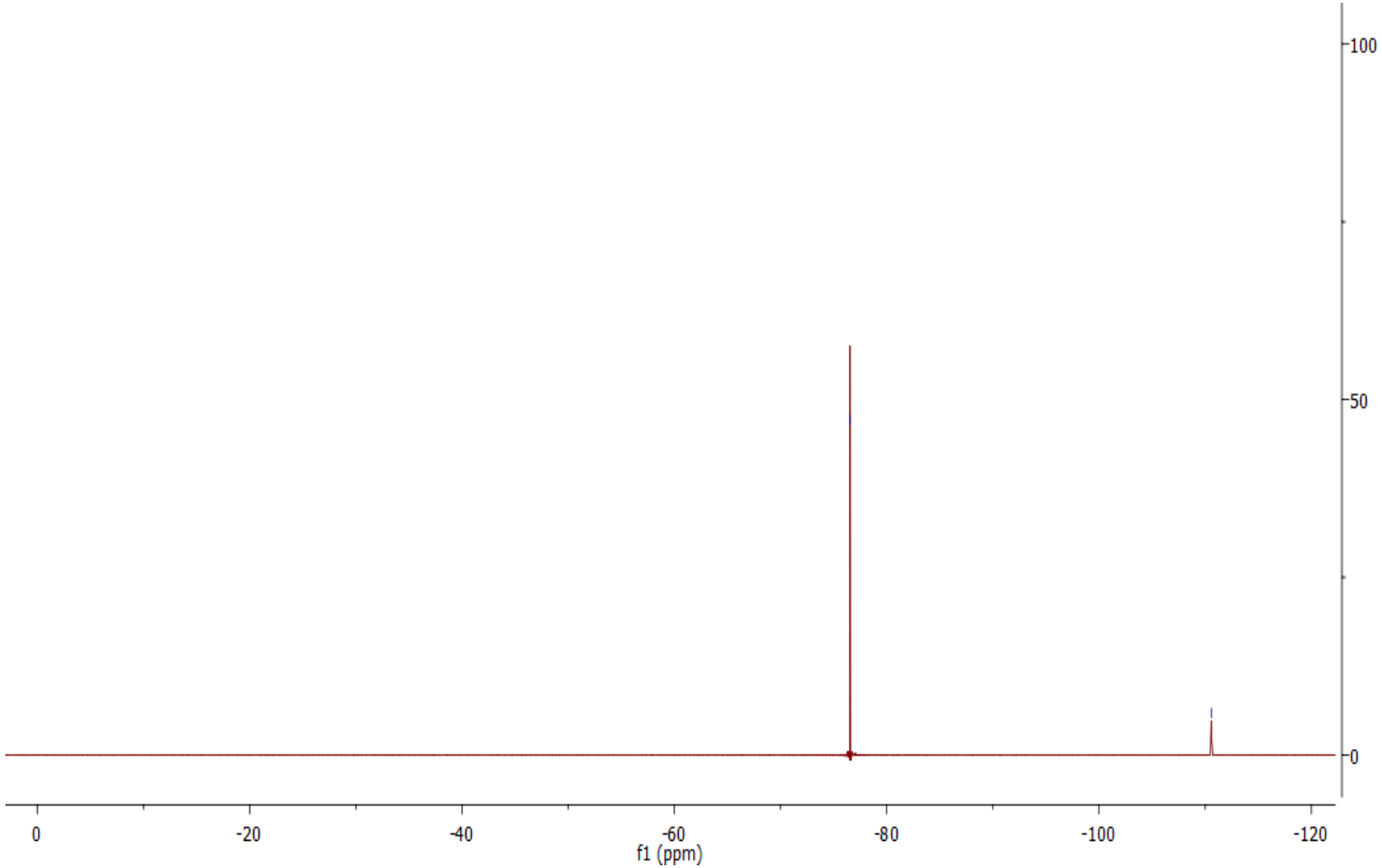

Figure 5-8. $^{19}F\{^{1}H\}$ NMR spectrum of **26** in D_2O. The signal at $\delta^{19}F$ -76.55 is TFA

Table 5-1 NMR results for **26**

Reduced 2-FEC (26)

C number	**No. Of Hs**	**^{1}H NMR:** δ / ppm, *J*-coupling (Hz)	**^{13}C{^{1}H} NMR:** δ / ppm**,** *J*-coupling (Hz)	**^{19}F{^{1}H} NMR:** δ / ppm
1	0	-	126.0, d, $^{2}J_{CF}$ = 13.2	
2	0	-	159.2, d $^{1}J_{CF}$ = 244	-110.57
3	1	7.19, dd, $^{3}J_{HH}$ = 8.3 $^{3}J_{HF}$ = 11.0	115.4, d, $^{2}J_{CF}$ = 21.6	
4	1	7.44, m	130.2, d, $^{3}J_{CF}$ = 8.7	
5	1	7.57, t, $^{3}J_{HH}$ = 7.7	127.7, d, $^{4}J_{CF}$ = 3.9	
6	1	7.31, t, $^{3}J_{HH}$ = 7.5	124.7, d, $^{5}J_{CF}$ = 8.7	
7	1	5.45, d, $^{3}J_{HH}$ = 3.1	66.1, s	
8	1	3.69, dt, $^{3}J_{HH}$ = 9.0 $^{3}J_{HH}$ = 6.0	56.7, s	
9	2	3.17, m, $^{3}J_{HH}$ = 6.8, 6.3	40.8, s	
10	3	1.15, d, $^{3}J_{HH}$ = 6.8	9.6, s	
11	3	1.37, t, $^{3}J_{HH}$ = 7.2	10.5, s	

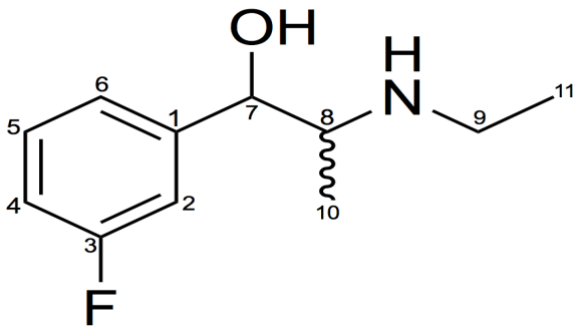

27

Figure 5-9. Structure of reduced 3-FEC (**27**)

The ^{1}H NMR spectrum of **27** is shown in Fig. 5-9. **27** produces nine unique proton environments. Again, the proton environments in the side chain incorporating the chiral centre are almost identical in all three isomers, because the side chain is unaltered, and changing the position of the fluorine atom in the aromatic ring has minimal effect on the side chain.

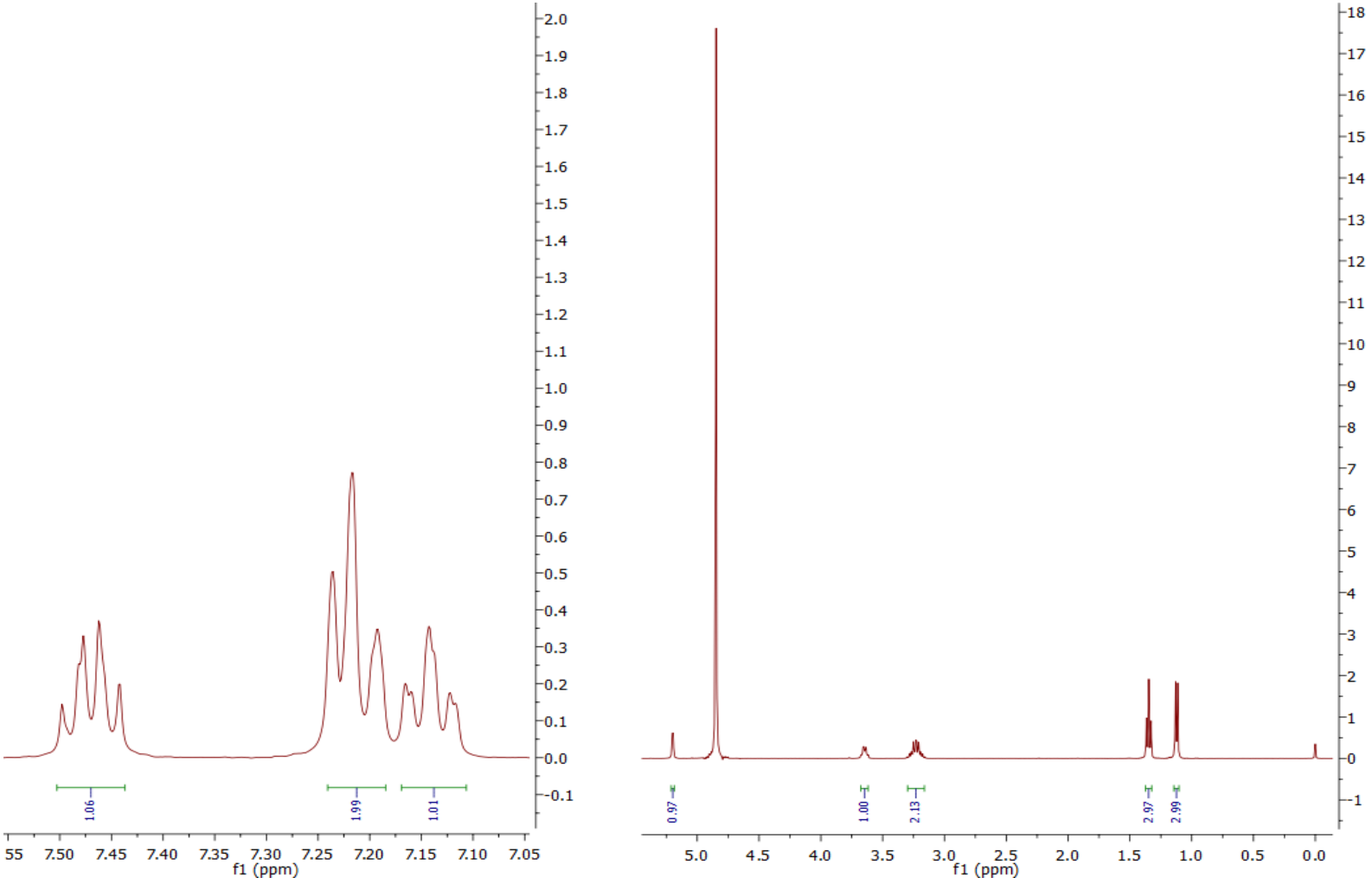

Figure 5-10. ^{1}H NMR spectrum of **27** collected in D_2O

However, comparing this side chain to the one on the FEC isomers, illustrates changes in the carbonyl group, which is now an alcohol group in the reduced form. Again, this results in the formation of an extra signal at δ 5.20 with a multiplicity of a doublet, with a $^{3}J_{HH}$ coupling of 3.2 Hz. The $^{3}J_{HH}$ coupling from the proton located on position 7 to the one located on the chiral centre is reflected in the observation of a cross-peak in the ^{1}H-^{1}H COSY spectrum (Fig. 5-11). The same observations were also made for **28**.

In the aromatic ring the position of the ^{1}H nuclei were identified using the J_{HF} coupling. The proton located on position 5 possesses a $^{4}J_{HF}$ coupling of 2.5 Hz in addition to two $^{3}J_{HH}$ and $^{4}J_{HH}$ couplings of 8.1 and 8.7 Hz . Furthermore, a cross peak is observed in the ^{1}H-^{1}H COSY NMR spectrum.

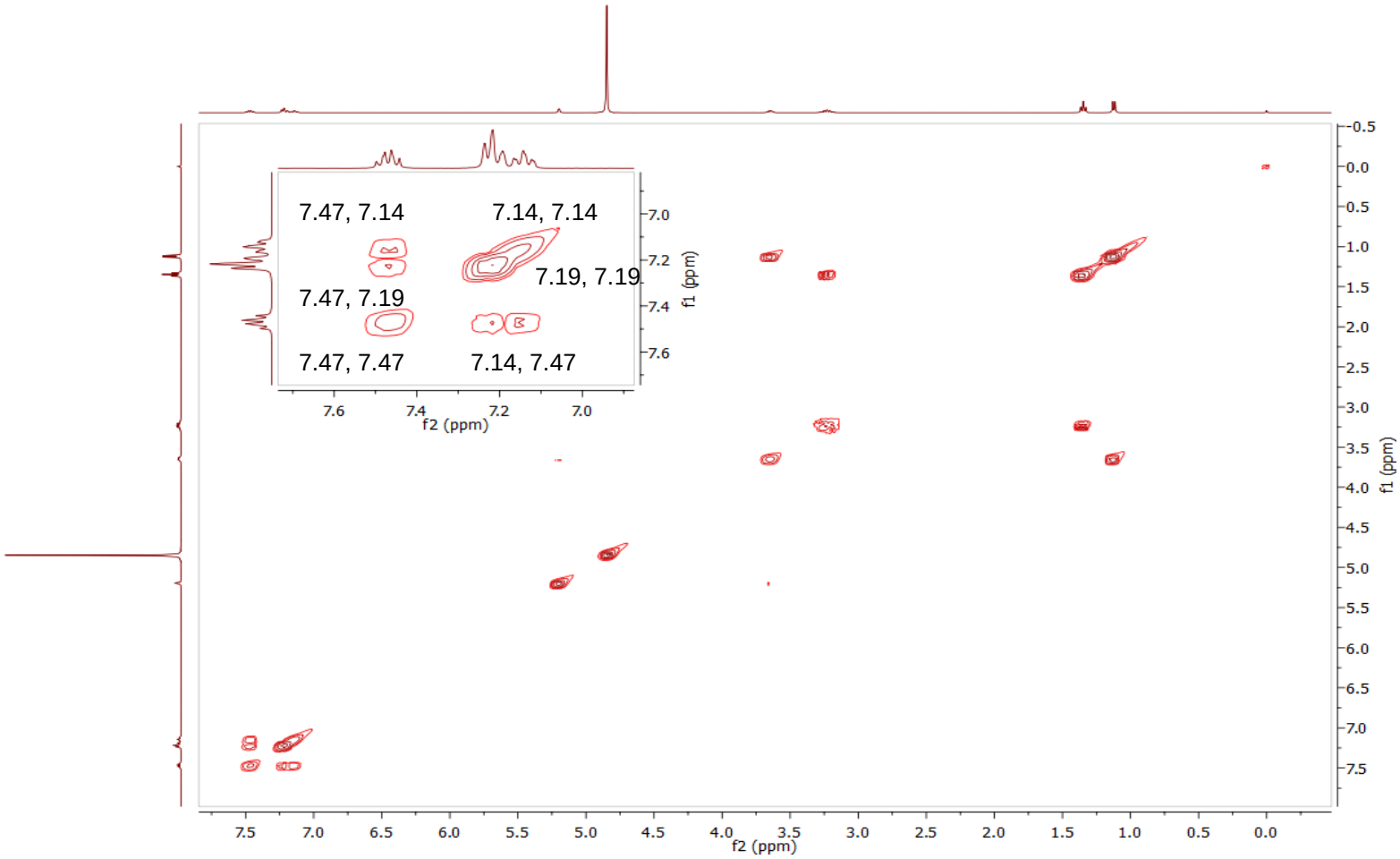

Figure 5-11. ^{1}H-^{1}H COSY NMR spectrum of **27** collected in D_2O

Similar to the $^{13}C\{^{1}H\}$ NMR spectrum of **26**, **27** (Fig. 5-12) possesses eleven unique carbon environments. When the $^{13}C\{^{1}H\}$ DEPT-135 spectrum was collected, this also simplified to nine environments. Again, the quaternary carbon and the carbon possessing the fluorine atom are not observed in the $^{13}C\{^{1}H\}$ DEPT-135 spectrum (Fig. 5-13). The carbon possessing a $^{2}J_{HF}$ coupling to the fluorine atom is found to have the highest chemical shift at δ 164.04 due to the electronegativity of fluorine leading to deshielding at this position. Moreover, the $^{13}C\{^{1}H\}$ NMR spectrum also determines that carbon 3 possesses the fluorine atom since it has the highest $^{1}J_{HF}$ coupling of 244.0 Hz.

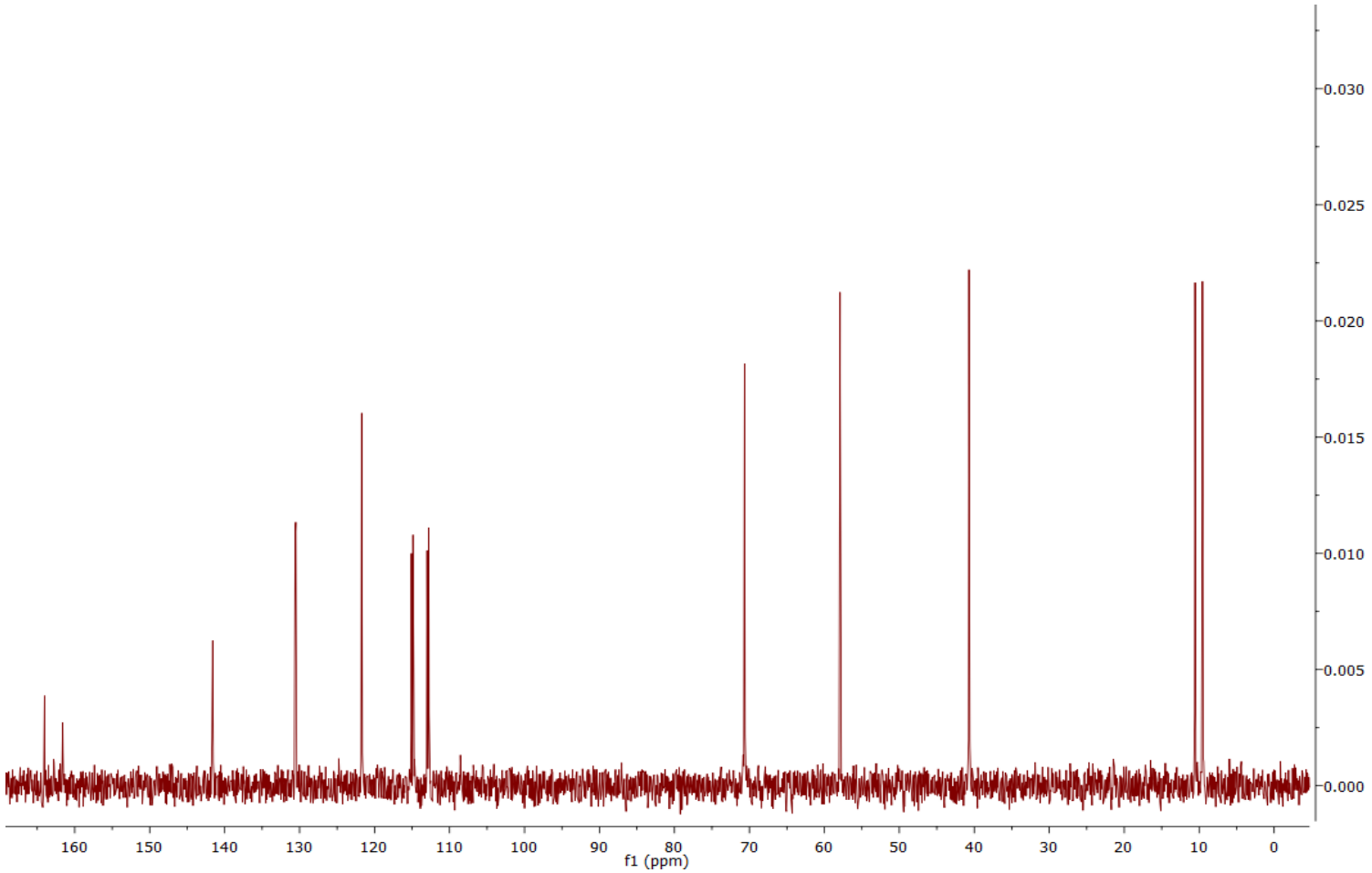

Figure 5-12. $^{13}C\{^{1}H\}$ NMR spectrum of **27** collected in D_2O

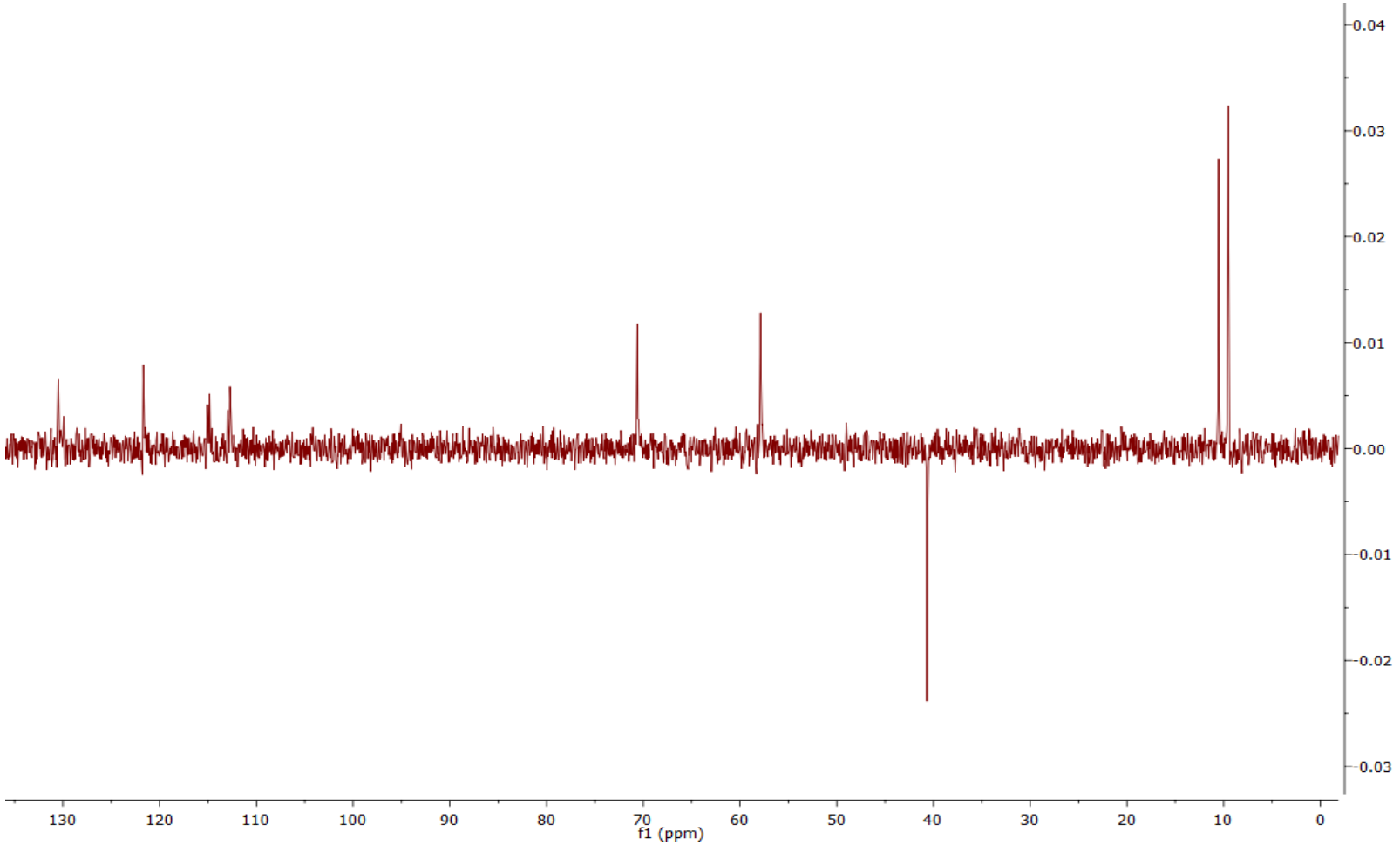

Figure 5-13. $^{13}C\{^{1}H\}$ DEPT-135 NMR spectrum of **27** collected in D_2O

The HMQC spectrum of **27** was used to connect ^{1}H environments identified from the ^{1}H NMR spectrum to those of the ^{13}C domain. The spectrum is shown in Fig. 5-14 and the results tabulated in Table 5-2.

According to the HMQC spectrum, there is a correlation between the ^{1}H peak at δ 7.47 and ^{13}C at δ 130.6; this demonstrates that the peak relates to the carbon at position 2 of the CH ring and this is the most deshielded carbon. Conversely, the carbon at position 5 has a ^{1}H-^{13}C correlation of δ 7.14 and δ 114.99 respectively, and is therefore, the most shielded CH ring site.

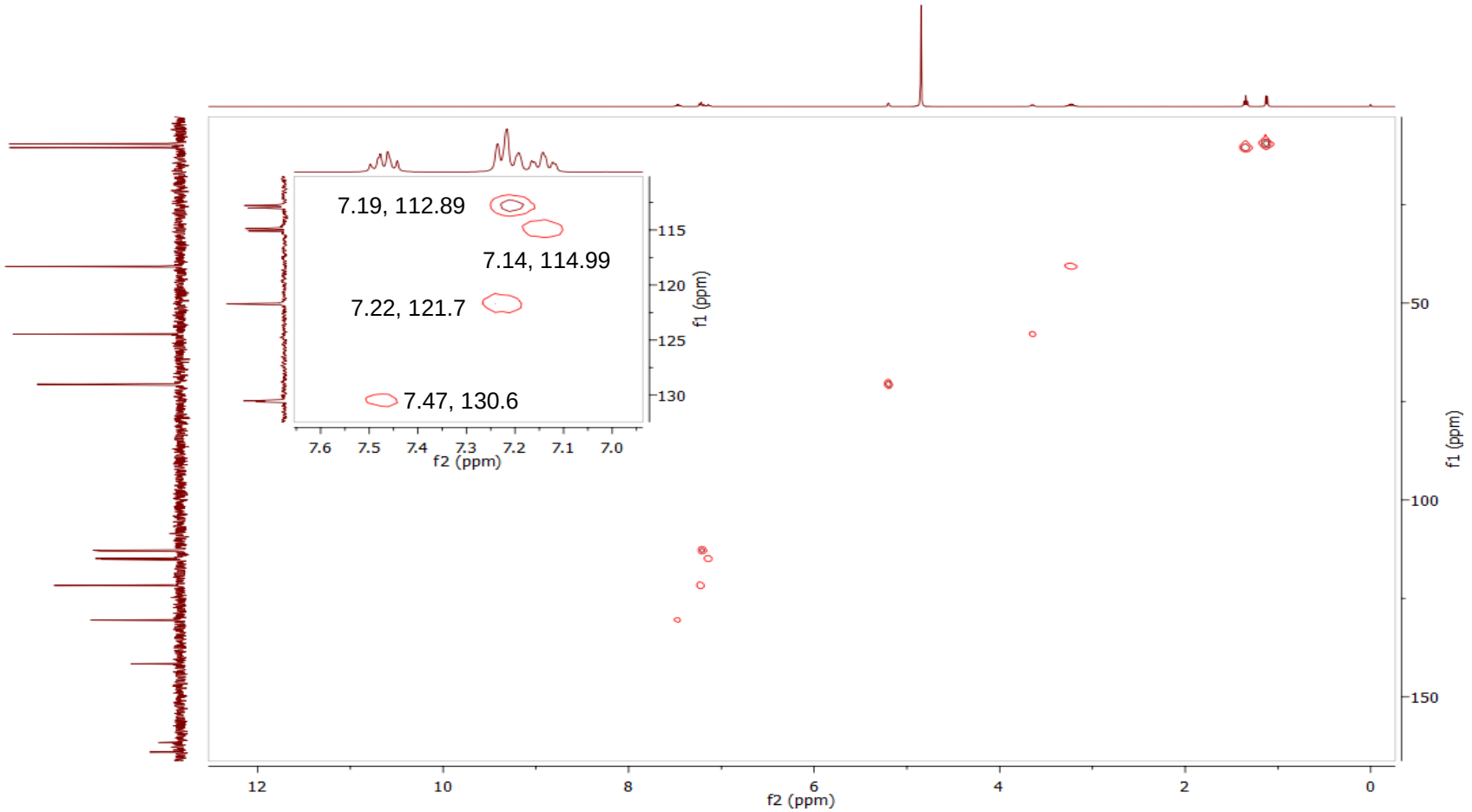

Figure 5-14. ^{1}H-^{13}C HMQC NMR spectrum of **27** collected in D_2O

The HMBC spectrum of **27** also produced only one quaternary carbon at δ 141.63. Also, the HMBC spectrum allowed the position of each carbon assigned to its corresponding proton as well as the adjacent carbon processing protons, by identifying $^{2}J_{CH}$ and $^{3}J_{CH}$ interactions (Fig. 5-15).

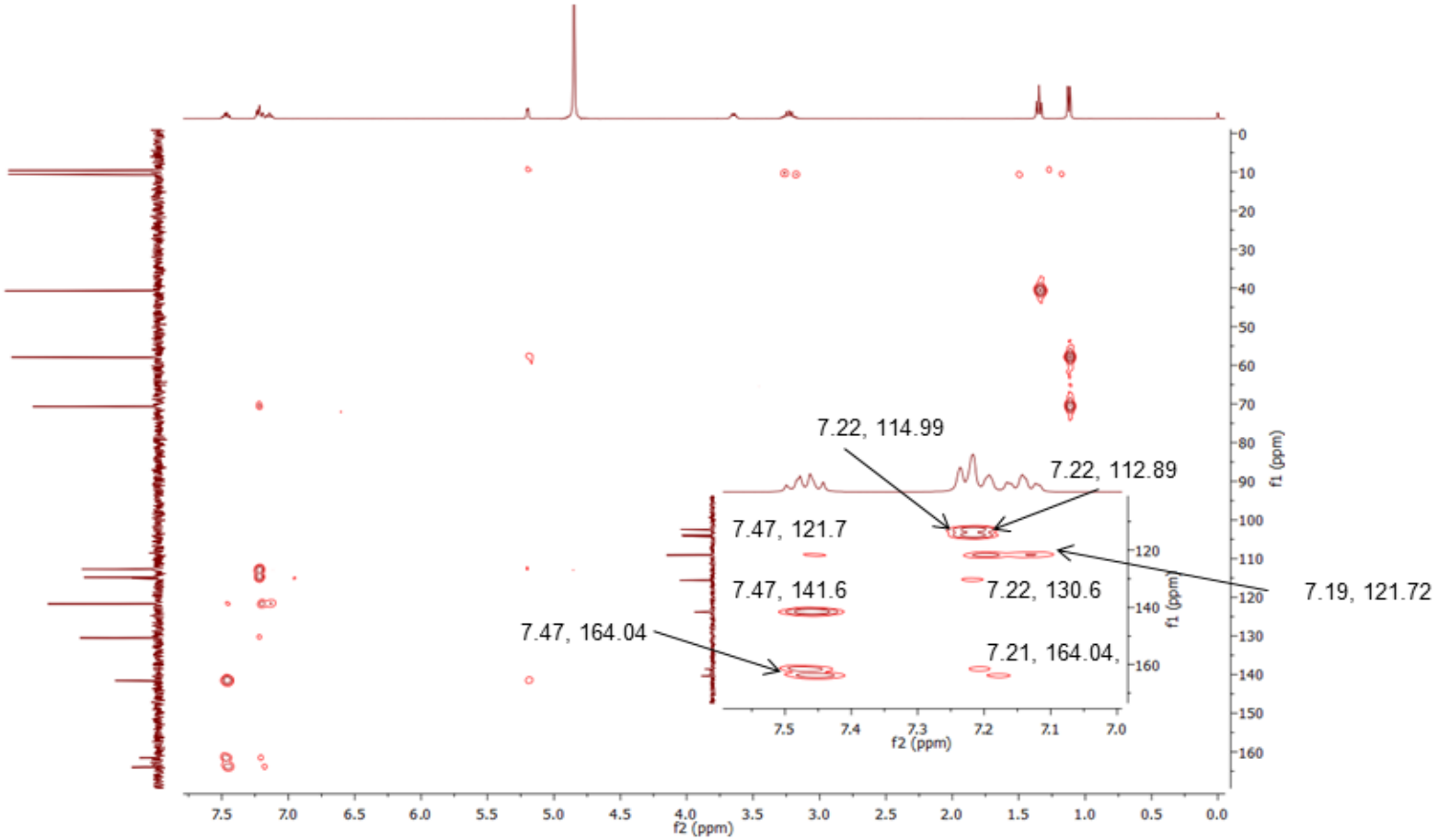

Figure 5-15. ^{1}H-^{13}C HMBC NMR spectrum of **27** collected in D_2O

Again, similar to other compounds discussed herein, **27** possesses a single ^{19}F nucleus. The $^{19}F\{^{1}H\}$ NMR spectrum (Fig. 5-16) of **27** reveals a single peak at δ -114.04, which is very similar to that of **26**. Therefore, it is difficult to distinguish between the two isomers by only $^{19}F\{^{1}H\}$ NMR spectrum analysis.

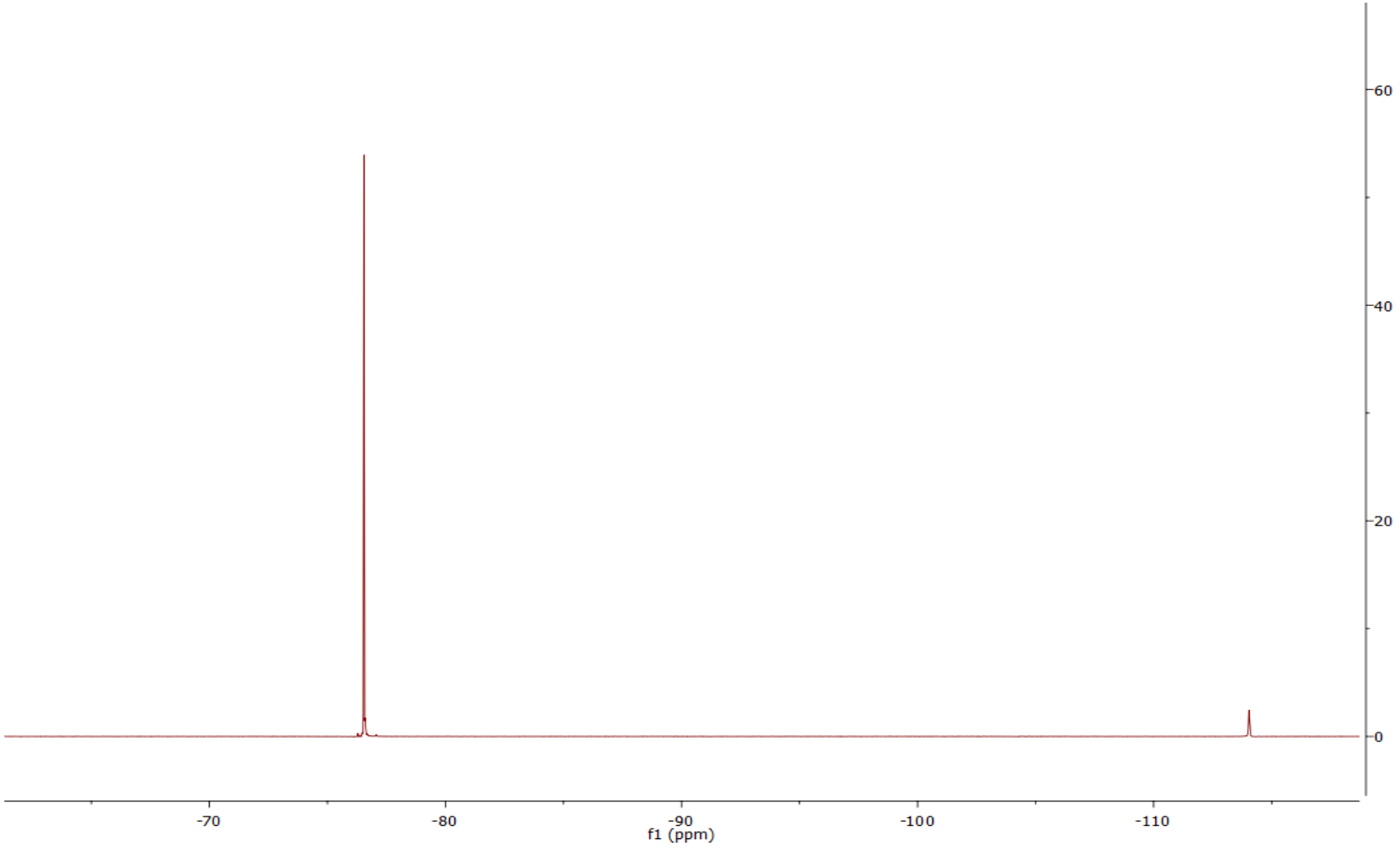

Figure 5-16. $^{19}F\{^{1}H\}$ NMR spectrum of **27** collected in D_2O. The peak at $\delta^{19}F$ -76.55 is TFA

Table 5-2 Table of NMR results for **27**

Reduced 3-FEC (27)

C number	**No. Of Hs**	**^{1}H NMR:** δ / ppm, *J*-coupling (Hz)	**^{13}C{^{1}H} NMR:** δ / ppm**,** *J*-coupling (Hz)	**^{19}F{^{1}H} NMR:** δ / ppm
1	0	-	141.63, d, $^{3}J_{CF}$ = 6.9	
2	1	7.47, td, $^{3}J_{HF}$ = 8.2, $^{4}J_{HH}$ = 6.0	130.60, d, $^{2}J_{CF}$ = 21.4	
3	0	-	164.04, d, $^{1}J_{CF}$ =244	-114.04
4	1	7.19, t, $^{4}J_{HH}$ = 2.1	121.72, d, $^{2}J_{CF}$ = 22.9	
5	1	7.14, td, $^{3}J_{HH}$ 8.7, $^{4}J_{HH}$ 8.1, $^{5}J_{HF}$ 2.5	114.99, d, $^{3}J_{CF}$ = 8.3	
6	1	7.22, m	112.89, d, $^{4}J_{CF}$ = 8.3	
7	1	5.20, d, $^{3}J_{HH}$ = 3.2	70.65, s	
8	1	3.65, qd, $^{3}J_{HH}$ = 6.9 $^{4}J_{HH}$ = 3.2	57.91, s	
9	2	3.24 m	40.70, s	
10	3	1.12, d, $^{3}J_{HH}$ = 6.9	9.6, s	
11	3	1.35, t, $^{3}J_{HH}$ = 7.3	10.5, s	

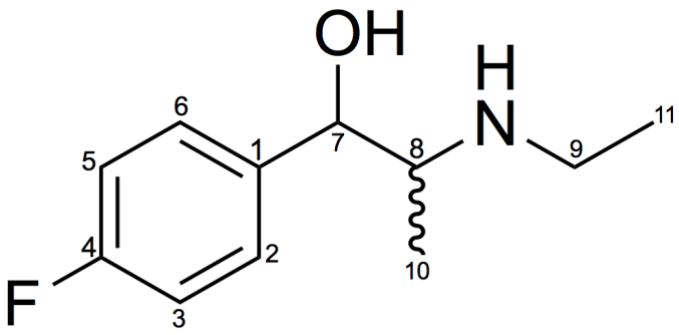

28

Figure 5-17. Structure of reduced 4-FEC (**28**)

The ^{1}H NMR spectrum of **28** is shown in Fig. 5-18. The structure of **28** possesses eight unique ^{1}H NMR environments and this is reflected in the ^{1}H NMR spectrum. The ^{1}H environments located on carbons C4/C6 and C3/C5 are identical; consequently, only two ^{1}H environments result in the aromatic ring. Therefore, in comparison to **26** and **27** there are fewer ^{1}H NMR signals observed. For example, the protons located at positions 2 and 6 appear as a multiplicity of a doublet of doublet of triplets, with a $^{4}J_{HF}$ coupling of 2.3 Hz in addition to two $^{3}J_{HH}$ and $^{4}J_{HH}$ couplings of 7.8 and 5.0 Hz, respectively. Similarly, the protons located at positions 3 and 5 appear as a multiplicity of a pseudo triplet from which a $^{3}J_{HF}$ coupling of 2.3 and a $^{3}J_{HH}$ coupling of 7.1 were identified. The $^{3}J_{HH}$ coupling from the proton located on position 2 and 6 to the ones located on position 3 and 5 and vice-versa is reflected in the observation of a cross-peak in the ^{1}H-^{1}H COSY spectrum (Fig. 5-19).

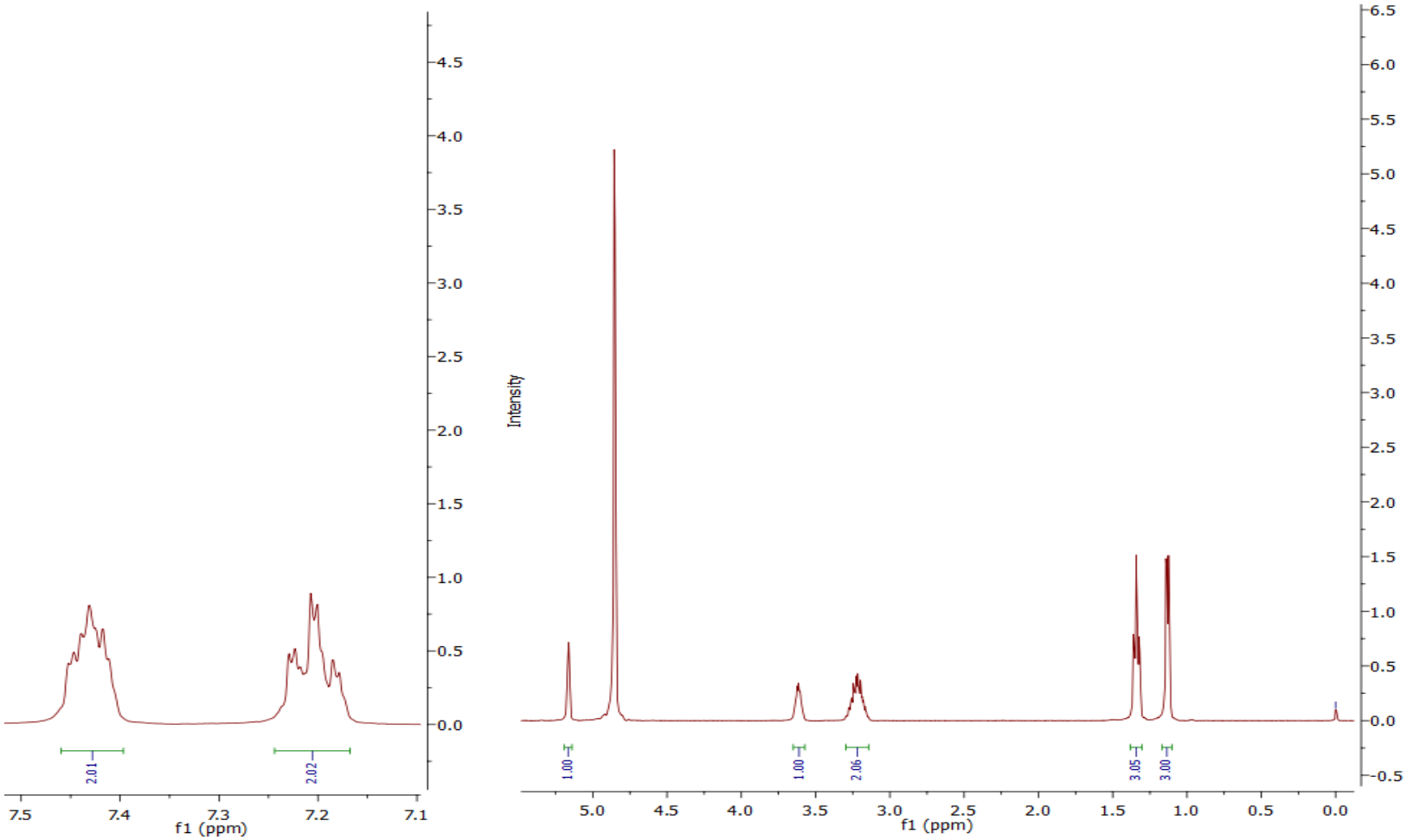

Figure 5-18. ^{1}H NMR spectrum of **28** collected in D_2O

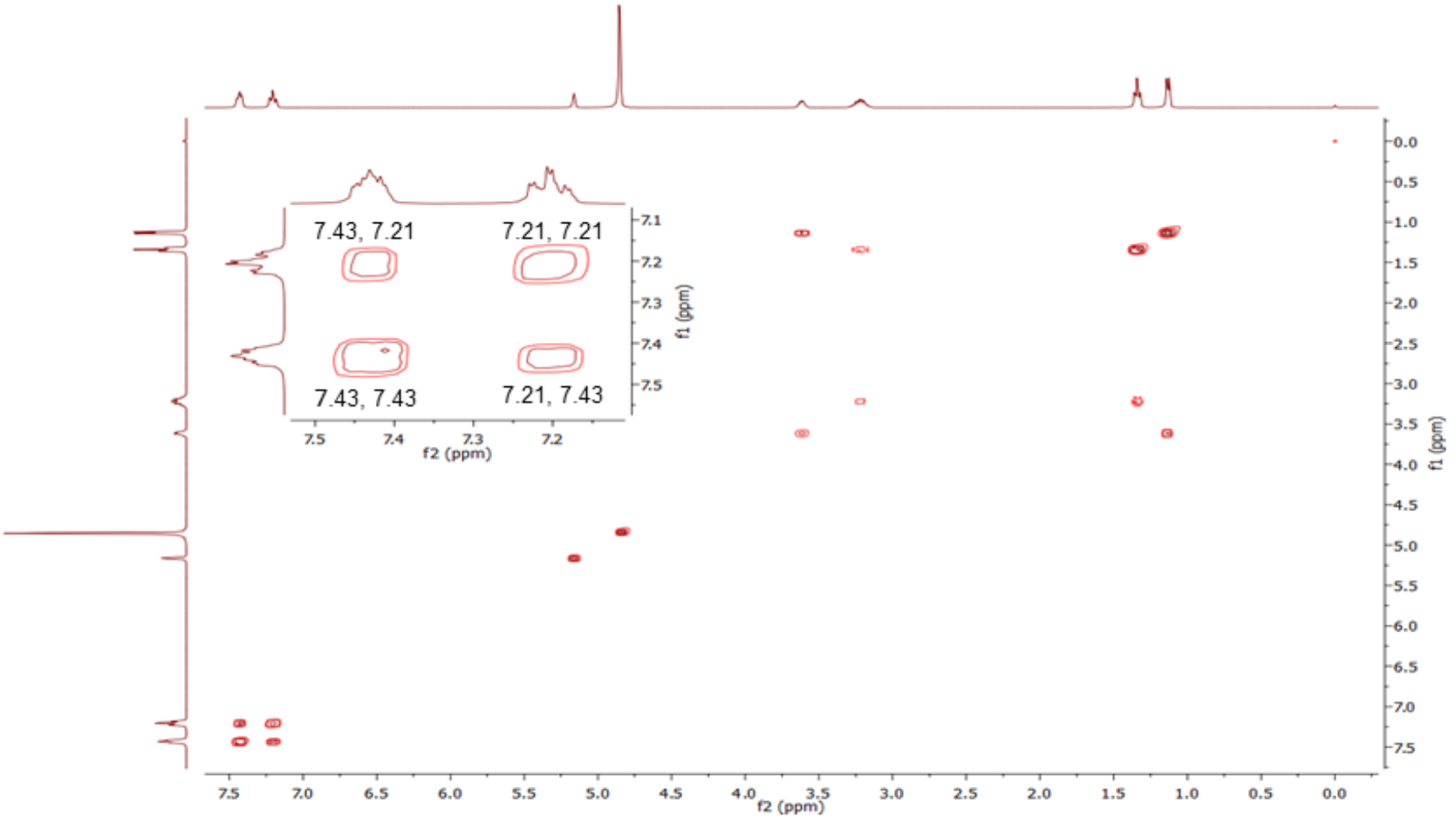

Figure 5-19. ^{1}H-^{1}H COSY NMR spectrum of **28** collected in D_2O

As with the other compounds, $^{13}C\{^{1}H\}$ NMR and $^{13}C\{^{1}H\}$ DEPT-135 spectra of **28** were also obtained (Fig 5-20 and 5-21) and revealed similar observations to other compounds studied. For example, the CH_2 moiety was identified at δ 40.7 in the ^{13}C NMR spectrum due to the presence of an emission peak in the corresponding $^{13}C\{^{1}H\}$ DEPT-135 spectrum. This is the only CH_2 in the compound.

The CH (carbon 7) is observed at δ 70.87 in both the $^{13}C\{^{1}H\}$ NMR and $^{13}C\{^{1}H\}$ DEPT-135 spectra, this also reflects the change of C=O to CH moiety. The ^{13}C chemical shift for this peak is very similar to that of **27** (δ 70.65).

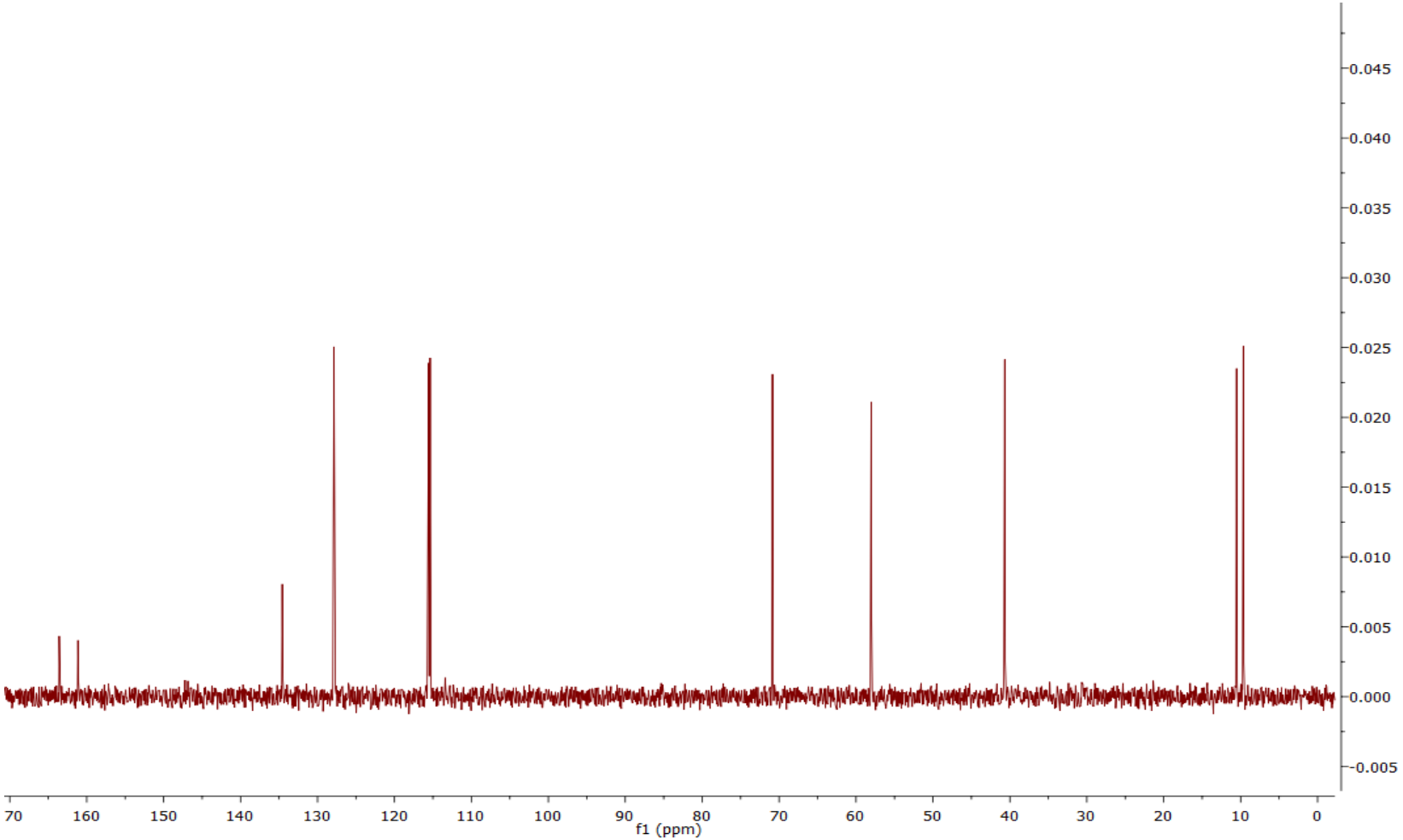

Figure 5-20. $^{13}C\{^{1}H\}$ NMR spectrum of **28** collected in D_2O

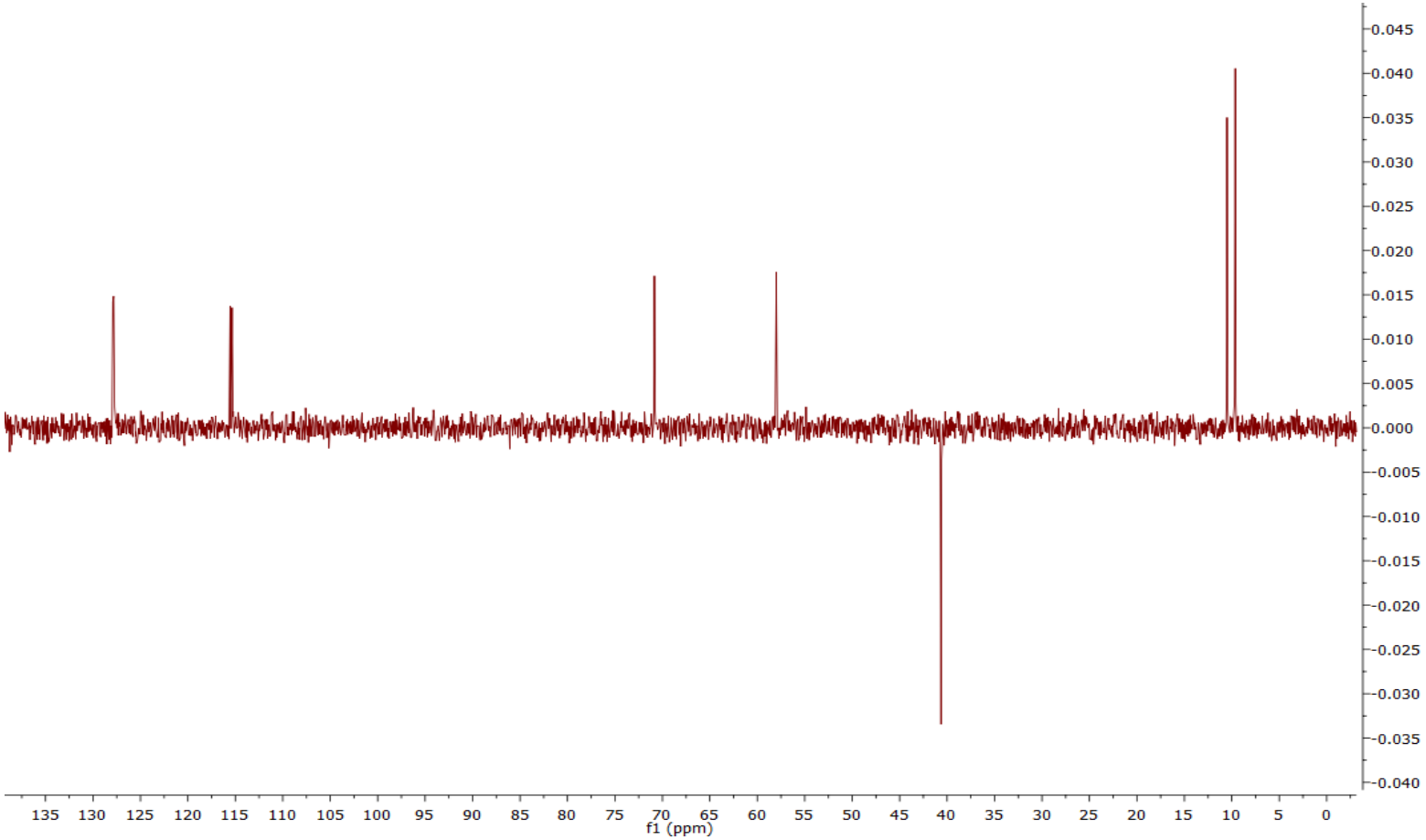

Figure 5-21. $^{13}C\{^{1}H\}$ DEPT-135 NMR spectrum of **28** collected in D_2O

The HMQC spectrum of **28** was also employed to connect the ^{1}H environments identified from the ^{1}H NMR spectrum to those of the ^{13}C domain. From the spectrum it is observed that there is a correlation between ^{1}H and ^{13}C of δ 7.21 and δ 155.5 on carbon position 2/6 as well as ^{1}H and ^{13}C correlation of δ 7.44 and δ 127.9 on carbon 3/5. The spectrum is shown in Fig. 5-22 and the results tabulated in Table 5-3.

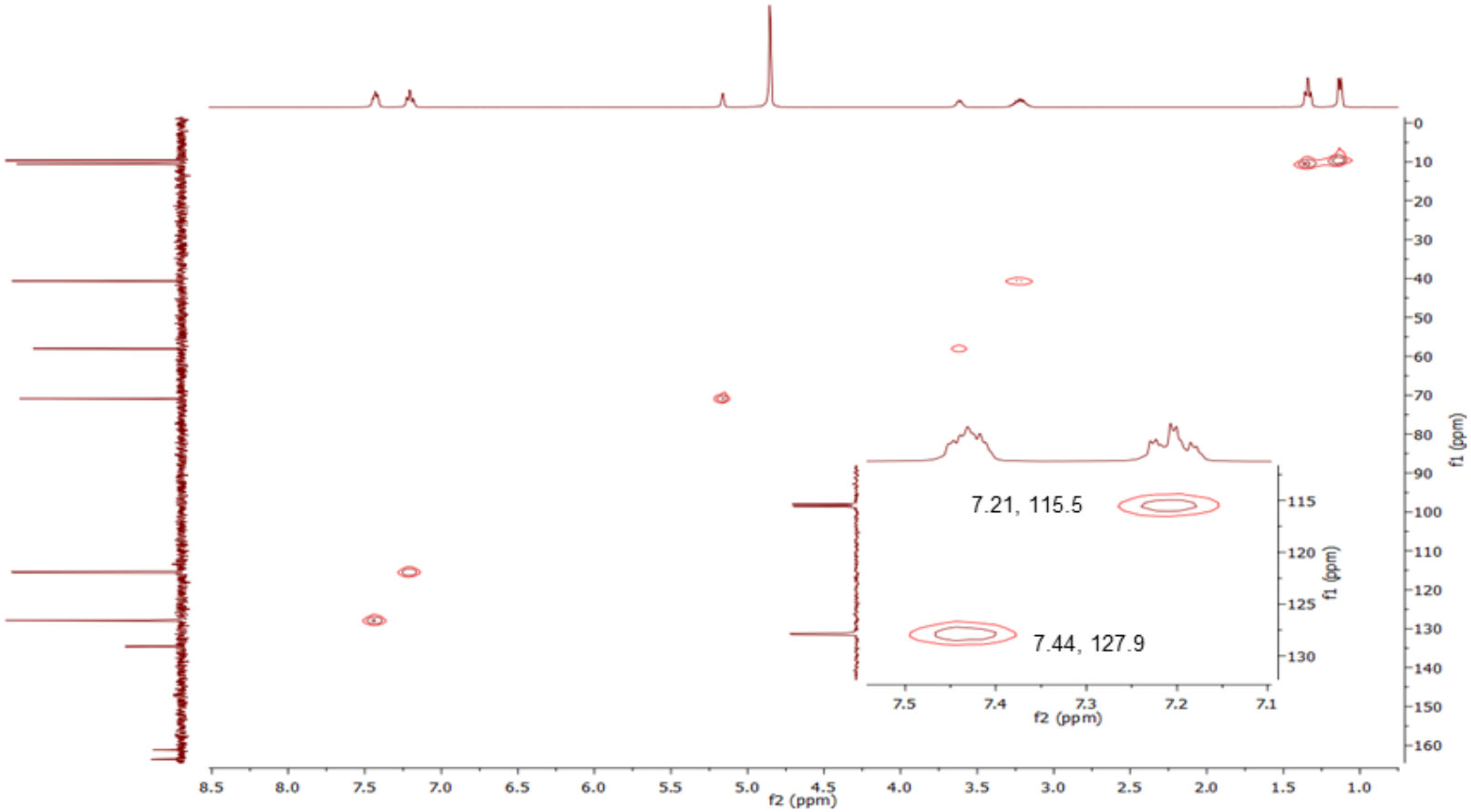

Figure 5-22. ^{1}H-^{13}C HMQC NMR spectrum of **28** collected in D_2O

The HMBC (Fig. 5-23) spectrum was collected to detect the ^{1}H-^{13}C interactions as well as to identify the quaternary carbon due to $^{2}J_{CH}$ interaction with proton nuclei in its local vicinity. This spectrum confirms that the peak at δ 134.61 in the ^{13}C NMR corresponds to the quaternary carbon at position 1.

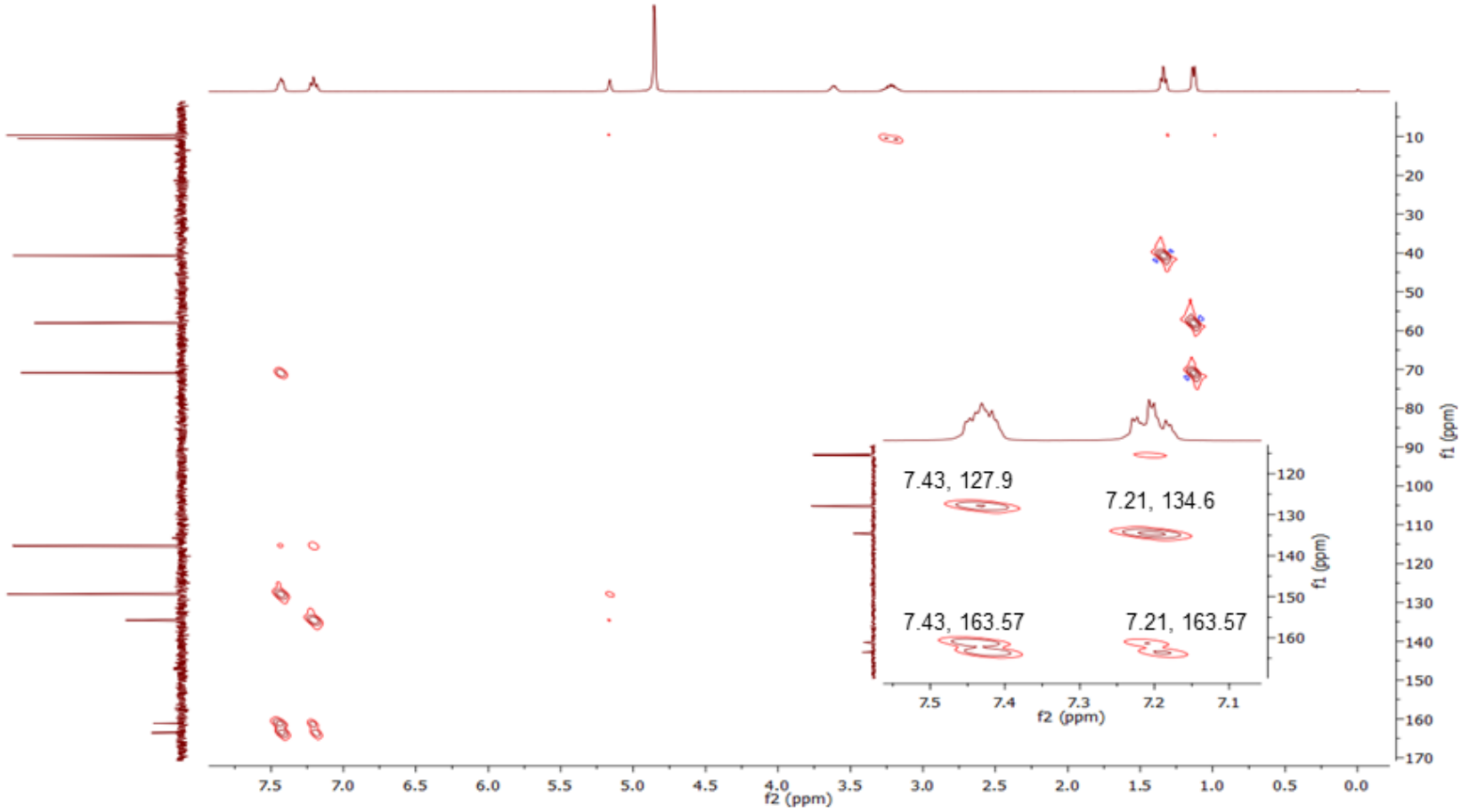

Figure 5-23. ^{1}H-^{13}C HMBC NMR spectrum of **28** collected in D_2O

As with the other FEC compounds, **28** also possesses a single ^{19}F nucleus. The $^{19}F\{^{1}H\}$ NMR spectrum (Fig. 5-24) of **28** reveals a single peak at δ -115.78.

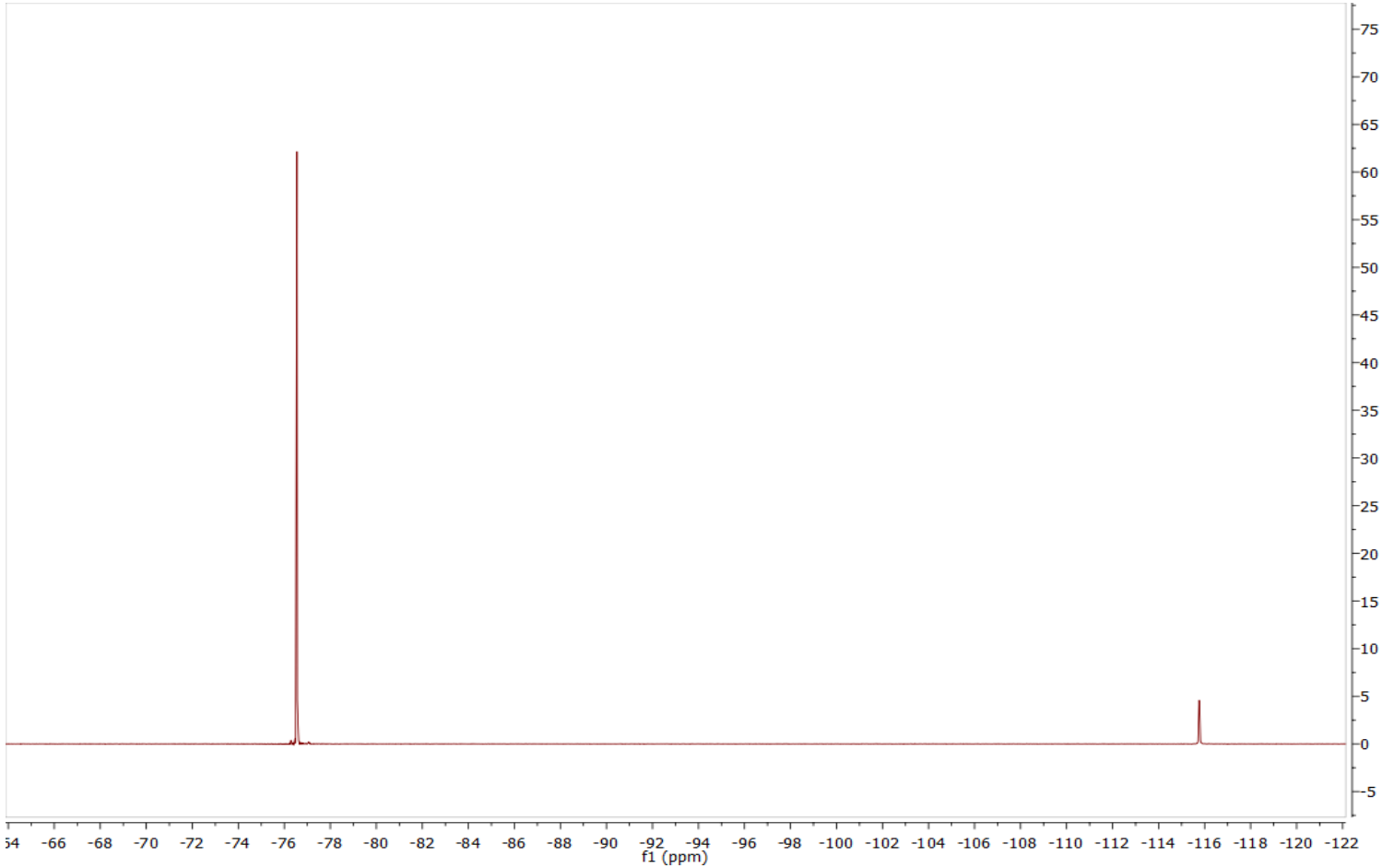

Figure 5-24. $^{19}F\{^{1}H\}$ NMR spectrum of **28** collected in D_2O.The peak at $\delta^{19}F$ -76.55 is TFA

Table 5-3 Table of NMR results for **28**

Reduced 4-FEC (28)

C number	**No. Of Hs**	**^{1}H NMR:** δ / ppm, *J*-coupling (Hz)	**^{13}C{^{1}H} NMR:** δ / ppm**,** *J*-coupling (Hz)	**^{19}F{^{1}H} NMR:** δ / ppm
1	0	-	134.6, d, $^{4}J_{CF}$ = 1.9	
2	1	7.43, ddt, $^{3}J_{HH}$ = 7.1 $^{4}J_{HH}$ = 5.0 $^{4}J_{HF}$ = 2.3	127.9, d, $^{3}J_{CF}$ = 8.5	
3	1	7.21, t $^{3}J_{HH}$ = 7.1, $^{3}J_{HF}$ = 2.3	115.5, d, $^{2}J_{CF}$ = 21.5	
4	0	-	163.57, d, $^{1}J_{CF}$ = 244	-115.78
5	Same as 3			
6	Same as 2			
7	1	5.17, d, $^{3}J_{HH}$ = 3.3	70.87, s	
8	1	3.62, dt, $^{4}J_{HH}$ = 6.4, 3.0	58.0, s	
9	2	3.23 m	40.7, s	
10	3	1.14, d, $^{3}J_{HH}$ = 6.8 $^{4}J_{HH}$ = 2.5	9.7, s	
11	3	1.34, t, $^{3}J_{HH}$ = 7.2 $^{4}J_{HH}$ = 2.4	10.52, s	

5.2 Attenuated Total Reflectance Fourier Transform infrared spectroscopy (ATR-FTIR)

The infrared spectra of the reduced FEC compounds were collected on an attenuated total reflection infrared (ATR–FTIR) spectrometer and the results are recorded in Table 5-4. **26**-**28** display strong C-O absorption bands at 1107.35, 1099.92, 1101.57 cm^{-1}, respectively. The samples also exhibit additional broad C=C absorptions at 1032.39, 1065.44, 1037.13 cm^{-1} respectively, indicative of an aromatic nucleus in all compounds, and 1577.41, 1612.79, 1604.93 cm^{-1} due to NH stretching, as well as an O-H stretch at 3297.82, 3332.51, 3351.11 cm^{-1} respectively (Fig 5-25 - 5-27).

In comparison to the FEC compounds, an O-H stretch is observed in all the reduced FEC compounds, in addition to a C-O band at around 3000 cm^{-1} instead of C=O, which verifies complete reduction of the FEC to the reduced form.

Table 5-4 Infrared analysis of the three reduced FEC isomers

STRETCH	26 / cm^{-1}	27 / cm^{-1}	28 / cm^{-1}
O-H	3297.82	3332.51	3351.11
=C-H	2981.60	2974.77	2976.99
CH_2	2792.36	2822.08	2846.13
N-H	1577.41	1612.79	1604.93
C=C aromatic	1482,05	1590.13	1570.97
C-F	1406.89	1406.45	1413.79
C-N	1218.29	1262.82	1223.04
C-O	1107.35	1099.92	1101.57
C-C	1032.39	1065.44	1037.13
C-H	792.45	788.19	777.12

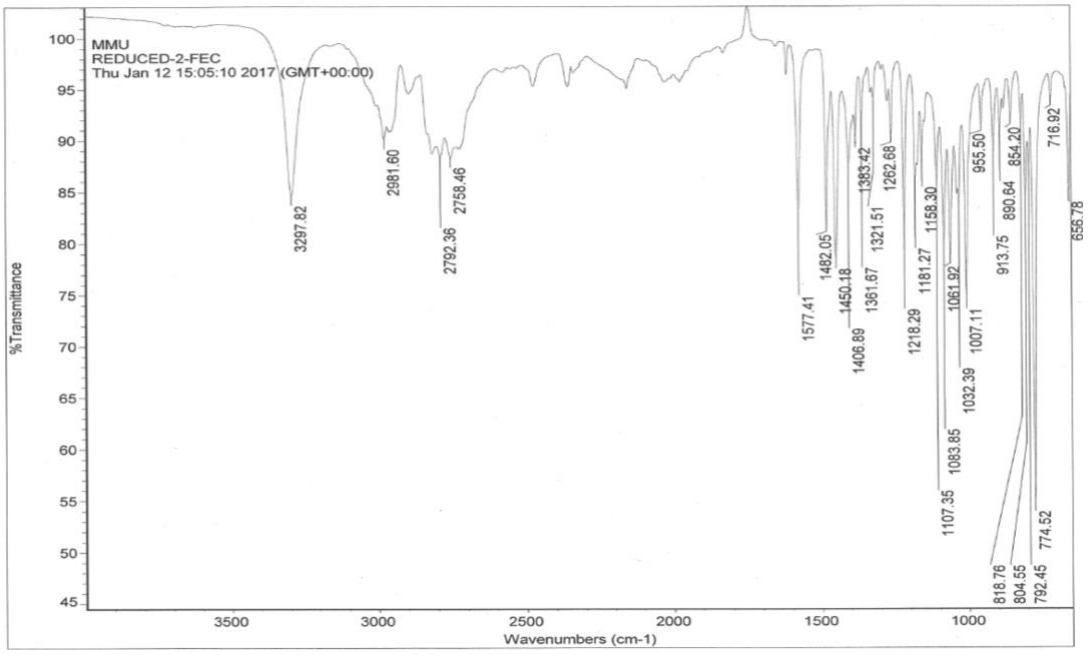

Figure 5-25. Infrared spectrum of **26**

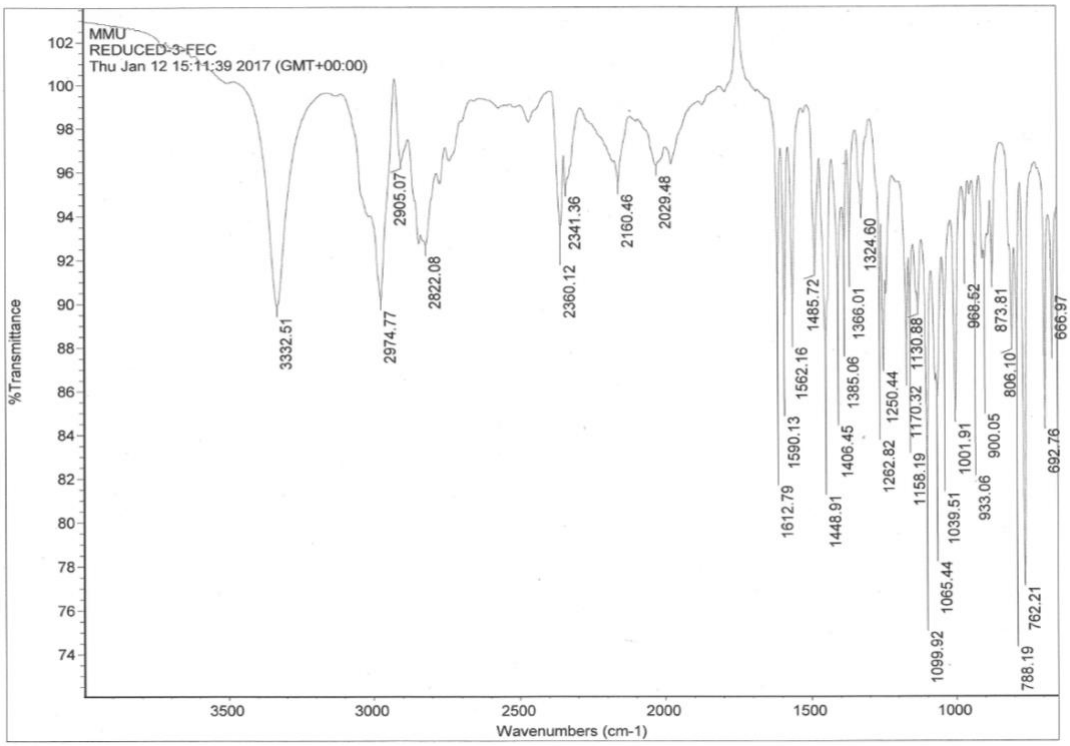

Figure 5-26. Infrared spectrum of **27**

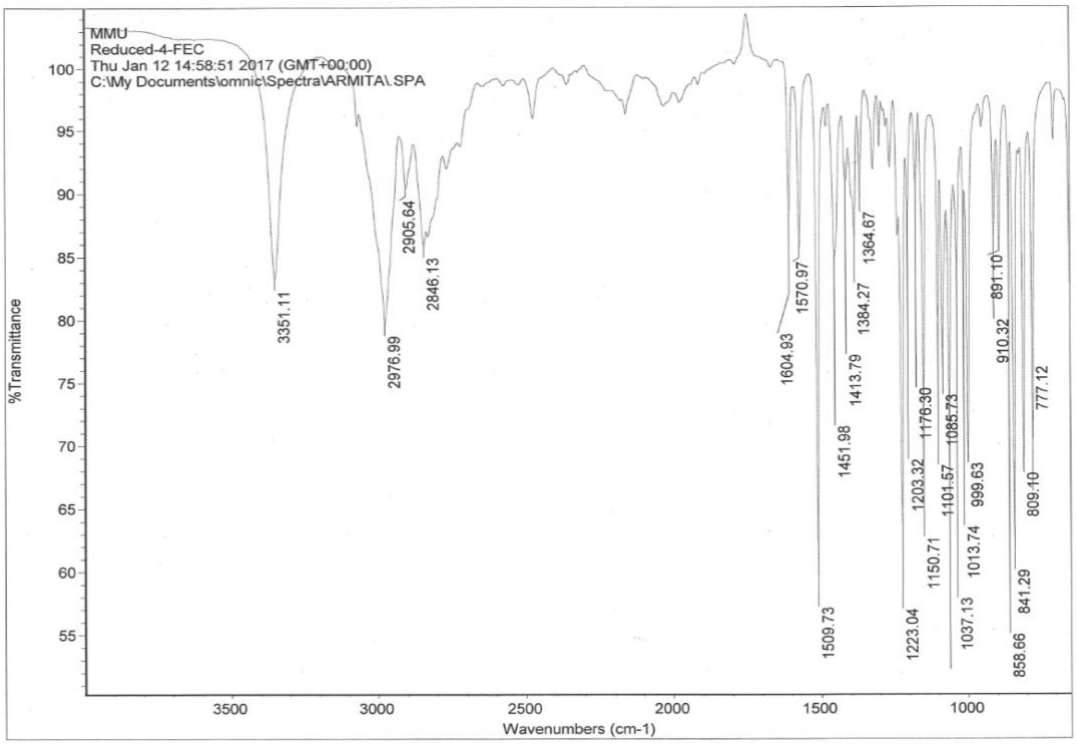

Figure 5-27. Infrared spectrum of **28**

5.3 Melting point analysis

The average melting points for **26**, **27** and **28** were observed in the ranges of 223-228°C and 229-233°C and 236-241°C, respectively. These results illustrated higher melting points than **23** and **24** (149°C and 196°C respectively), whereas the melting point of **28** is lower than that of **25** (256°C).

5.4 Thin layer chromatography (TLC)

TLC was established as an identification method for the cathinone compounds; TLC analysis of the isomers of fluoroethcathinone compounds produced bright pink coloured spots, when ninhydrin solution was employed.

The examination of R_f validates some separation of the reduced FEC regioisomers (R_f = 0.41, 0.33 and 0.26 for **26**, **27** and **28** respectively). These values are lower than the corresponding FEC and FMC derivatives. The presence of the alcohol must lead to stronger interactions with the silica and hence lower R_f values. R_f of FEC compounds were also measured as reference standards to confirm validity of these results. Since ephedrine isomers are more polar than cathinone isomers, R_f values are significantly smaller in ephedrine.

The %RSDs values calculated for **26**, **27** and **28** are 2.01%, 2.36%, and 2.91% respectively. Analogous to the FEC samples, %RSD of reduced forms are less than 3%, therefore the R_f results obtained by 6 repetitive tests are within a small range, hence they are valid.

5.5 Colour presumptive tests

Various presumptive tests of ephedrine derivatives illustrate that Chen Kao is the most appropriate colour preservative test for the analysis of ephedrine isomers as a powder.[25] However, the ephedrine isomers did not react with any of the colour testing agents as a solution. Chen Kao reagent results in formation of a violet colour upon a symmetrical chelate formation reaction with the ephedrine isomers as powders. However, the stability and solubility of this reagent is affected by the structural and steric differences of the alkylamine part of the molecule.

In tables 5-5 to 5-10, a negative (-) sign indicates that no colour change occurred, whereas a positive (+) sign indicates a reaction of the compound with the reagents.

Table 5-5 Colour changes of reduced FEC regioisomers using *Marquis*, *Mandelin*, *Simon*, and *Robadope's* tests in solution after 20 minutes

Colour change of reduced FEC isomers in solution after 20 minutes

	Marquis	**Mandelin**	**Simon**	***Robadope***
BLANK	Colourless	Dark yellow	Peach	Colourless
26	(-)	(-)	(-)	(-)
27	(-)	(-)	(-)	(-)
28	(-)	(-)	(-)	(-)

Table 5-6 Colour changes of reduced FEC regioisomers using *Scott*, *Zimmerman*, *Liebermans*, and *Chen Kao* tests, samples in solution after 20 minutes

Colour change of reduced FEC isomers in solution after 20 minutes

	Scott	**Zimmerman**	**Liebermans**	**Chen Kao**
BLANK	Dark peach	Colourless (Cloudy)	Colourless (Cloudy)	Blue
26	(-)	(-)	(-)	Colourless
27	(-)	(-)	(-)	Colourless
28	(-)	(-)	(-)	Colourless

Table 5-7 Immediate colour changes of reduced FEC regioisomers powders using *Marquis*, *Mandelin*, *Simon*, and *Robadope's* tests.

Immediate colour change of the reduced FEC isomers as powders

	Marquis	**Mandelin**	**Simon**	***Robadope***
BLANK	Colourless	Yellow	Bright pink	Colourless
26	(-)	(-)	(-)	(-)
27	(-)	(-)	(-)	(-)
28	(-)	(-)	(-)	(-)

Table 5-8 Immediate colour changes of the FEC regioisomers as powders, using *Scott*, *Zimmerman*, *Liebermans*, and *Chen Kao* tests.

Immediate colour change of reduced FEC isomers as powders

	Scott	**Zimmerman**	**Liebermans**	**Chen Kao**
BLANK	Peach	Colourless (Cloudy)	Colourless	Bright blue
26	(-)	(-)	(-)	Violet (+)
27	(-)	(-)	(-)	Violet (+)
28	(-)	(-)	(-)	Violet (+)

Table 5-9 Colour changes of the FEC regioisomers as powders, using *Marquis*, *Mandelin*, *Simon*, and *Robadope's* tests, after 20 minutes.

	Colour change of reduced FEC isomers as powders after 20 minutes			
	Marquis	**Mandelin**	**Simon**	***Robadope***
BLANK	Bright peach	Intense yellow	Peach	Colourless
26	(-)	(-)	(-)	(-)
27	(-)	(-)	(-)	(-)
28	(-)	(-)	(-)	(-)

Table 5-10 colour changes of the FEC regioisomers as powders, using *Scott*, *Zimmerman*, *Liebermans*, and *Chen Kao* tests, after 20 minutes.

	Colour change of reduced FEC isomers as powders after 20 minutes			
	Scott	**Zimmerman**	**Leibermans**	**Chen Kao**
BLANK	Peach	Colourless (Cloudy)	Colourless	Bright blue
26	(-)	(-)	(-)	Violet (+)
27	(-)	(-)	(-)	Violet (+)
28	(-)	(-)	(-)	Violet (+)

Chapter 6 Low-field NMR Analysis

6.1 HETCOR- Heteronuclear Correlation (HETCOR)

In order to tackle the forensic issues of rapid, selective and sensitive field screening, low-field NMR spectroscopy was employed.

The NMR characterisation of the regioisomers of FEC revealed the similarity in the chiral centre containing chain. There are, however, differences in the appearance of the aromatic ring component and the chemical shift of the unique ^{19}F signal. These properties can be used to resolve one regioisomer from another using 2D NMR techniques. One such technique is HETCOR (Heteronuclear Correlation).[38]

HETCOR provides the correlation between nuclei such as ^{13}C or ^{19}F and ^{1}H by polarisation transfer. H-H couplings are removed in HETCOR. Furthermore, HETCOR leads to the production of cross-peaks for all the protons and carbon nuclei, for example, that are connected by a ^{13}C-^{1}H coupling over one bond.[38-39]

HETCOR can also be used to establish the connectivity between ^{1}H and ^{19}F environments. Given that the FEC and FMC regioisomers all possess a single ^{19}F, it was envisaged that HETCOR could be used to differentiate the three isomers in each class. This is not achievable using ^{1}H and ^{19}F NMR due to the convoluted nature of the aromatic region for the former, and the fact that the FEC and FMC ^{19}F NMR signals have very similar δ values, thus they cannot be resolved readily using conventional 1D methods. An

example of the $^{19}F\{^{1}H\}$ NMR spectra of the three regioisomers of FEC is shown in figure 6-1.

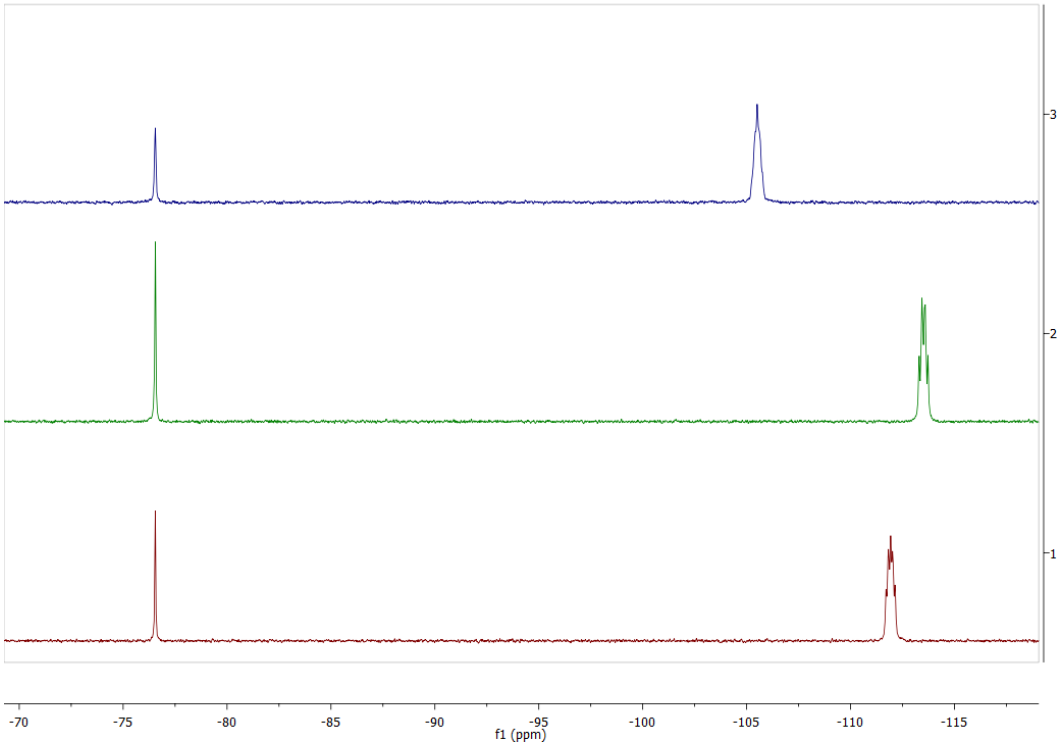

Figure 6-1. Stacked $^{19}F\{^{1}H\}$ NMR spectra of the three regioisomers of FEC; spectrum 1: **23**, spectrum 2: **24**, spectrum 3: **25**

To overcome this problem, HETCOR was employed in an attempt to resolve the regioisomers of FEC and FMC. The ^{19}F-^{1}H HETCOR NMR spectrum of the three regioisomers of FEC is shown in Fig.6-2. From this spectrum, it is apparent that **25** has only two correlations. This is due to the symmetry that is found within the aromatic ring. **23** and **24** both possess four correlations each. This is expected given that the ^{19}F nucleus interacts with four ^{1}H nuclei in the aromatic ring.

The HETCOR NMR data shows that the three isomers can be separated from one another, provided that the chemical shift of the ^{19}F nucleus is known for each regioisomer. However, without any prior knowledge of the regioisomers, only **25** can be readily identified using this method based on the number of ^{19}F-^{1}H correlations it possesses.

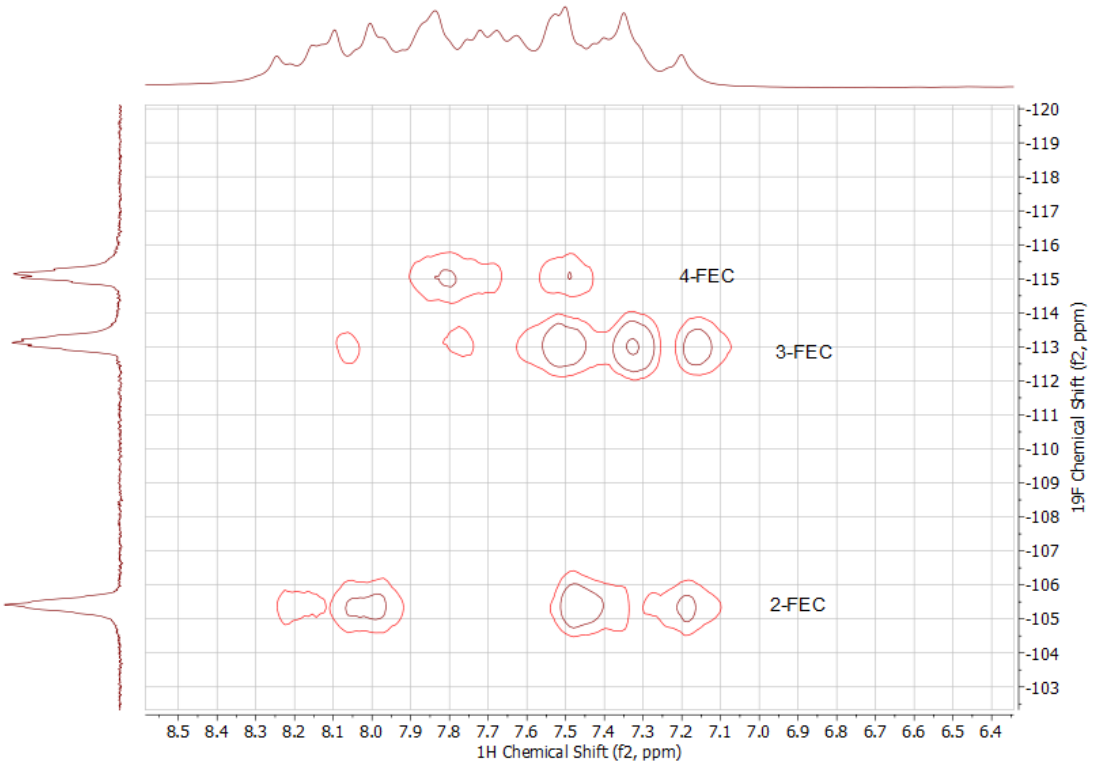

Figure 6-2. ^{19}F-^{1}H HETCOR NMR spectrum of the three regioisomers of FEC

A ^{19}F-^{1}H HETCOR NMR spectrum of the regioisomers of FMC was also collected (Fig. 6-3). Upon inspection, the spectrum appears to have similar characteristics to that of the FEC equivalent. This was expected based on the characterisation data that has been obtained for all of the regioisomers discussed in this thesis. Again, two correlations are observed for 4-FMC whereas four are seen for 2-FMC and 3-FMC. The similarity of this spectrum

relative to the FEC equivalent makes the likelihood of being able to resolve efficiently a mixture of all six regioisomers difficult. However, to prove this hypothesis, a ^{19}F-^{1}H HETCOR NMR spectrum of all six regioisomers was collected and analysed. This spectrum is shown in Fig. 6-4.

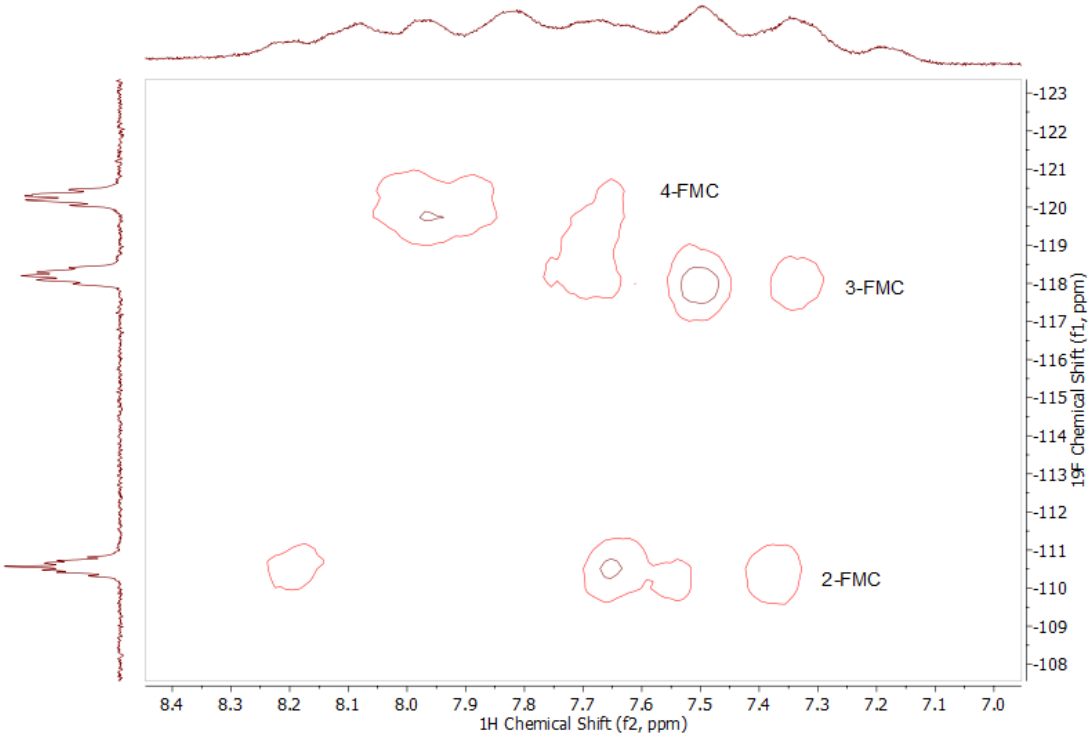

Figure 6-3. ^{19}F-^{1}H HETCOR NMR spectrum of the regioisomers of FMC

The ^{19}F-^{1}H HETCOR NMR spectrum of all six regioisomers highlights the problem associated with using HETCOR to resolve the six regioisomers; the similarity of the ^{19}F chemical shift of the corresponding FEC / FMC regioisomers results in the employment of this method being impractical. This is because there are only three distinct rows of cross-peaks observed, if the experiment had been successful, then six should have been observed.

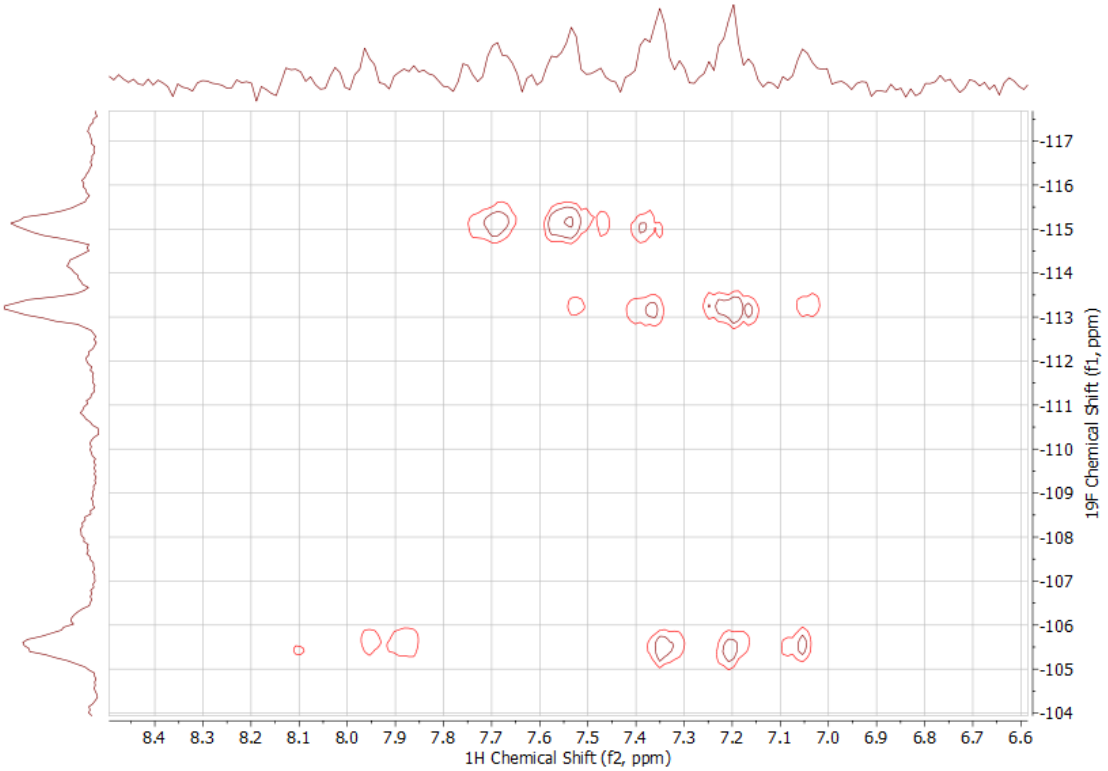

Figure 6-4. ^{19}F-^{1}H HETCOR NMR spectrum of all six FEC and FMC regioisomers

In summary, ^{19}F-^{1}H HETCOR can be utilised to resolve the individual regioisomers of FEC or FMC from a mixture comprised of a single class. However, it cannot be used to resolve individual regioisomers from a complex mixture consisting of both FEC and FMC classes.

6.2 *J*-resolved spectroscopy (*J*-RES)

The HETCOR experiments described in the previous section rely upon using chemical shift to differentiate the regioisomers present. An alternative is to use the *J*-coupling that exists between ^{19}F and those ^{1}H nuclei to which it couples. To do this, *J*-resolved spectroscopy was employed.[38]

It is usually difficult to separate different isomers of a compound using only 1D NMR i.e. ^{1}H NMR. It can be a challenge to distinguish between multiplets of the same resonance, and observe their splitting pattern, since they can overlap and form more complex multiplets. [38] An example of the overlapping nature of the multiplets in the ^{1}H NMR spectrum of all six FEC and FMC regioisomers is shown in Figure 6-5.

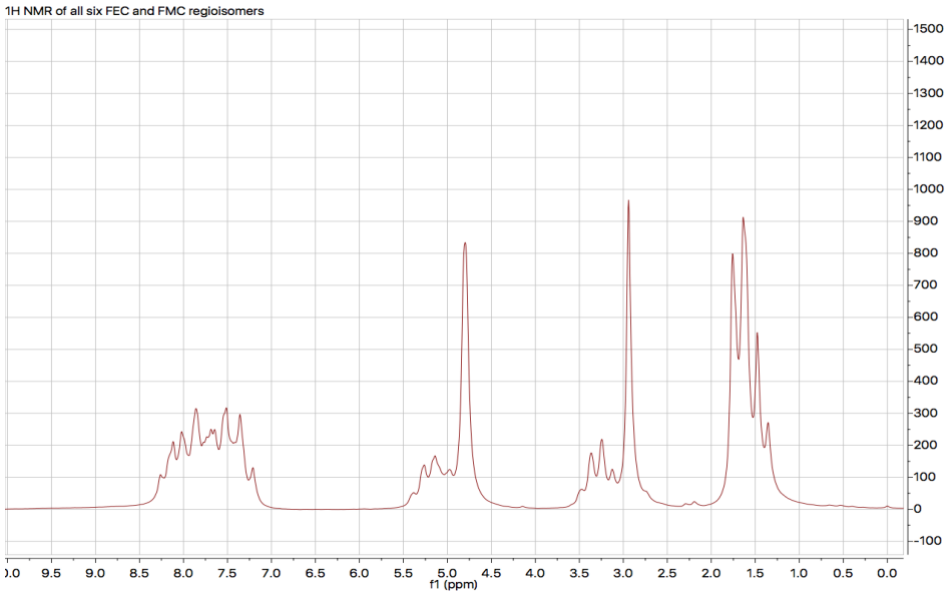

Figure 6-5. ^{1}H NMR spectrum of all six FEC and FMC regioisomers

Consequently, 2D spectra can be obtained to resolve this complexity. *J*-RES produces a spectrum that links the chemical shift of an environment with that of the *J*-coupling it possesses. In a homonuclear ^{1}H-^{1}H experiment, the indirect dimension is the proton-proton coupling, whereas the direct dimension is the chemical shifts of the ^{1}H nuclei.

Again, the presence of a single ^{19}F nucleus was utilised as this was hoped to simplify the resulting *J*-RES spectrum. In a similar vain to the HETCOR

study, the two individual classes were examined independently (Fig. 6-6 and 6-7) prior to analysing a mixture of all six regioisomers (Fig. 6-8).

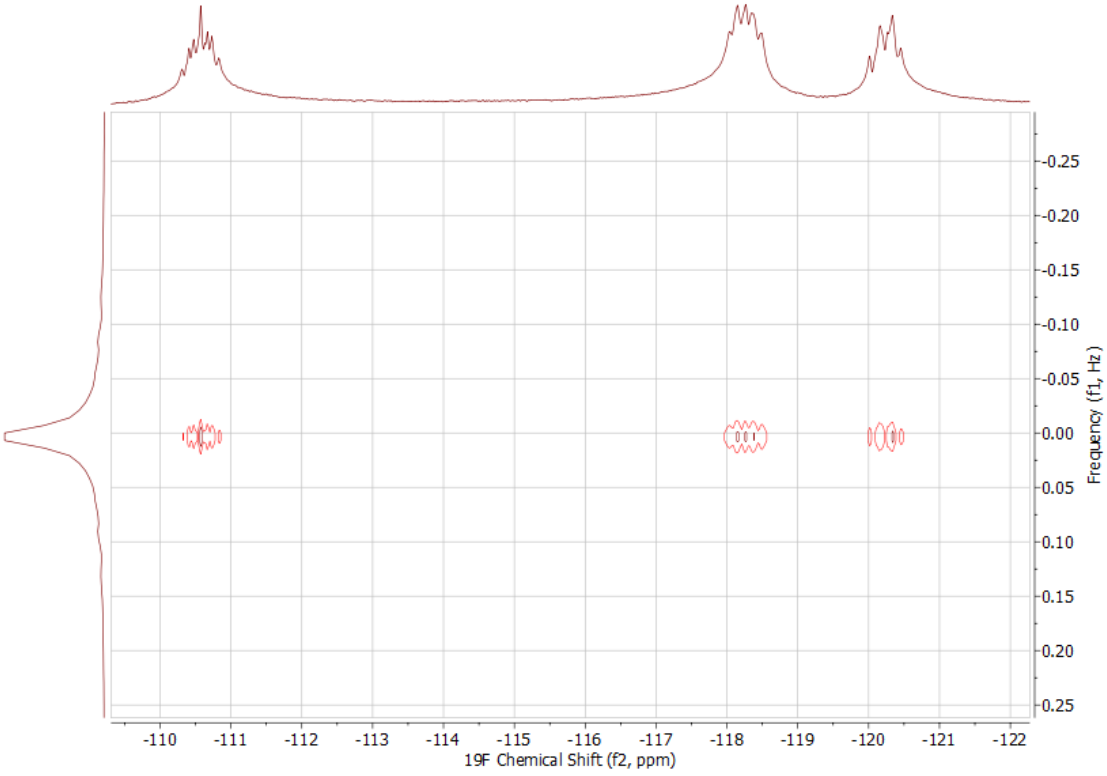

Figure 6-6. ^{19}F *J*-RES spectrum of the three isomers of FEC

Effectively, coupling to proton is observed along the f2 dimension. ^{19}F-^{19}F coupling, if present, would be visible along the f1 direction. This simplifies the spectrum and makes it easier to detect chemical shifts and coupling arrangement. The observation of three distinct peaks in the *J*-RES spectrum again relates to each FEC compound present.

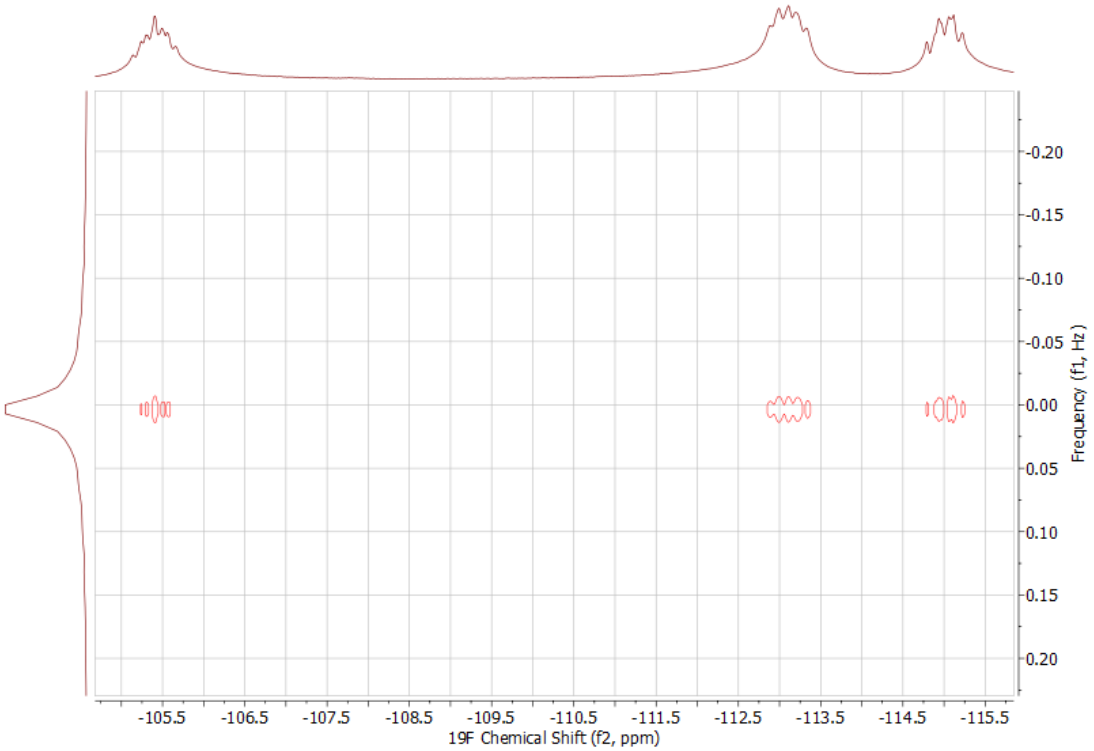

Figure 6-7. ^{19}F *J*-RES spectrum of the three isomers of FMC

Figures 6-6 and 6-7 show the proton coupling of each isomer of FEC and FMC separately but because they have a very similar structure it is difficult to resolve them from each other because they overlap. The overlapping nature of the FEC and FMC regioisomers is shown in Fig. 6-8. Only three peaks are observable, whereas to resolve all six regioisomers successfully, six peaks should be present. Thus, the structural similarities of FEC and FMC isomers make them difficult to differentiate by HETCOR and *J*-RES. This is due to the structural change in the backbone having no marked effect on the chemical shifts of the nuclei of the aromatic ring, and the couplings they possess. This means that HETCOR and *J*-RES are not suitable NMR techniques to successfully resolve the regioisomers of FEC and FMC when combined in a mixture.

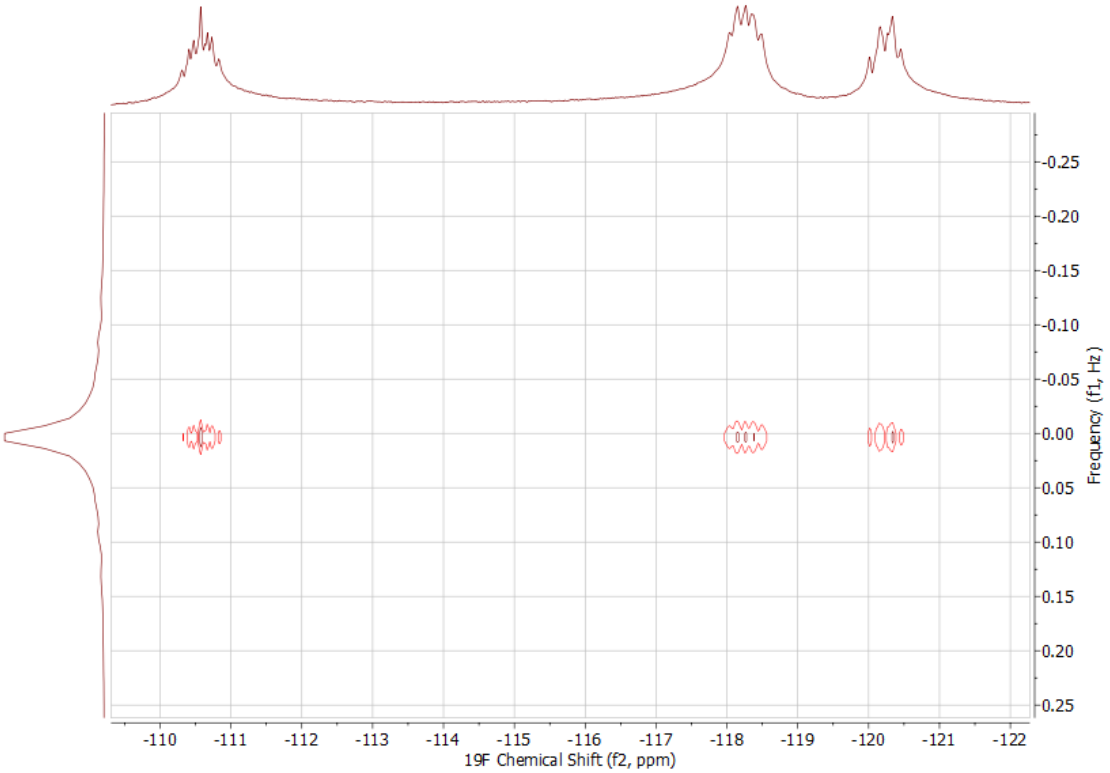

Figure 6-8. ^{19}F *J*-RES spectrum of all six isomers of FEC and FMC

6.3 *J*-resolved spectroscopy (*J*-RES) of the 4-FEC and 4-FMC with benzocaine

Evidence has shown that adulterants have been added to NPS containing street samples. In the *J*-RES analysis of the FEC and FMC regioisomers, the samples were characterised and resolved in their pure form. The presence of common adulterants was used to determine the selectivity of the *J*-RES methodology i.e. could FEC (**28**) or FMC (**29**) regioisomers still be resolved effectively. Therefore, benzocaine (**30**), which is a local anaesthetic, was added as an adulterant to the samples investigated.

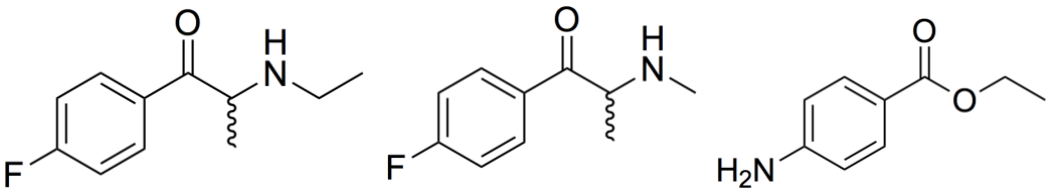

28 **29** **30**

Figure 6-9. 4-FEC (**28**) and 4-FMC (**29**) with benzocaine (**30**)

The spectra shown in Figs. 6-10 and 6-11 show the proton coupling of **28** and **29** with **30** separately, from which it is clear that they are resolved. The lack of a ^{19}F nucleus in benzocaine means that this result was to be expected. However, the similarity of the ^{19}F-^{1}H coupling of **28** and **29** in the f2 direction is notable. Thus, when **28** and **29** were mixed together (Fig. 6-12), and because they have similar structures, it is again difficult to resolve them from each other because their signals overlap. This has further ramifications in that a mixture of **28** and **30,** and **29** and **30**, cannot be differentiated from one another using this technique alone. The chemical shift of the fluorine nuclei in **28** and **29**, and their resultant couplings to ^{1}H, are too similar. Thus, in order to employ *J*-RES successfully, FEC and FMC isomers need to incorporate a second ^{19}F nucleus. This structural modification will produce homonuclear couplings in the f1 direction. The size of J_{FF} may be sufficient to resolve a FEC regioisomer from the same regioisomer of FMC, and vice versa. Currently, the lack of homonuclear couplings (J_{FF}) limits *J*-RES to differentiating either FEC or FMC regioisomers only, but not a mixture thereof. Arguably, ^{19}F NMR can achieve

this readily and negates the need to use a lengthy and more complicated pulse sequence.

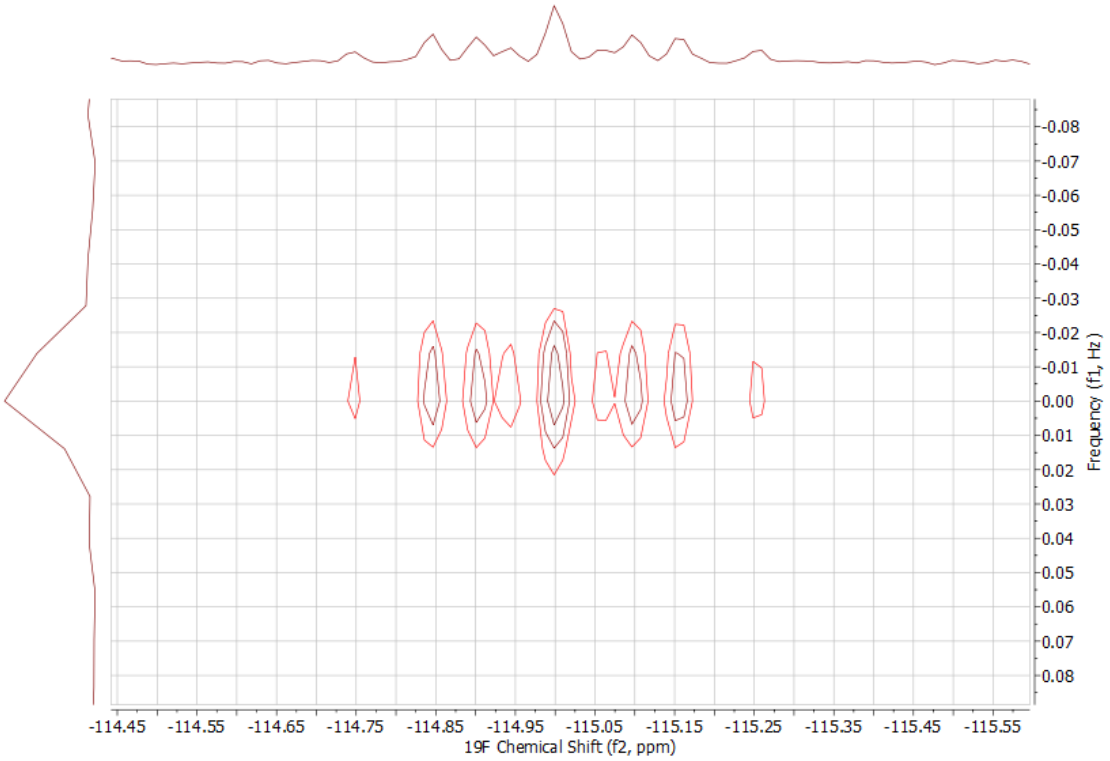

Figure 6-10. ^{19}F *J*-RES spectrum of **28** with **30** collected in DMSO

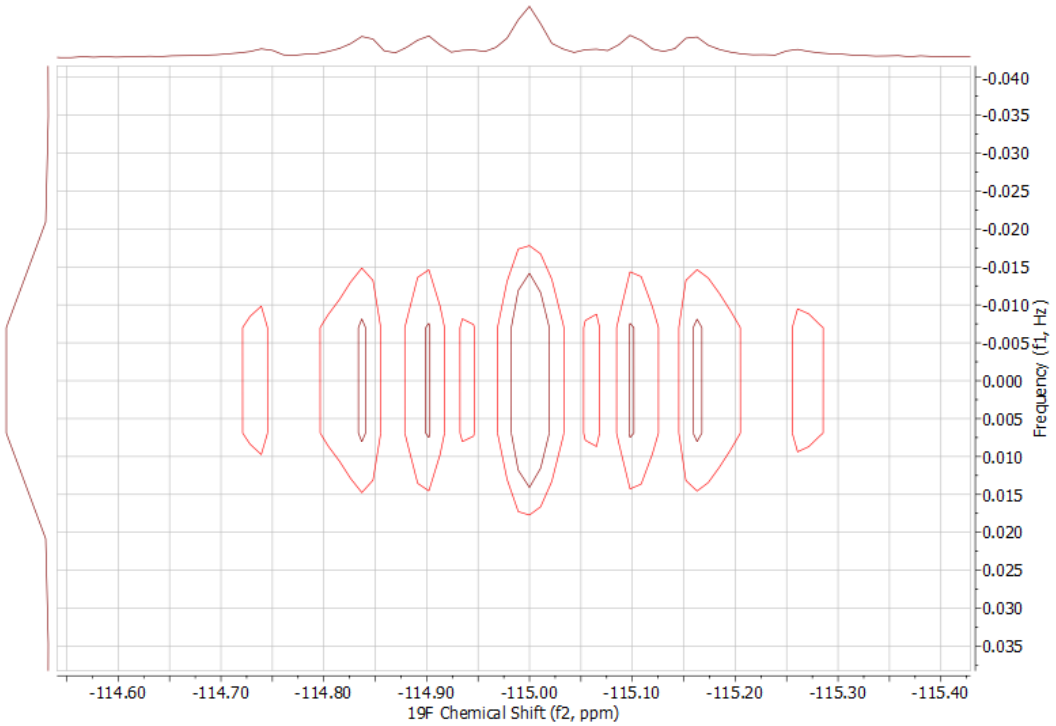

Figure 6-11. ^{19}F *J*-RES spectrum of **29** with **30** collected in DMSO

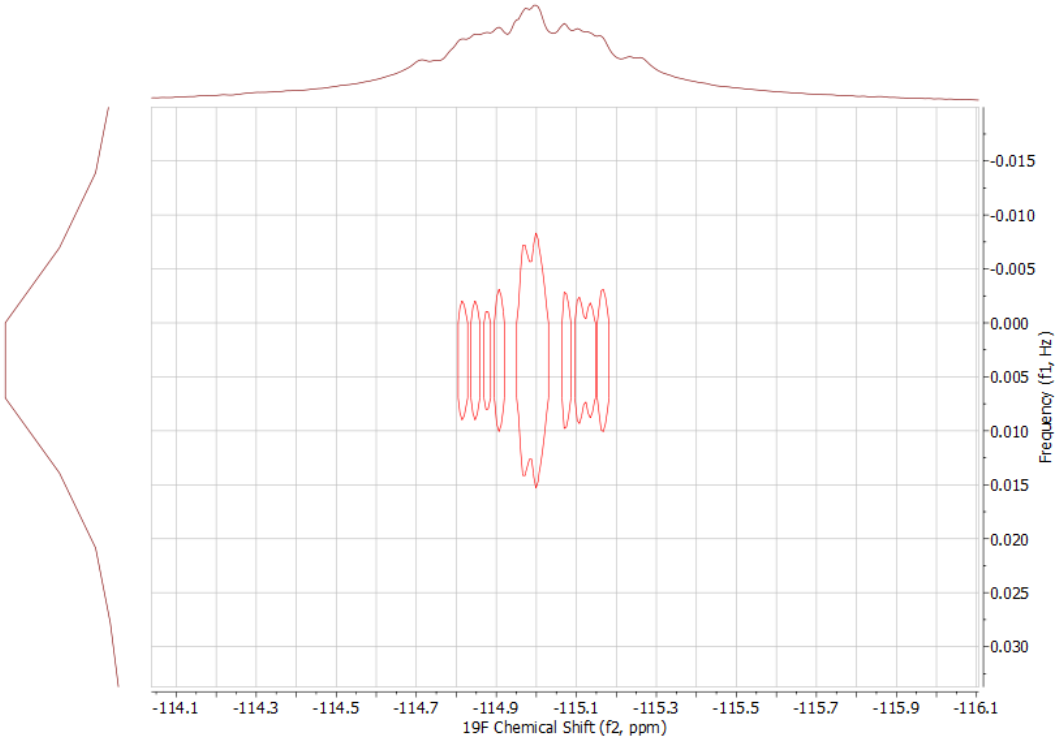

Figure 6-12. ^{19}F *J*-RES spectrum of **28** and **29** with **30** collected in DMSO

Chapter 7 Conclusion

The significant increase in the popularity of the NPSs, particularly synthetic cathinone and its derivatives as ‘legal highs’, in the past few years, has resulted in an urgent need for a simple, accessible and selective analytical method for their detection.

Regioisomers of fluoroethcathinone and its metabolites were successfully synthesised. They were fully characterised using analytical techniques such as high-field and low-field NMR spectroscopy, GC-MS, LC-MS, IR, TLC, colour presumptive test and melting point. Yields of the materials ranged from 19% and 65%. In all cases, the structural characterisation analysis verified that all six samples were mainly pure. Presumptive colour tests produced the expected colour changes, i.e. the Zimmerman’s test were positive for the FEC isomers whereas Chen Kao reacted with the ephedrine isomers to give a positive indicator.

TLC was established as an identification technique for the cathinone isomers and their derivatives. The R_f values of the reduced FEC isomers are lower than the corresponding FEC and FMC derivatives. The presence of the alcohol must lead to stronger interactions with the silica and hence lower R_f values. Since ephedrine isomers are more polar than cathinone isomers, R_f values are significantly smaller in ephedrine.

Analysis of GC spectra of both non-derivitised and derivitised compounds demonstrated that derivatisation is the way forward for cathinone

compounds, as the three derivatised compounds are very close to being baseline separated; also all three isomers were eluted under 20 mins with eicosane being employed as a reference in all cases. However, this research was not able to identify reduced FEC isomers using the same method that was developed.

HETCOR NMR data shows that the three regioisomers (either FEC or FMC) can be separated from one another. A mixture of FEC and FMC regioisomers are not distinguishable due to the similarity in the chemical structure in the vicinity of the ^{19}F. Moreover, *J*-RES spectral data mirrored that of the HETCOR NMR data; again, the regioisomers could be separated within their class but not as a mixture. A similar observation was true of a mixture of **28**, **29** and **30**, a common adulterant, although **28** and **29** were successfully resolved from benzocaine, they could not be resolved from one another in a mixture.

Chapter 8 Future Work

In terms of future work, High Performance-Liquid Chromatography technique (HPLC) could be used to separate the regioisomers of FEC in order to expand the method scope for separating these isomers. As highlighted in this thesis, GC-MS cannot be used, using the conditions described here; to successfully separate out the regioisomers and so other techniques could be investigated.

Also, the employment of GC-MS can be further investigated in relation to both FEC and reduced FEC derivatives, in order to obtain a better result in terms of separating the reduced FEC compounds.

Furthermore, the library of compounds could be expanded, to include those with more than one fluorine substituent (**31-34**) (J_{FF} couplings will aid in resolving the isomers in the HETCOR and *J*-RES spectra). Again, these compounds would need to be synthesised as reference compounds do not currently exist.

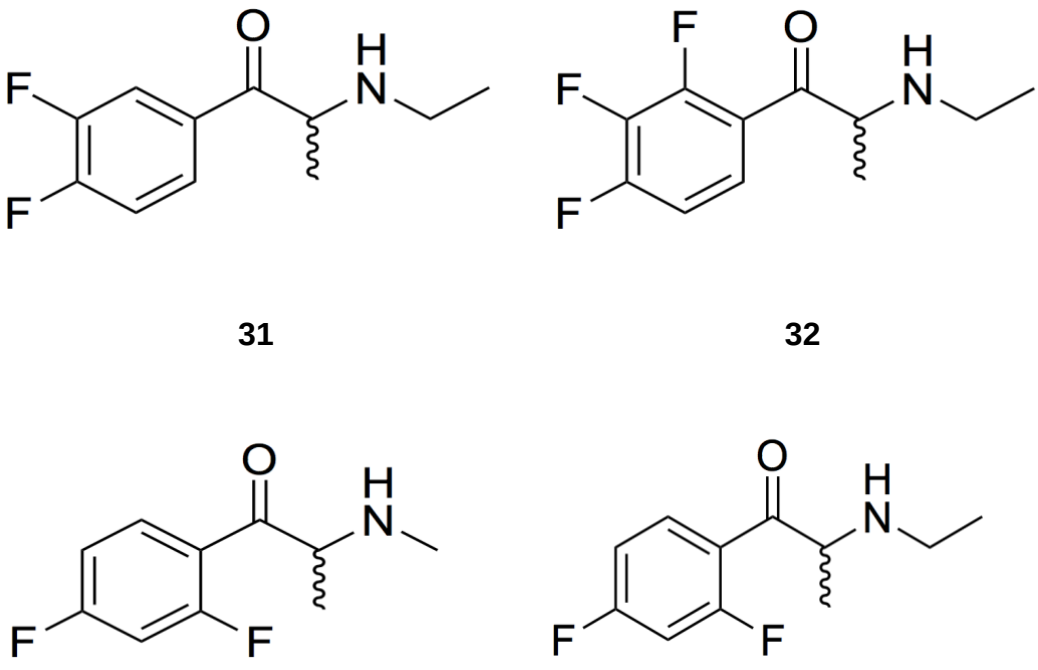

Figure 8-1. Chemical structures of cathinone derivatives possessing more than one fluorine substituent that could be investigated using 2D NMR spectroscopy

References

1. J. Smith, O. Sutcliffe and C. Banks, *The Analyst*, 2015, **140**, 4932-4948.

2. Psychoactive Substances:Legal Guidance : Crown Prosecution Service, http://www.cps.gov.uk/legal/p_to_r/psychoactive_substances/#a05, (accessed 15 October, 2016).

3. DrugWise, http://www.drugwise.org.uk/what-are-the-uk-drug-laws/, (accessed 15 October, 2016).

4. UNODC, World Drug Report 2015, United Nations, 2015.

5. N. Burgess, *Aberdeen Student Law Review*, 2017, **7**, 109-120.

6. T. Ayres and J. Bond, *BMJ Open*, 2012, 2.

7. M. Baumann, R. Glennon and J. Wiley, *Neuropharmacology of New Psychoactive Substances (NPS): The Science Behind the Headlines*, Springer, 1st edn, Switzerland, 2017.

8. N. Nic Daeid, K. Savage, D. Ramsay, C. Holland and O. Sutcliffe, *Science & Justice*, 2014, **54**, 22-31.

A. Abdullaha, K. Changa, S. Jayaramb and M. Sulaimanb, *Malaysian Journal of Forensic Sciences*, 2015, **6**, 30-43.

9. Unodc.org, https://www.unodc.org/LSS/Page/NPS, (accessed 14 October, 2017).

10. T. Ketema, M. Yohannes, E. Alemayehu and A. Ambelu, *BMC Immunology*, 2015, **16**, 9.

11. P. Kuś, J. Kusz, M. Książek, E. Pieprzyca and M.Rojkiewicz, *Forensic Toxicology*, 2016, **35**, 114-124.

12. *Talktofrank.com*, http://www.talktofrank.com/sites/default/files/drugs/Khat%201.JPG, (accessed 14 October, 2017).

13. M. Capriola, *Clinical Pharmacology: Advances and Applications*, 2013, 109

14. Vouga, R. .A. Gregg, M. Haidery, A. Ramnath, H. K. Al-Hassani, C. S. Tallarida, D. Grizzanti, R. B. Raffa, G. R. Smith, A. B. Reitz ,S. M.Rawls, *Neuropharmacology*, 2015, **91**, 109-116.

15. Davidson and F. Schifano, *Progress in Neuro-Psychopharmacology and Biological Psychiatry*, 2016, **64**, 267-274.

16. H. Manske, H. Holmes, Academic Press, 1953, **3**, 351-361

17. E. Ravina, *The Evolution of Drug Discovery: From Traditional Medicines to Modern Drugs*, Wiley-VCH, Germany, 1th edn, 2011.

18. A. J. Mullen, PHD thesis, Dublin City University, September 1991.

19. Booth, W. Sherman, P. Raven, J. Caffrey, T. Yorio, M. Forster, P. Gwirtz, *Warner-Lambert*, 1999.

20. J. Liles, *Journal of Pharmacology and Experimental Therapeutics*, 2005, **316**, 95-105.

21. Pearson, MSc (by Research), Manchester Metropolitan University, 2015.

22. K. Alsenedi and C. Morrison, *Anal. Methods*, 2017, **9**, 2732-2743.

23. What-when-how.com, http://what-when-how.com/forensic-sciences/presumptive-chemical-tests/, (accessed 14 October, 2017).

24. E. Toole, S. Fu, R. G. Shimmon and N. Kraymen, *Microgram J.,* 2012, **9**, 27-32.

25. G. Nagy, I. Szollosi, K. Szendrei, Colour Test for Precursor Chemicals of Amphetamine-Type Substances, Szeged University, Hungary, UNODC, 2005.

26. N. (NMR) and H. NMR, *Jeol.co.jp*, 2018.

27. M. Alotaibi, S. Husbands and I. Blagbrough, *Journal of Pharmaceutical and Biomedical Analysis*, 2015, **107**, 535-538.

28. R. Mewis, *1H, 19F and 13C analysis in under two minutes using Pulsar, Application Note*, Oxford Instruments, Oxford, 1st edn., 2017.

29. Y. Huang, S. Cai, Z. Zhang and Z. Chen, *Biophysical Journal*, 2014, 106, 2061-2070.

30. I.O. Khreit, C. Irving, E. Schmidt, J. Parkinson, N. Nic Daeid and O. Sutcliffe, *Journal of Pharmaceutical and Biomedical Analysis*, 2011, 61, 122-135.

31. E. Y. Santali, A.K. Cadogan, N. N. Daeid, K. A. Savage and O. B. Sutcliffe, Journal of Pharamaceutical and Biomedical Analysis, 2011, 246-255.

32. R. P. Archer, *Forensic Science International*, 2009, **185**, 10-20.

33. *Recommended methods for the identification and analysis of amphetamine, methamphetamine and their ring-substituted analogues in seized materials*, United Nations, New York, 2006.

34. Swgdrug.org, http://www.swgdrug.org/monographs.htm, (accessed 14 October, 2017).

35. M. Philp, S. Fu, *Drug Testing and Analysis*, 2017, 10, 95-108.

36. Darsigny, M. Leblanc-Couture and I. Desgagné- Penix, *Austin publishing group*, 2018, 5, 1-9.

37. K. Kovar, M. Laudszun, *UNITED NATIONS*, 1989, 13.

38. Tecmag, http://www.tecmag.com/pdf/HETCOR.pdf, (accessed 17 October, 2017).

39. Sh. Wu, *1D and 2D NMR Experiment Methods*, *NMR Research Center Chemistry Department,* Atlanta, May 2011.